

ROLE OF 14-3-3 ETA AND EPSILON IN GAMETOGENESIS

A dissertation submitted
to Kent State University in partial
fulfillment of the requirements for the
degree of Doctor of Philosophy

by

Alaa Abdulaziz Eisa

December 2019

© Copyright

All rights reserved

Except for previously published material

Dissertation written by

Alaa Abdulaziz Eisa

B.Sc., Umm Al-Qura University, Saudi Arabia 2008

M.Sc., Ball State University, USA, 2013

Ph.D., Kent State University, USA, 2019

Approved by

Douglas Kline. _____ , Chair, Doctoral Dissertation Committee

Srinivasan Vijayaraghavan _____ , Members, Doctoral Dissertation Committee

Kristy Welshhans _____

Gail Fraizer _____

Accepted by

Ernest Freeman _____ , Director, School of Biomedical Sciences

James L. Blank _____ , Dean, College of Arts and Sciences

TABLE OF CONTENTS

TABLE OF CONTENTS	III
LIST OF FIGURES	V
LIST OF TABLES	IX
ACKNOWLEDGEMENTS	XI
CHAPTER 1 INTRODUCTION.....	1
1.1 Cell division	1
1.2 Oogenesis	5
1.3 Spermatogenesis.....	17
1.4 Protein Phosphatase in gametogenesis	34
1.5 YWHA or 14-3-3 Proteins in gametogenesis.....	38
CHAPTER 2 MATERIALS AND METHODS.....	42
2.1 Materials and Methods for Aim 1 and 2	42
2.2 Materials and Methods for Aim 3	55
CHAPTER 3 AIM 1 AND 2	66
3.1 Aim 1: To identify the possible roles of PP1 in oocyte maturation	66
3.1.1 Rationale.....	66
3.1.2 Result.....	67
3.1.3 Discussion	90
3.2 Aim 2: To define the role of 14-3-3 eta and 14-3-3 epsilon in oocyte maturation .	94
3.2.1 Rationale.....	94
3.2.2 Results	95

3.2.3 Discussion	112
CHAPTER 4 AIM 3.....	117
4.1 Aim 3: To study the role of 14-3-3 eta and epsilon in spermatogenesis	117
4.1.1 Rationale.....	117
4.1.2 Results	119
4.1.3 Discussion	149
REFERENCES.....	155

LIST OF FIGURES

Figure 1. The difference between Mitosis and Meiosis	3
Figure 2. Phases of the cell cycle in somatic cells	4
Figure 3. Structure of the female reproductive system	6
Figure 4. Oogenesis and folliculogenesis	7
Figure 5. The oocyte maturation process of mammalian oocyte	9
Figure 6. The signaling pathway for the prophase I arrested oocyte	11
Figure 7. The signaling pathway for oocyte maturation initiated by LH.....	13
Figure 8. Embryonic development.....	16
Figure 9. Structure of the male reproductive system	17
Figure 10. Seminiferous tubule.....	18
Figure 11. Stages of spermatogenesis	22
Figure 12. The hypothalamus pituitary gonadal axis.....	24
Figure 13. Sperm structure.....	27
Figure 14. Mouse sperm head.....	29
Figure 15. Sperm flagellum structure	30
Figure 16. Progressive and hyperactivated motility in mammalian sperm.....	31
Figure 17. The family of Phosphoprotein Phosphatases (PPP)	36
Figure 18. PP1 γ 1 and PP1 γ 2 mRNA expression using RT-PCR technique	68
Figure 19. Validation of PP1 γ 1 and PP1 γ 2 antibodies using His-tagged recombinant proteins	72

Figure 20. Pull down of PP1 protein from mouse ovaries using microcystin beads	73
Figure 21. Pull down of PP1 γ 2 protein from mouse ovaries using microcystin beads.....	74
Figure 22. Western blot analysis of lysates probed with anti-PP1 γ 2 antibody.....	76
Figure 23. PP1 γ 1 and 2 localization in mouse oocytes and eggs.....	77
Figure 24. Expression of PP1 isoforms and PP2A proteins in mouse eggs shown by immunofluorescence using isoform specific antibodies.....	79
Figure 25. Expression of PP1 isoforms and PP2A proteins in mouse eggs shown by immunofluorescence using PP1 (E9) antibody	80
Figure 26. Expression of PP1 α in both PP1 γ KO and WT ovaries, oocytes and eggs	82
Figure 27. Expression of PP1 α isoform in mouse eggs shown by immunofluorescence using PP1 α antibody	83
Figure 28. Fluorescent intensity of PP1 α expression in both PP1 γ KO and WT oocytes	84
Figure 29. Pull down of CDC25B protein from WT ovaries by using His-tagged PP1 γ 1 and PP1 γ 2 recombinant proteins	86
Figure 30. Immunoprecipitation of CDC25B protein from both PP1 γ KO and WT ovaries by using PP1 α antibody	88
Figure 31. Diagrammatic summary of the production of 14-3-3 eta oocyte-specific conditional knockout	98
Figure 32. Whole animal genotyping identifies those females with global and oocyte specific gene deletion	99
Figure 33. Validation of 14-3-3 epsilon ablation in both 14-3-3 epsilon CKO and GKO eggs by western blot	100

Figure 34. <i>In vivo</i> breeding for 14-3-3 eta and epsilon KO females.....	103
Figure 35. <i>In vitro</i> maturation of the 14-3-3 eta CKO and GKO oocytes	104
Figure 36. <i>In vitro</i> maturation of the 14-3-3 epsilon CKO and GKO oocytes	105
Figure 37. <i>In vitro</i> maturation of the 14-3-3 eta/epsilon double CKO oocytes	106
Figure 38. <i>In vitro</i> maturation rate of 14-3-3 eta KOs, epsilon KOs and eta/epsilon double CKO.....	107
Figure 39. <i>In vitro</i> fertilization of eggs from 14-3-3 epsilon knockout females.....	109
Figure 40. Embryonic development of the 14-3-3 epsilon KO mice.....	110
Figure 41. Expression of 14-3-3 eta and epsilon in mouse testis and sperm by using western blot.....	120
Figure 42. Messenger RNA expression of 14-3-3 epsilon in developing testis by using qPCR.....	121
Figure 43. Pan 14-3-3 and 14-3-3 epsilon expression in mouse sperm by using immunofluorescence technique	122
Figure 44. 14-3-3 epsilon expression in mouse seminiferous tubules	123
Figure 45. Whole animal genotyping identifies those males with global and testes specific gene deletion.....	125
Figure 46. Validation of 14-3-3 eta ablation in both 14-3-3 eta CKO and GKO testis by western blot.....	126
Figure 47. Validation of 14-3-3 epsilon ablation in 14-3-3 epsilon CKO testis and sperm by western blot.....	127

Figure 48. Validation of 14-3-3 epsilon ablation in 14-3-3 epsilon GKO testis and sperm by western blot.....	127
Figure 49. Validation of 14-3-3 epsilon ablation in 14-3-3 epsilon CKO testis by immunoflourescent technique.....	128
Figure 50. <i>In vivo</i> breeding for 14-3-3 eta and epsilon KO males.....	130
Figure 51. <i>In vitro</i> fertilization of sperm from 14-3-3 epsilon CKO knockout males....	131
Figure 52. Sperm count of 14-3-3 eta and epsilon KO mice	133
Figure 53. Total and progressive motility of 14-3-3 eta KO sperm.....	134
Figure 54. Total and progressive motility of 14-3-3 epsilon KO sperm.....	135
Figure 55. Speed parameters of 14-3-3 epsilon KO sperm.....	136
Figure 56. Mitochondrial potential and ATP assay of 14-3-3 epsilon KO sperm	138
Figure 57. DIC images of 14-3-3 epsilon KO sperm.....	140
Figure 58. Sperm abnormalities of 14-3-3 epsilon KO sperm.....	141
Figure 59. Histological sections of 14-3-3 epsilon KO testis	142
Figure 60. Post-translational modification of GSK3 and PP1 in 14-3-3 epsilon KO sperm	144
Figure 61. GSK3 activity of 14-3-3 epsilon KO sperm	145
Figure 62. Immunoprecipitation of PP1 γ 2 protein by using two different 14-3-3 epsilon antibodies.....	146
Figure 63. Immunoprecipitation of 14-3-3 epsilon by using PP1 γ 2 antibody	147
Figure 64. Western blot analysis of sperm extract probe with anti phospho(Ser)14-3-3 binding motif antibody	148

LIST OF TABLES

Table 1. Primers used to detect presence of each PP1 γ isoform by RT-PCR.....	45
Table 2. Primers used to detect LoxP and <i>Ywhah</i> in female mice	52
Table 3. Primers used to detect LoxP and <i>Ywha</i> genes in male mice	61
Table 4. Expression of Ppp1c and Cdc25 isoforms mRNA in single cell	69
Table 5. Expression of 14-3-3 isoform mRNAs in single oocytes	96

This thesis is dedicated to

“My everything in this life: Mom and Dad”

“My strength throughout the time: my Wife”

“My happiness throughout this journey: my Kids”

ACKNOWLEDGEMENTS

I would like to start my acknowledgement with an Arabic expression that says, “Who does not thank people, does not thank God”. So first of all, I would like to express my special thanks of gratitude to my advisor Dr. Douglas Kline who gave me the golden opportunity to work with him and under his supervision. I am so grateful for every moment I spent in his laboratory. He provided me with his invaluable guidance throughout my PhD journey. He opened my eyes into new views, taught me how to carry out my work, and how to deal with any difficulties I might face. Dr. Douglas Kline was the source of my motivation, encouragement and support. It was my pleasure and honor to work under his supervision and guidance.

I would like also to express my deep and sincere gratitude to my co-advisor, Dr. Srinivasan Vijayaraghavan, for his continuous support, patience, motivation, and for sharing his knowledge. I am very grateful for having him and Dr. Kline as advisors and mentors through my PhD journey. I would like to thank them for giving me the chance to join their labs and work with them. I am extremely grateful for what both of them have offered me.

Beside my advisors, I would like to thank my committee members, Dr. Kristy Welshhans and Dr. Gail Fraizer, for their support throughout this journey. My big thanks for my previous and current lab mates, (Santanu De, Ariana Detwiler, Eva Gilker, Travis Mollick, Nidaa Awaja, Rahul Bahattacharjee, Suranjana Goswami, and Priyanka Rana) their support and encouragement. Special thanks to my brothers and closest friends Abdulaziz Aloliqi, Alexander Ignatious, Wesam Nofal, Souvik Dey and Cameron Brothag for the good times we spent together and for the hard times we have been through, but we were there for each other. Thank you for your friendship and empathy.

My family has contributed to the success of this project in numerous ways. My deepest gratitude goes to my beloved father Mr. Abdulaziz Eisa and mother Mrs. Naeema Bukhari. They were with me here in spirit even though they were overseas. Their prayers and support always strengthened me during this project and throughout my life. I am extremely thankful to them for all of the sacrifices they have made just to help me achieve my dream. I'm very thankful to my sisters Ola, Alyaa and Afraa, and my brother Amer for their endless love, prayers and encouragement and being with me whenever I needed them.

I am greatly indebted to my devoted wife Weaam. Her support, encouragement, quiet patience and unwavering love allow me to pursue my own goals. She was the strength that I used throughout this journey. My journey would not be accomplished without her support and love. She is the love of my life. Special gratitude goes to my kids Abdulaziz, Naeema and Abdulwahed for their love, support and patience.

Lastly, I would like to thank the Saudi government and Tibah University for giving me the scholarship to study abroad and achieve my goals. My PhD journey has now come to an end, but I am grateful for every moment I spent during this journey.

Alaa Abdulaziz Eisa

October/30/2019, Kent, Ohio

CHAPTER 1

Introduction

1.1 Cell division

The mammalian body is composed of trillions of cells that are capable of dividing to help the organism to grow, repair damage, and to respond to environmental changes. This type of division used by somatic cells is called mitosis. Unlike the somatic cells, the germ cells in the mammalian body use a different form of cell division called meiosis. The primary function of meiosis is to create genomic diversity within the species. This diversity is accomplished by two phenomena, independent assortment and crossing over. Independent assortment produces gametes with many different assortments of homologous chromosomes, this is happening at metaphase I and during the random orientation of homologous chromosome pairing. On the other hand, crossing over occurs during prophase I, when the arms of the chromatids swap to create more genetic variation in the gametes (Gottlieb & Tegay, 2019) (Fig.1).

The cell cycle is composed of four phases that include Gap phase1 (G1), DNA synthesis (S), Gap phase 2 (G2) and Mitosis (M). The successful completion of each cycle will produce two daughter cells in mitosis. In each phase of the cell cycle, the cell will undergo cellular modification that will help the cell to progress to the next step. At the G1 phase, for example, the cell will start to transcribe genes that control cell cycle, synthesize proteins, conduct series checks and increase its size before entering into the DNA synthesis phase. At the S phase, the replication of the entire cell genome occurs.

The cell then will be prepared for division at the G2 phase by checking the size and for DNA replication errors. Later on, the nuclear envelop breaks down, the chromatin is condensed, and the DNA is separated into two diploid daughter cells at the M phase. After the completion of the cell cycle, the cell may choose one of two fates. The cell either goes again to the G1 phase and on to another round in the cell cycle or will remain at G0 phase in which the cell will be in quiescent (Tan, Duncan, & Slawson, 2017) (Fig.2).

Mitosis occurs in somatic cells mainly, while the process of meiosis occurs only in reproductive cells. The main goal for this reduction division, or in another word meiosis, is to produce haploid cell gametes. A gamete in the male is sperm and in the female is an oocyte. These gametes combine during the fertilization process and form a diploid cell. The process of gamete formation in the male is called Spermatogenesis, while in the female it is called Oogenesis. In general, gametogenesis is composed of Meiosis I and Meiosis II, which represent the two rounds of cell cycles that are involved in this processing. Meiosis I is the first round, and it involves homologous chromosome pairing, crossing over of chromosomes and separation of homologous chromosomes. In contrast, Meiosis II involves a separation of sister chromatids. Unlike the process of mitosis, the end product for meiosis is four genetically different daughter cells (Ohkura, 2015).

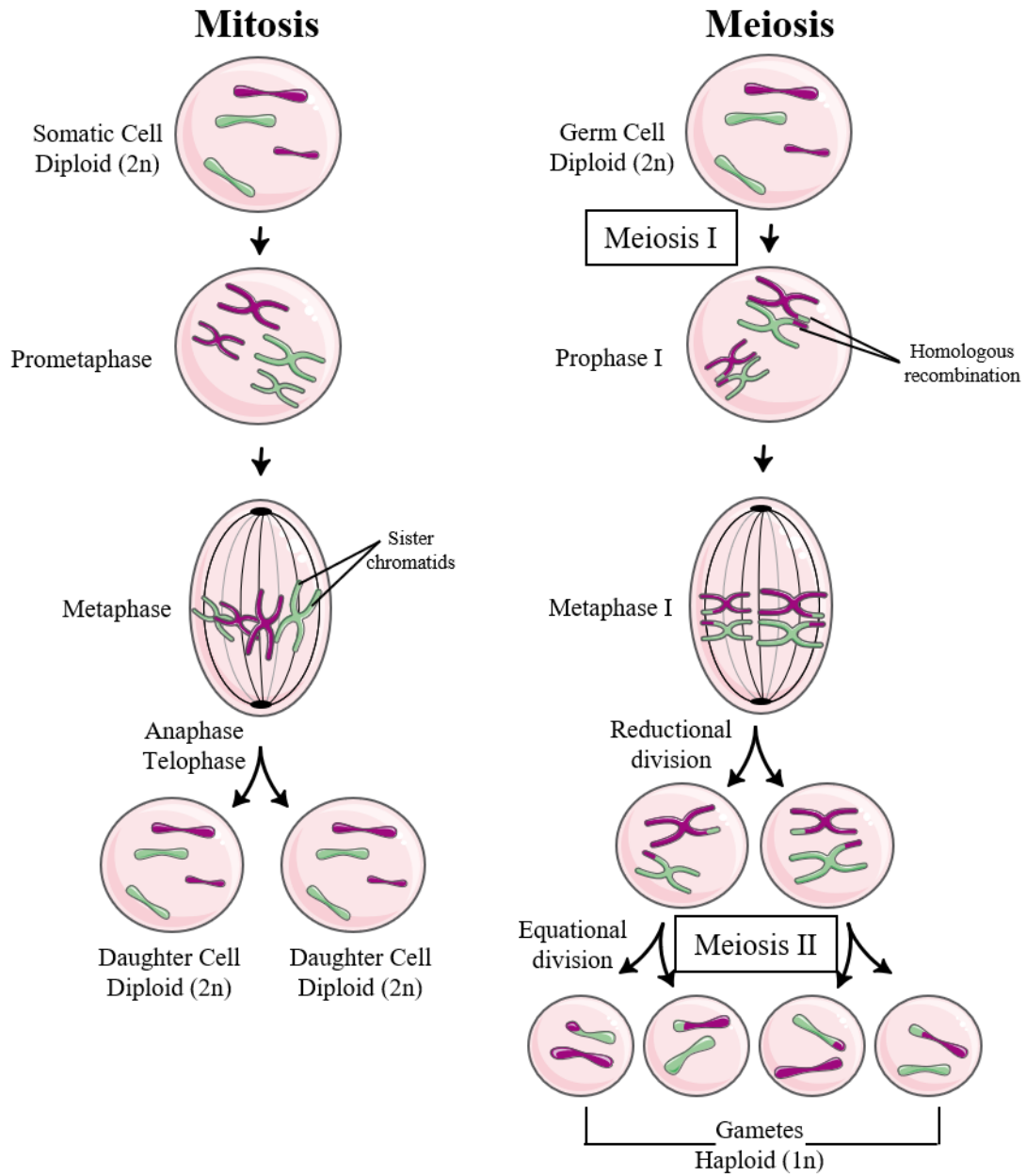


Figure 1. The difference between Mitosis and Meiosis. Mitosis occurs in somatic cells mainly and gives two diploid ($2n$) daughter cells. In contrast, meiosis occurs in gametes and provides four haploid cells ($1n$).

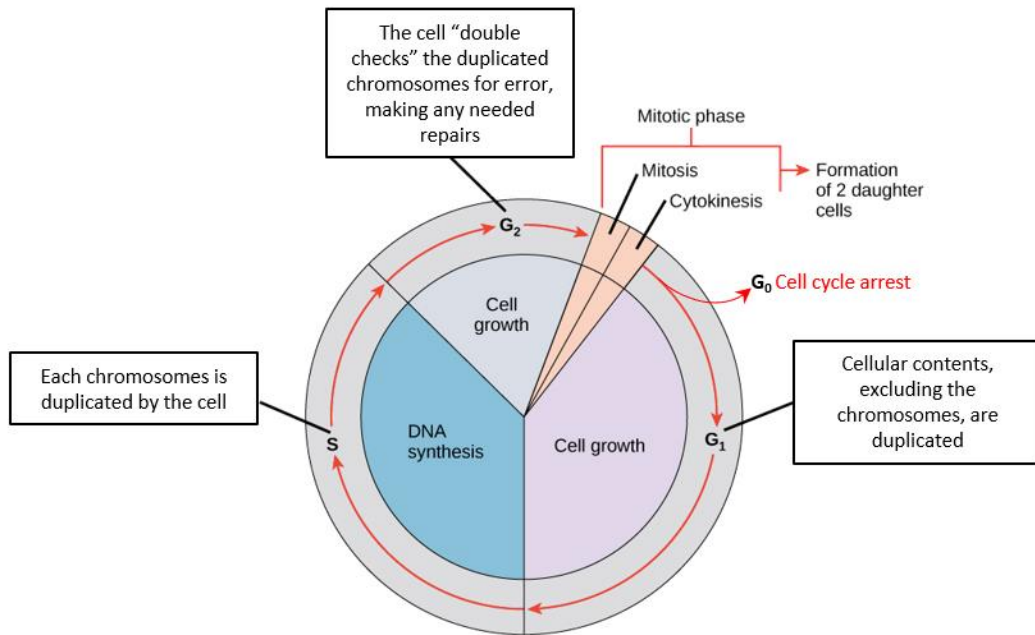


Figure 2. Phases of the cell cycle in somatic cells. Interphase is divided into G₁, S, and G₂ phases. The M phase is started with the cell entering into mitosis.

1.2 Oogenesis

The female reproductive system is composed of external and internal sex organs. The function of the external sex organs is varied between helping the sperm to enter the body, protecting the internal organs, and providing sexual stimulus. Alternatively, the primary functions of the internal organs are to produce oocytes in the ovaries, help the sperm to meet an egg within the fallopian tube and provide an accommodating environment for the fertilized embryo in the uterus (McGee & Hsueh, 2000) (Fig.3). The ovary is also an endocrine gland. Besides its role in producing eggs, the ovary has secretes hormones that are essential for follicular development and the estrous cycle (Hirshfield, 1991).

The process of mammalian oogenesis starts early in fetal life. The oogonia, which are the primordial germ cells in the female, start to grow in number by mitotic division. Before birth, these oogonia differentiate into primary oocytes surrounded by granulosa cells. The oocytes and the first single layer of granulosa cells are called primordial follicles. The oocytes at this stage are arrested by the prophase stage of Meiosis I and encapsulated within the primordial follicular cells. In mouse ovaries, there is a pool of 8000 arrested oocytes. Just for selected oocytes, the growth of follicular cells around the oocyte will occur in preparation for ovulation. Some follicles start to grow around the oocytes to form secondary follicles. This growth will continue sometime further to form a pre-ovulatory follicle, or Graafian follicle, which is the last stage of the maturing follicle. The oocyte in the Graafian follicle are surrounded by 2-3 layers of granulosa cells, also called a cumulous mass. The cumulus mass oocytes complex (COC) is connected by Gap

junctions, and the cavity of the follicle is filled with fluid. The oocytes in the Graafian follicle become meiotically competent, and the resumption of meiosis occurs before ovulation. The most important sign for the meiotic resumption is the germinal vesicle breakdown (GVBD) also known as nuclear envelope breakdown (Bachvarova, 1985; Jones, 2004; Mehlmann, 2005) (Fig.4).

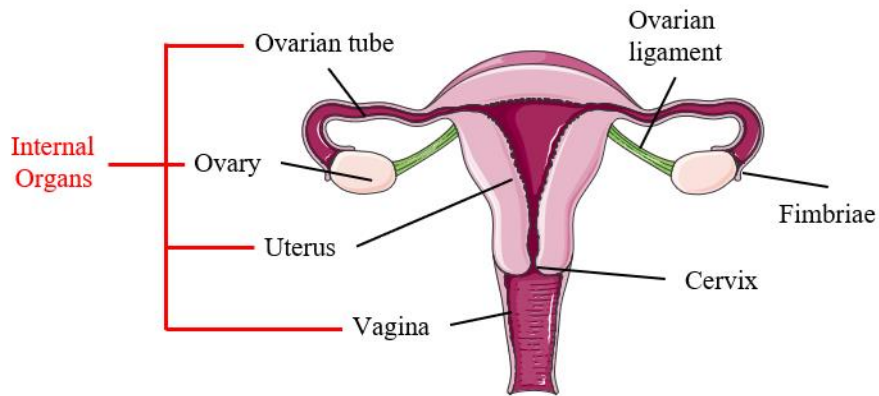


Figure 3. Structure of the female reproductive system. The female reproductive system is composed of internal and external organs. The primary function for the internal organs is to produce oocytes, help in fertilization and embryogenesis. In contrast, the external organs play a role in protecting the internal organs and providing sexual stimulus.

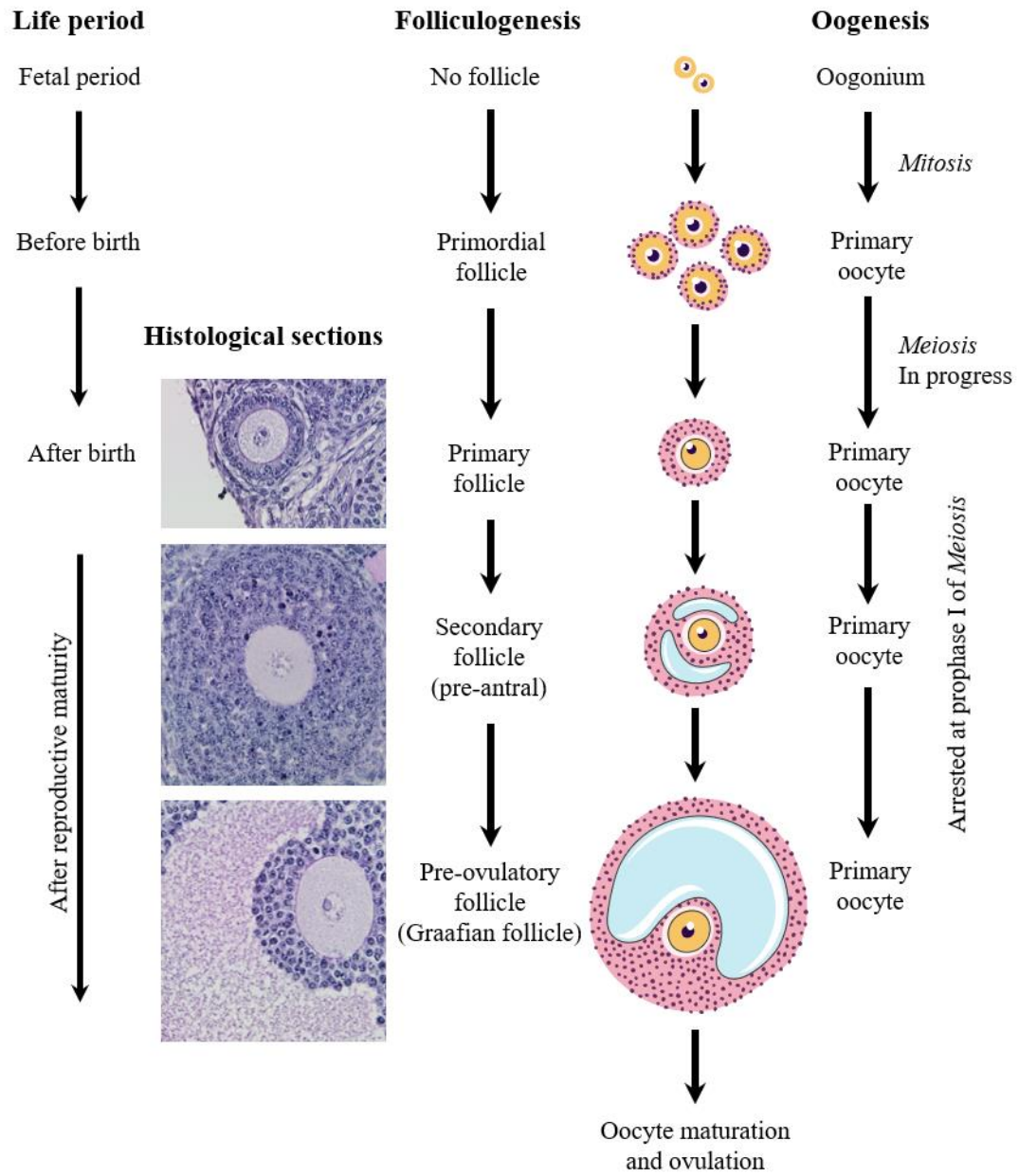


Figure 4. Oogenesis and folliculogenesis. The oogonium undergoes mitosis and then differentiates into a primary oocyte. Later on, the primordial follicle cells wrap the arrested oocyte. The follicle cells then continue the differentiation process and develop into primary follicles after the birth of the female. Once the female reaches maturity, some follicles will continue to enlarge and develop into a secondary and subsequently tertiary (Graafian) follicle.

Meiotic Arrest and Oocyte Maturation in Mammals

Meiosis is the process of making haploid gametes from diploid cells and is essential for sexual reproduction in mammals. In males, meiosis is completed, and the four products of meiosis each differentiate into sperm cells. In females, only one cell of the four products of meiosis becomes an oocyte and meiosis is arrested at two distinct points. The primary oocyte, or immature oocyte, is arrested at prophase I of meiosis after DNA replication and homologous recombination. During this long period of arrest, the oocytes grow in size and start to accumulate the proteins and RNA transcripts that are necessary for oocyte maturation, fertilization, and pre-implantation development. In mammals, a surge in luteinizing hormone (LH) or removal of the oocyte from the follicle releases the cell from meiotic arrest. The nuclear envelope, or germinal vesicle, breaks down (GVBD) and the oocyte completes Meiosis I, to form the first polar body and continues to metaphase of Meiosis II when the cell is arrested for a second time. Fertilization of the mature egg triggers release from meiotic arrest and meiosis is completed (Jones, 2004; Mehlmann, 2005) (Fig.5).

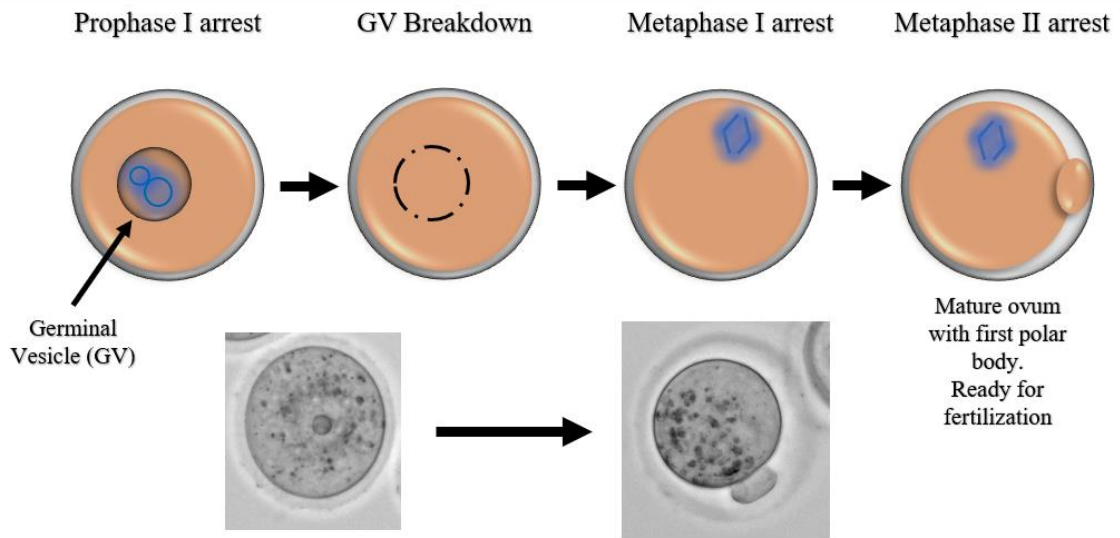


Figure 5. The oocyte maturation process of mammalian oocyte. The surge in LH or the removal of the oocyte from the follicle releases the cell from meiotic arrest causing germinal vesicle breakdown (GVBD). Completing Meiosis I produces the first polar body and the cell continues to metaphase of Meiosis II producing a mature egg (ovum). After this maturation, the cell is arrested again at metaphase.

Prophase I meiotic arrest is associated with the inactivated state of the complex of Cyclin-Dependent Kinase 1 (CDK1) and cyclin B, known as Maturation Promoting Factor (MPF) (Adhikari & Liu, 2014; Bury, Coelho, & Glover, 2016; Ohkura, 2015). CDK1, which is the catalytic subunit of MPF, must bind to cyclin to be active; however, it is maintained in the inactive state by phosphorylation by WEE2. WEE2 is activated by Protein Kinase A in the presence of cyclic AMP (cAMP) (Conti *et al.*, 2002; Duckworth *et al.*, 2002; Mehlmann, 2005; Schindler, 2011). Within the oocyte, cAMP is maintained at a relatively high concentration by a constitutively active G-protein-linked receptor, the GS protein, and activation of adenylyl cyclase (Mehlmann, 2005; Mehlmann *et al.*, 2004). The phosphodiesterase, which would normally inactivate cAMP (converting it to 5'AMP), is inhibited by cyclic GMP (cGMP) entering from cumulus cells connected to the oocyte through gap junctions (Mehlmann, Jones, & Jaffe, 2002; Shuhaibar *et al.*, 2015).

Protein kinase A (PKA), the cAMP-dependent kinase, plays a dual role in oocyte arrest. The first role for this kinase is to activate the WEE2 by phosphorylation on residue S15. Activating WEE2 will ensure arrest by its inhibitory mechanism on CDK1 (Figure 6). The second role is phosphorylation of CDC25B (Pirino, Wesco, & Donovan, 2009; Seung, Chen, Paronetto, & Conti, 2005) to prevent nuclear accumulation and inhibit its dephosphorylation activity on CDK1. The phosphorylation of CDC25B enhances its interaction with tyrosine 3-monooxygenase/tryptophan 5-monooxygenase activation (YWHA) proteins, also known as 14-3-3 (Oh, Han, & Conti, 2010; Zhang *et al.*, 2008).

Indeed, it is thought that CDC25B is maintained in an inactive state by binding with 14-3-3.

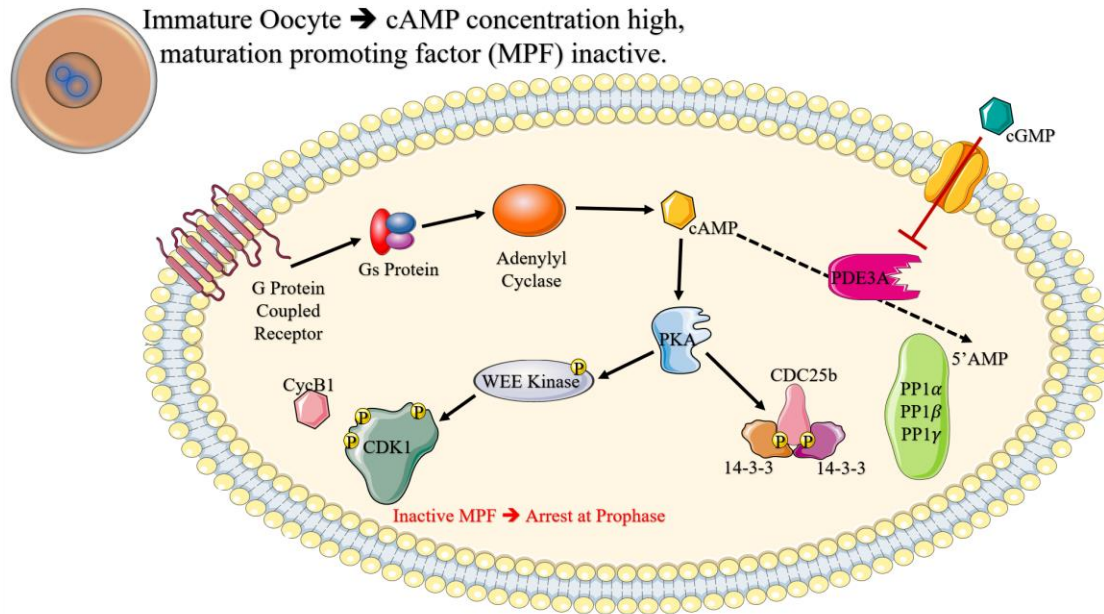


Figure 6. The signaling pathway for the prophase I arrested oocyte. High cAMP is produced through the G-protein coupled receptor. Activation of PKA induces the activity of WEE2 kinase. WEE2 kinase then inhibits the MPF (CDK1+CyclinB1), which causes oocyte arrest. PKA also inhibits CDC25B activity. PDE3A inhibition prevents cyclic AMP degradation. The dotted line represents an inactive pathway.

Within the ovary, some oocytes will resume meiosis in response to the LH surges that begin after puberty. The LH acts not on the oocyte, but on granulosa cells of large follicles. LH acts via a G-protein-linked pathway to inactivate guanylyl cyclase in these somatic cells of the follicle and, as a result, the high level of cGMP within the entire follicle and cumulus cells adjacent to the oocyte decreases and cGMP diffuses out of the oocyte relieving the inhibition of phosphodiesterase PDE3A within the oocyte (Shuhaibar *et al.*, 2015) (Figure 7). This mechanism is supported by the observation that the absence of PD3A in a genetically modified mouse prevents the normal resumption of Meiosis as cAMP and is not reduced in concentration even as LH is elevated (Masciarelli, Horner, & Liu, 2004). Thus, the LH surge decreases cGMP levels in the follicle and cAMP levels in the oocyte, leading to a reduction in the PKA activity in a selected follicle. CDC25B then becomes active and dephosphorylates CDK1. This dephosphorylation, in addition to the reduction of WEE2 phosphorylation, will activate the MPF. Activation of MPF then induces meiotic resumption, and subsequently germinal vesicle breakdown. In all mammals, removing the oocyte from the follicle manually triggers oocyte maturation. This is due to the reduction of the high concentration of cGMP that was surrounding the oocyte within the follicle. Adding a membrane-permeable cAMP or a PDE3A inhibitor to the culture medium will mimic the meiotic arrest *in vitro* (Conti *et al.*, 2002; Dekel & Beers, 1978).

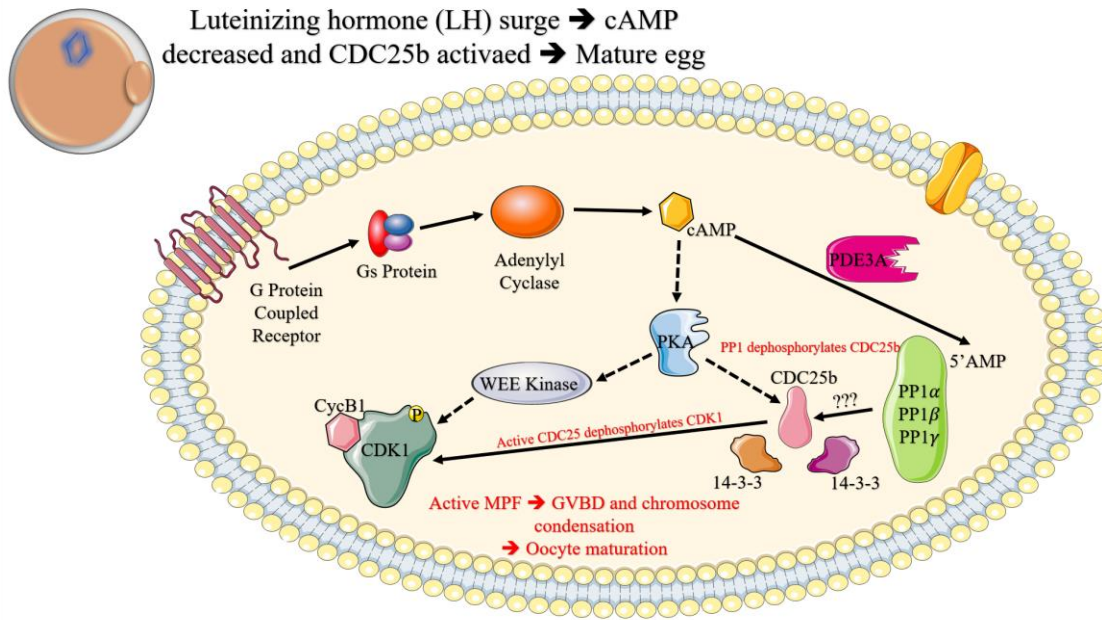


Figure 7. The signaling pathway for oocyte maturation initiated by LH. An increase in luteinizing hormone increases the concentration of PDE3A, which is accountable for breaking down cAMP. Lower cAMP level decreases PKA activity, thus enabling the oocyte to resume meiosis. The dotted represents an inactive pathway.

In mammals, CDC25, also known as a CDK activating phosphatase, is expressed as three different isoforms A, B, and C. Members of this family are known to be required for transition in the M phase in both mitosis and meiosis (Kim, Fernandes, & Lee, 2016; Mochida & Hunt, 2012). CDC25B is apparently the only isoform that is needed for the resumption of meiosis (Lincoln *et al.*, 2002). Absence of CDC25B in female mice leads to sterility due to the inability of those oocytes to resume meiosis. While CDC25A and CDC25B are present in the oocyte, there is no clear role for CDC25C, and there is no indication of the ability for these other isoforms of CDC25A and CDC25C to substitute for CDC25B loss. CDC25A may play a role in oocyte maturation and can release cells from meiotic arrest if overexpressed; however, the role of this isoform is not completely defined (Solc *et al.*, 2009).

CDC25B is localized in the cytoplasm of arrested oocytes. This cytoplasmic localization depends on PKA activity (Duckworth *et al.*, 2002; Oh *et al.*, 2010). In somatic cells, phosphorylated CDC25B is thought to be bound to the regulatory protein 14-3-3 that sequesters this phosphatase in the oocyte cytoplasm (Forrest & Gabrielli, 2001; Rebelo, Santos, Martins, da Cruz e Silva, & da Cruz e Silva, 2015). Moreover, human CDC25B in somatic cells expresses a high-affinity binding site for 14-3-3 eta and 14-3-3 zeta (Rie Mils *et al.*, 2000). CDC25B is thought to be activated by dephosphorylation by Protein Phosphatase 1 (PP1) and/or Protein Phosphatase 2 (PP2) and released from a complex with 14-3-3. PP1 and PP2A were previously shown to be present in mouse oocytes (Smith, Sadhu, Mathies, & Wolf, 1998). However, the specific phosphatase involved in dephosphorylating of CDC25B in oocytes is not entirely known.

The oocyte is known to be a specialized cell since it can store and flourish RNA and proteins to the embryo until early development. The nuclear materials and the cytoplasm of the oocytes undergo maturation during oogenesis that includes storage of maternal mRNA, proteins, and nutrients to help and support the embryonic development. During folliculogenesis, the transcription process for the oocytes will continue. This transcription will stop when the oocytes become fully grown. At this point and until the formation of the zygote, the oocytes will be dependent on the stored mRNA and proteins (Bell, Calder, & Watson, 2008). The beginning of embryonic transcription is varied among the mammalian species. In mice, the embryos start the transcription as early as the 2-cell stage. Pig and human embryos start transcription between the 4 and 8 cell stages while sheep and bovine embryos start later between stage 8 and the 16 cell stage (Li, Lu, & Dean, 2013) (Figure 8).

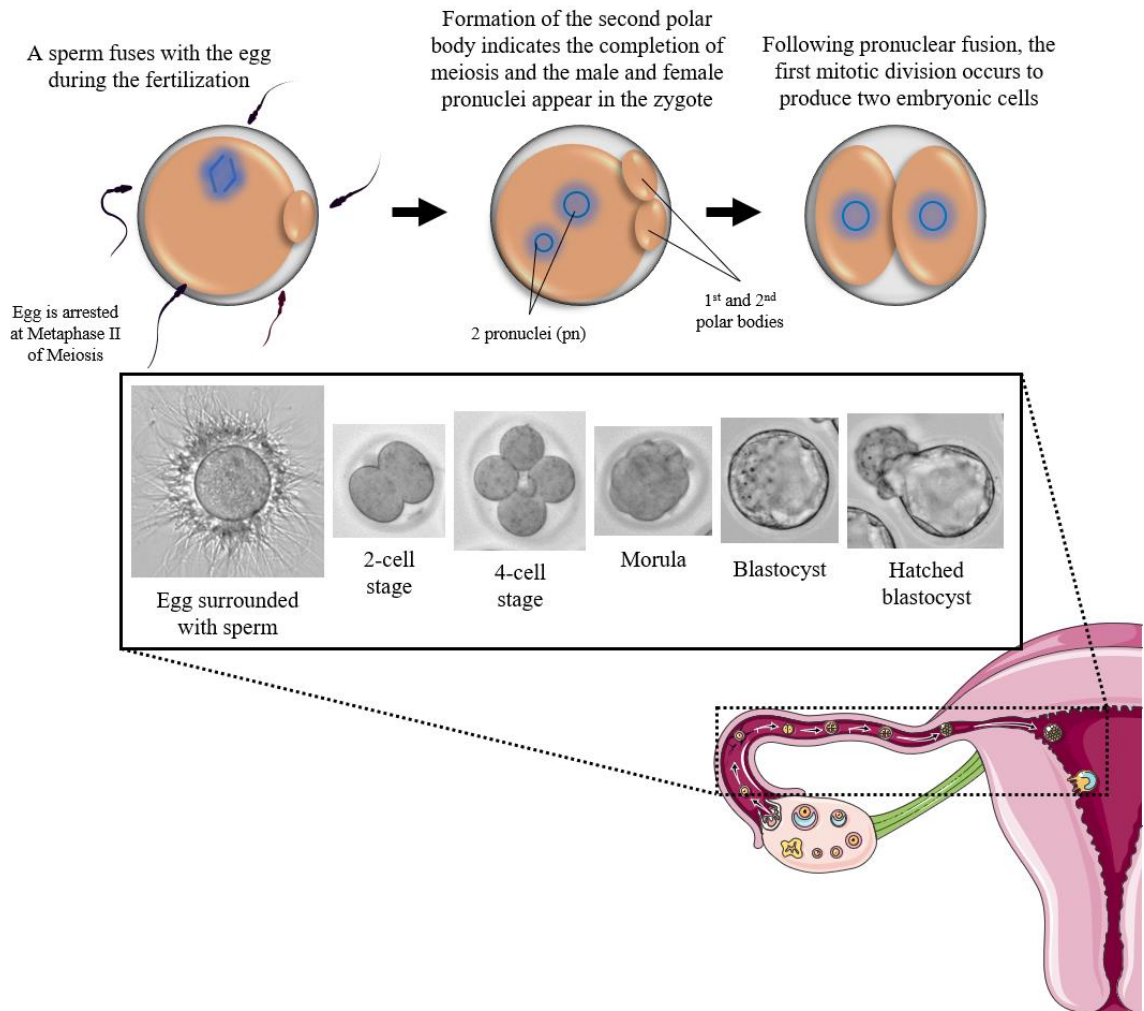


Figure 8. Embryonic development. Fertilization of the egg at the fallopian tube triggers release from the second meiotic arrest. Early embryonic development is dependent on stored maternal mRNA, proteins, and nutrients from oogenesis. Embryonic transcription in mice starts at the 2-cell stage. Embryonic development continues by mitotic cell division to produce the blastocyst, which implants in the uterus.

1.3 Spermatogenesis

The male reproductive system is composed of internal (testis, epididymis, vas deferens, and accessory glands) and external (penis and scrotum) organs. The testis in the male produces sperm and androgen hormones. *Tunica albuginea* is a fibrous tissue that encloses the seminiferous tubules. Inside the seminiferous tubules, the production of sperm from germ cells occurs by the process of spermatogenesis (Jacob & Jacob, 2012) (Figure 9).

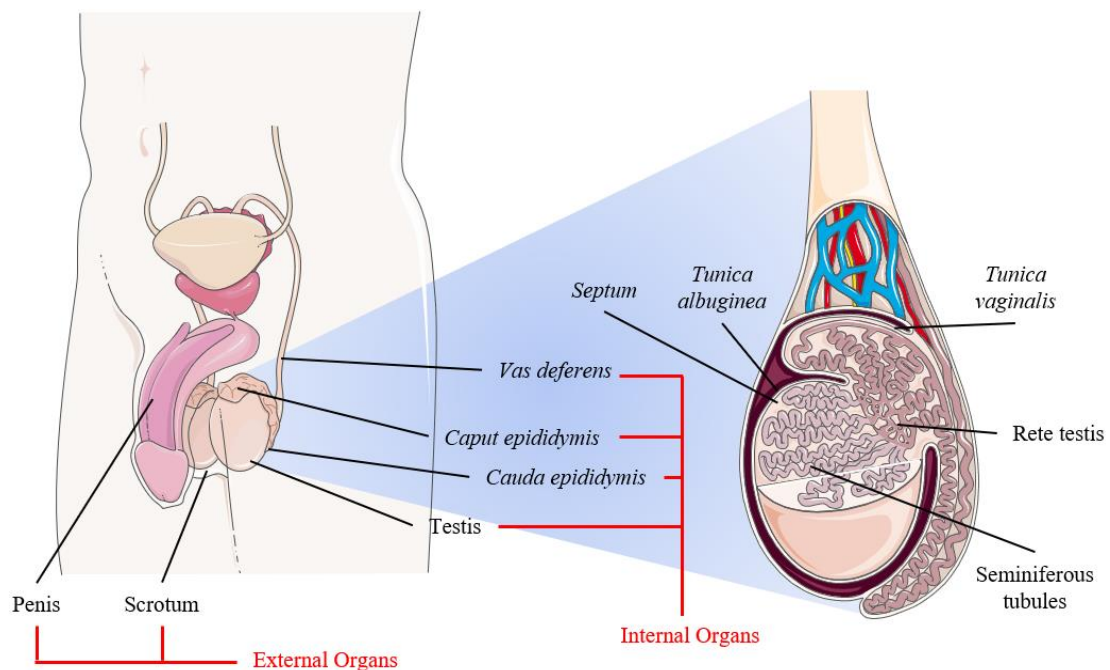


Figure 9. Structure of the male reproductive system. The male reproductive system is composed of internal and external organs. The primary function for the internal organs is to produce sperm and hormones, while the primary purpose of the external organs is to protect the testes and deliver the sperm into the female reproductive tract.

The cells inside the testis consist of Leydig cells, Sertoli cell, germ cells, and peritubular myoid cells. The peritubular myoid cells have an important role in giving structural support to the seminiferous tubules (Maekawa, Kamimura, & Nagano, 1996). Outside the seminiferous tubules, the Leydig cells are located. The main function for this type of cell is to produce the hormone testosterone, which is essential for spermatogenesis and male sexual development (Shima *et al.*, 2013). Two main cells are located in the seminiferous tubules, the Sertoli cells and germ cells. The germ cells are important in making and producing sperm while the Sertoli cells aid the sperm development during spermatogenesis. The Sertoli cells also help by absorbing the extra cytoplasm from mature sperm at the spermiation stage. The adjacent Sertoli cells have an important role in preventing an auto-immune reaction, this occurs by blocking the antibodies from the blood from entering into the seminiferous tubules, by forming the blood-testis barrier (Griswold, 1995; Wright, Musto, Mather, & Bardin, 1981) (Figure 10).

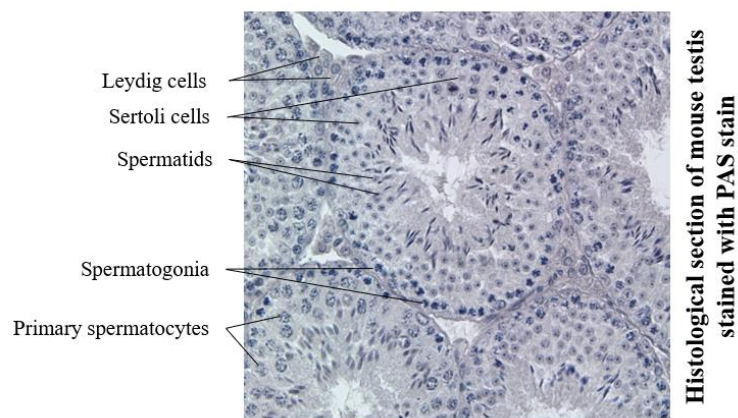


Figure 10. Seminiferous tubule. Cross-section of mouse testis shows the somatic and different stages of germ cells in and around the seminiferous tubules.

Spermatogenesis is one of the most complex biological processes because it is composed of mitotic, meiotic and, differentiation phases. It involves the production of a highly specialized cell, the spermatozoan. In the early stages of male fetal life, the developing testis prepares a pool of spermatogenic stem cells that are produced by rounds of mitotic divisions. At the onset of puberty, and under the control of gonadotropins, spermatogenesis begins with the differentiation of spermatogonia into spermatocytes, which then undergo meiosis to generate haploid spermatids.

Morphogenesis of spermatids yields structurally mature spermatozoa which are released into the lumen of the seminiferous tubules, then stored in the epididymis where further maturation and motility initiation occurs. This transitional journey involves dramatic changes in the transcriptional profile of germ cells which occurs at two stages. The first at the beginning of meiosis, where many genes involved in cell cycle regulation and cell division are upregulated. The second stage takes place in post-meiotic cells during morphogenesis of spermatids. This stage involves the expression of many testis-specific genes and testis-specific variants of ubiquitously expressed genes. Later, testicular spermatozoa become transcriptionally inactive due to chromatin condensation, leaving post-translational modifications of proteins the main regulatory mechanism of cellular processes (Cheng, Pilder, Nairn, Ramdas, & Vijayaraghavan, 2009).

After the Spermiation, which is the process of releasing the sperm from the Sertoli cells, the sperm then travel from the seminiferous tubules into the epididymis to mature and through the rete testis and efferent ducts. The mature sperm will later be ready to ejaculate after leaving the epididymis by the vas deferens (Jacob & Jacob, 2012).

The Mitotic Phase

The germ cells are first divided into type A spermatogonia when they reach the gonads. The type A spermatogonia then settle in the basal lamina of the tubular epithelium. This type A spermatogonium is an undifferentiated stem cell that can undergo mitosis to raise other intermediate cells that can differentiate later into type B spermatogonia. Four different phases for type A spermatogonia (A1 - A4) were identified in rodents. Type A1 sequentially divide into A2, A3, and A4. Type A1-4 populations are self-renewing cells which allows this population be maintained in testis. The type A4 spermatogonia face one of three fates in the testis. This type of cell can differentiate into intermediate cells, proliferate and produce more type A1 or undergo apoptosis. The mechanism behind the differentiation of type A1 is still unknown. After the differentiation of type A4 spermatogonia to intermediate cells, these cells will undergo mitotic division to make type B spermatogonia. Type B spermatogonia will undergo one last mitotic division to make primary spermatocytes which undergo Meiosis. Cytokinesis will never occur during all of these divisions. The cells are connected to each other by cytoplasmic bridges (Dym & Fawcett, 1971; Gilbert & Barresi, 2017).

The Meiotic Phase

The primary spermatocyte, which is the largest spermatogenic cell type, is located in the midway of the seminiferous tubules. Primary spermatocytes eventually undergo Meiosis I to produce two secondary spermatocytes. Each secondary spermatocyte, after completion of Meiosis II, will give rise to two haploid spermatids. These spermatids will

remain connected by the cytoplasmic bridge that helps in gene diffusion between neighboring cells (Gilbert & Barresi, 2017; Neill et al., 2006).

The Differentiation Phase

This phase is also called spermiogenesis. Each haploid spermatid is developed and matures into a spermatozoon. During this stage, several changes will occur to the sperm shape that would help the sperm later with fertilization. These changes include acrosomal formation, chromatin condensation, mitochondrial arrangement, Tail growth and removal of cytoplasmic material by Sertoli cells (Neill *et al.*, 2006) (Figure 11).

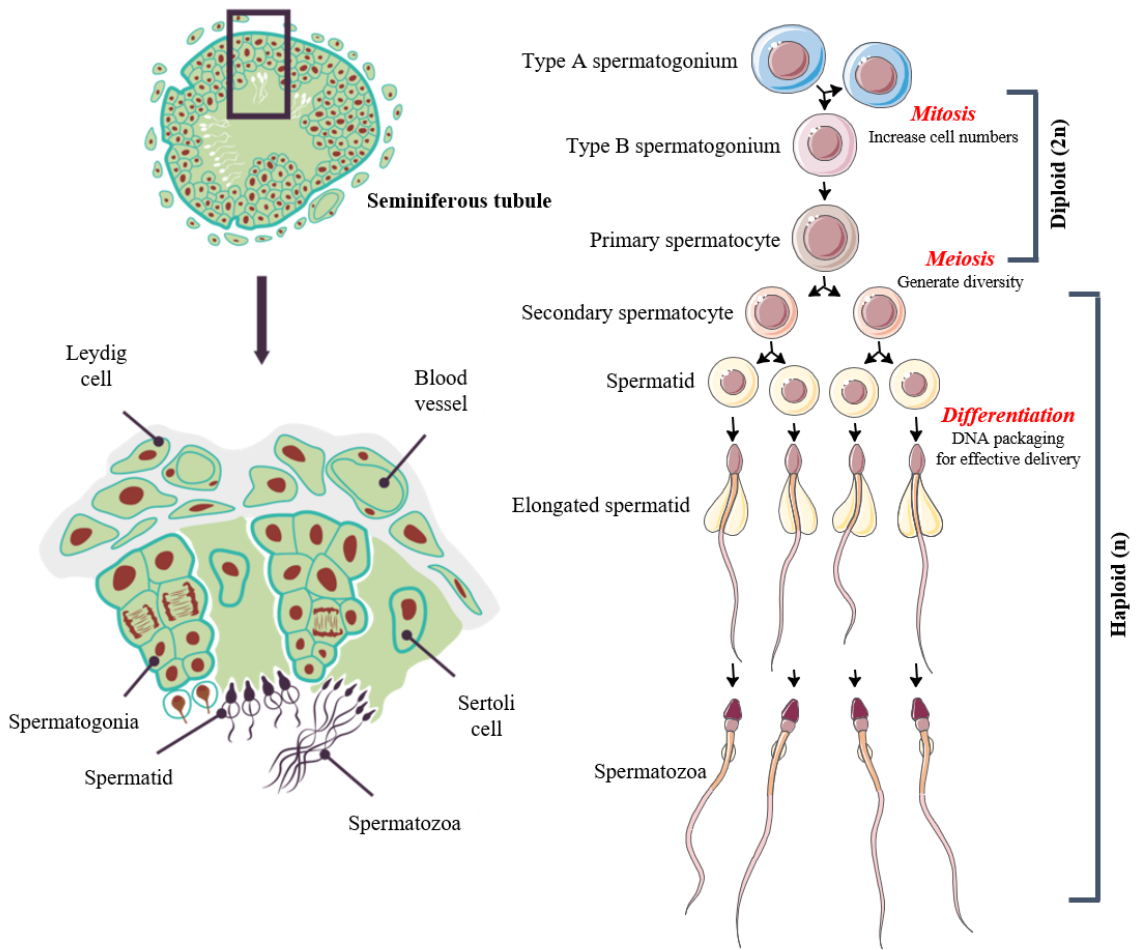


Figure 11. Stages of spermatogenesis. Diagrammatic cross-section of seminiferous tubule illustrating different phases of spermatogenesis. The spermatogonium goes through mitosis, meiosis and differentiation phases to give four sperm at the end.

The regulation of Spermatogenesis

The proteins that are essential to spermatogenesis are continually produced during different stages of spermatogenesis. These proteins are involved in meiosis, acrosome formation, nuclear chromatin condensation, tail formation *etc.* The genes that are responsible for these proteins are regulated by extrinsic, interactive and intrinsic factors.

Extrinsic Factors (Hormonal)

Spermatogenesis is regulated hormonally by the hypothalamic-pituitary-gonadal (HPG) axis. Gonadotropin-Releasing Hormone (GnRH) is produced by the GnRH expressing neuron in the hypothalamus. The GnRH passes through the hypophyseal portal system and travels down to the anterior part of the pituitary gland. In response to the GnRH, the secretory cells of the adenohypophysis produce LH and FSH, which travel into the bloodstream. Leydig cells in the testis produce testosterone and androgens under LH influence. FSH with testosterone binds to Sertoli cellular receptors to boost multiple functions such as hormonal synthesis (estrogen and inhibin), meiosis and sperm maturation. Secretion of inhibin, estrogen, and testosterone have negative feedback on gonadotropic hormone production (Walker & Cheng, 2005) (Figure 12).

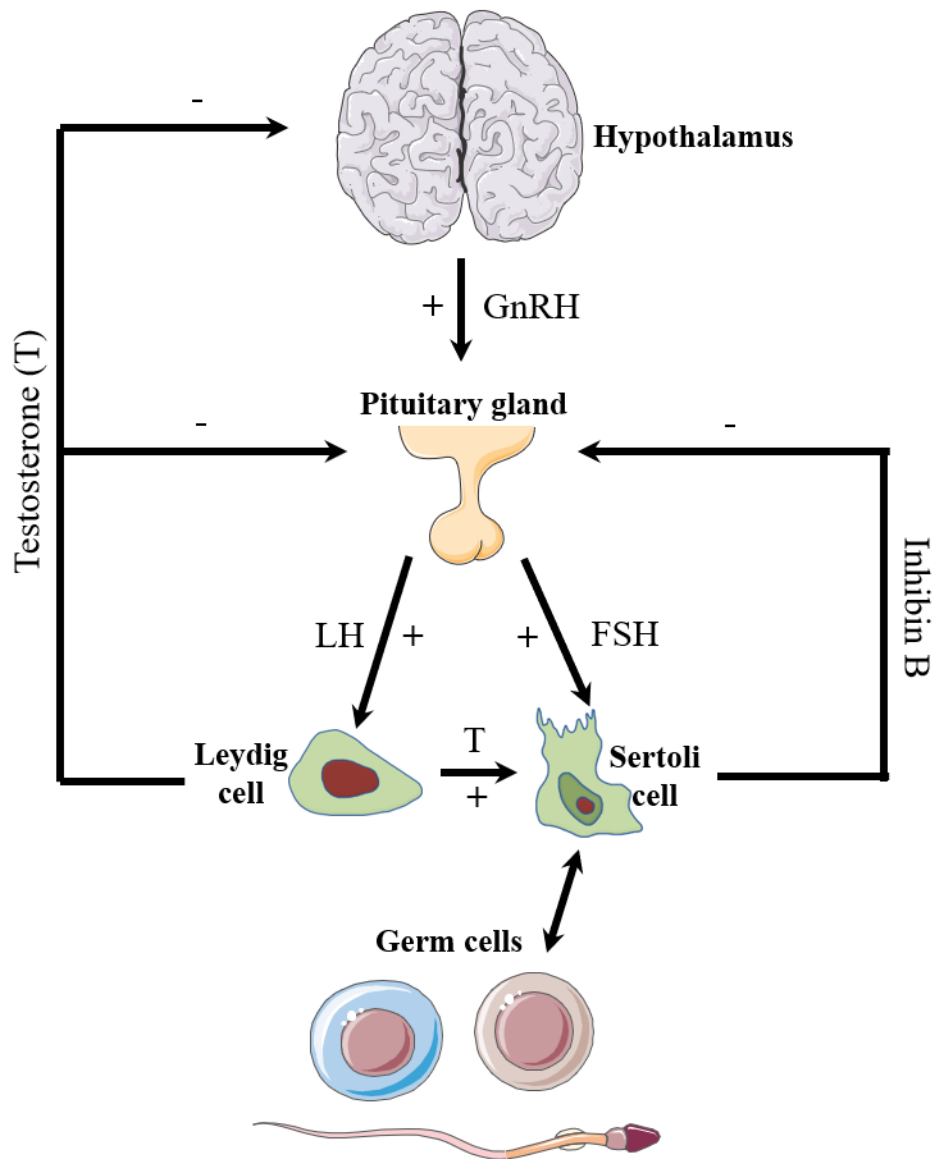


Figure 12. The hypothalamus pituitary gonadal axis. Follicle-stimulating hormone (FSH) and luteinizing hormone (LH) are stimulated by the pituitary (GnRH). LH stimulates the production of testosterone (T) by Leydig cells. FSH and testosterone directly stimulate the activity of Sertoli cells, which in turn controls the growth of germ cells. GnRH is controlled by testosterone with negative feedback. The negative feedback of testosterone also controls the pituitary secretions of LH and FSH. Inhibin B is generated by Sertoli cells and causes FSH production to be selectively inhibited. Adapted from (Borg, Wolski, Gibbs, & O’Bryan, 2009).

Interactive factors

Sertoli cells play a crucial role in nurturing germ cells and regulating spermatogenesis. The gene expression pattern in Sertoli cells is believed to be changed when the germ cell progress in spermatogenesis (Griswold, 1998; Zabludoff, Charron, Decerbo, Simukova, & Wright, 2001). The interaction between the Sertoli cells and the germ cells is seen in the c-Kit transmembrane tyrosine kinase receptor and ligand. The c-kit receptor is found in the spermatogonia while the Sertoli cells produce the c-kit ligand. Mutation in the gene *Kitl* that produces the ligand will disrupt the development of germ cells (Manova, Nocka, Besmer, & Bachvarova, 1990; Rossi, Albanesi, Grimaldi, & Geremia, 1991; Yoshinaga et al., 1991).

Intrinsic factors

Differential gene expression during spermatogenesis is regulated at different levels (transcriptional, translational, and post-translational). The primary mechanism for gene expression in spermatogenesis is transcriptional regulation. The spermatogenic cells contain unique transcription factors that are upregulated during spermatogenesis, such as (HSF-2, SPRM1, OCT-2, OVOL1, CREM, etc.) (Eddy, 1998). CREM is the best-studied transcription factor in testis, and it is known to be the master controller of spermatogenesis. The CREM knockout mice are infertile due to the spermatogenesis arrest at round spermatids. In response to the upregulation for many transcription factors during spermatogenesis, the target gene expression will increase as well (Eddy, 1998; Kimmins, Kotaja, Davidson, & Sassone-Corsi, 2004). The peak expression of genes in mouse testis has been identified. The first peak occurs during the mitotic phase (0-8 days

postnatal). The second peak occurs at the onset of meiosis (around 14 days postnatal) while the third peak occurs at 20 days postnatal and during spermiogenesis (Laiho, Kotaja, Gyenesei, & Sironen, 2013). These upregulated genes can be either testis-specific or genes that are ubiquitously expressed in all tissues. The testis-specific genes can also be genes that have no somatic homologs such as (AKAP3) or genes that have somatic homologs such as (Pgk2) (Robinson, McCarrey, & Simon, 1989; Vijayaraghavan *et al.*, 1999).

Post-transcriptional regulation has two ways to regulate gene expression, and both of them occur at the mRNA level. This is either by alternative splicing of the gene or silencing the transcript with miRNA. Alternative splicing produces two or more protein isoforms for the same gene (Yeo, Holste, Kreiman, & Burge, 2004). While miRNA, on the other hand, will disrupt the mRNA by either obstructing translation of the mRNA or promoting its degradation (Ha & Kim, 2014).

This translational regulation occurs after spermatogonial cells enter the meiotic phase. During this phase, the transcriptional levels are reduced and stopped entirely with the cell progressing toward later stages of meiosis. The reason for transcriptional arrest during this phase is nuclear condensation. The DNA becomes inaccessible to transcription factors due to the tighter condensation by protamines (Eddy, 1998; Schäfer, Nayernia, Engel, & Schäfer, 1995). The translational regulation helps the germ cells at later stages of spermatogenesis to go back and synthesize essential proteins for sperm formation. This can be accomplished by keeping the transcripts in an inactive form before DNA condensation through binding them to mRNA binding protein or delaying this

translation by increasing the length of poly A tail (Iguchi, Tobias, & Hecht, 2006; M. Xu & Hecht, 2011).

Mature Sperm Structure

The spermatozoon is a highly specialized cell composed of a head and tail. The main role of sperm is to transfer the haploid male chromosome through fertilizing the female egg (Figure 13).

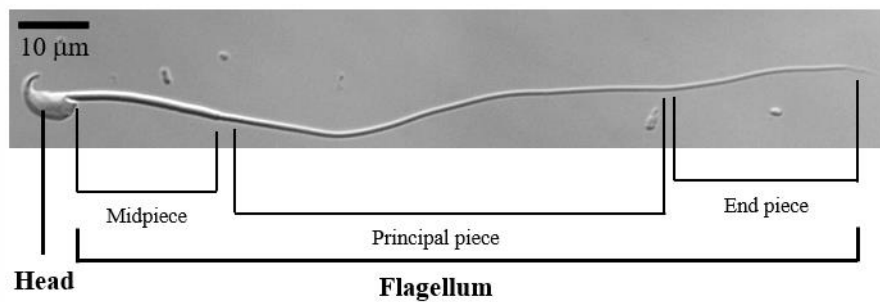


Figure 13. Sperm structure. DIC image shows the structure of mouse sperm. The sperm is composed of head and tail (flagellum). The tail is further subdivided into midpiece, principal and end pieces.

Spermatozoon head

The sperm head has different shapes among different species. For example, the human, bovine, and rabbit sperm have paddle-shaped head while the rodents have a hook-shaped head. The sperm head in different species shares the same structure, such as the presence of the nucleus, acrosome, cytoskeleton and cytoplasm. The nucleus is enclosed by the nuclear envelope which has less pores compared to somatic cells. The nucleus also has the condensed haploid male DNA (Yelick *et al.*, 1989). The major cytoskeletal components for the sperm head are actin, tubulin, and spectrin which play a role in shaping the sperm head (Neill *et al.*, 2006). The cell membrane around the sperm head is divided into acrosomal and post-acrosomal regions. The acrosomal region is further divided into the acrosomal (anterior) and equatorial (posterior) segments. The acrosome is a secretory vesicle that is made from the Golgi complex. Exocytosis of the acrosome release proteases and hydrolytic enzymes that help the sperm to penetrate the *zona pellucida* surrounding the mature egg (Buffone, Foster, & Gerton, 2008; Mack, Bhattacharyya, Joyce, Van Der Ven, & Zaneveld, 1983; Scialli, 1993) (Figure 14).

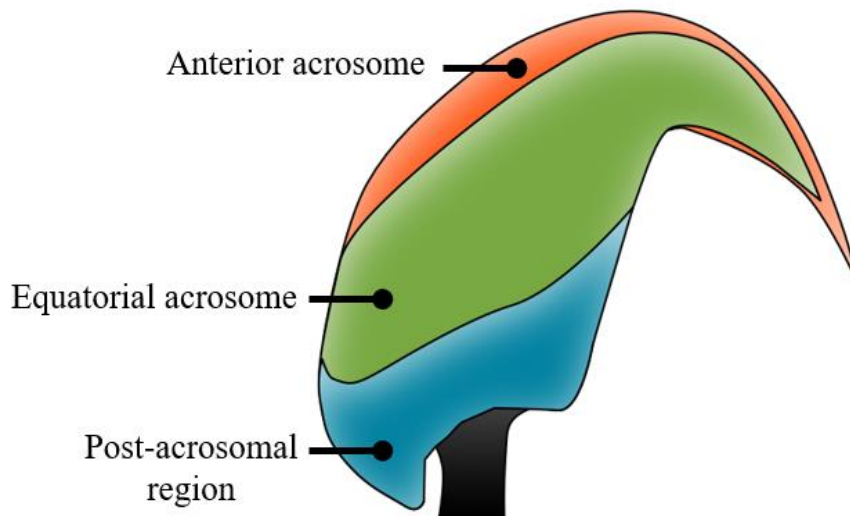


Figure 14. Mouse sperm head. The sperm head is divided into anterior acrosomal, equatorial acrosomal, and post acrosomal regions.

Sperm flagellum

The main function of the flagellum is to help with sperm movement and egg penetration. It is divided into the connecting piece, midpiece, principal piece, and end piece. The connecting piece attaches the rest of the flagella into the sperm nucleus. The axoneme is the main structural component of the flagella and is structurally similar to cilia in the oviduct, sensory organs, and trachea. The axoneme 9+2 arrangement of microtubules is conserved among the eukaryotic cilia and flagella. This arrangement is composed of nine doublet microtubules (a fused pair of tubules) each one contains a complete A-tubule and incomplete B-tubule. These nine doublet microtubules surround two central microtubules. The motor protein, dynein generates the sliding force through

ATPase activity and is responsible for cilia and flagellar motion as well as sperm motility. Midpiece of the sperm flagella are surrounded by dense outer fibers (ODF) and a mitochondrial sheath. The principle midpiece are also surrounded by ODF and a fibrous sheath (Inaba, 2003, 2011; Petersen, Füzesi, & Hoyer-Fender, 1999) (Figure 15).

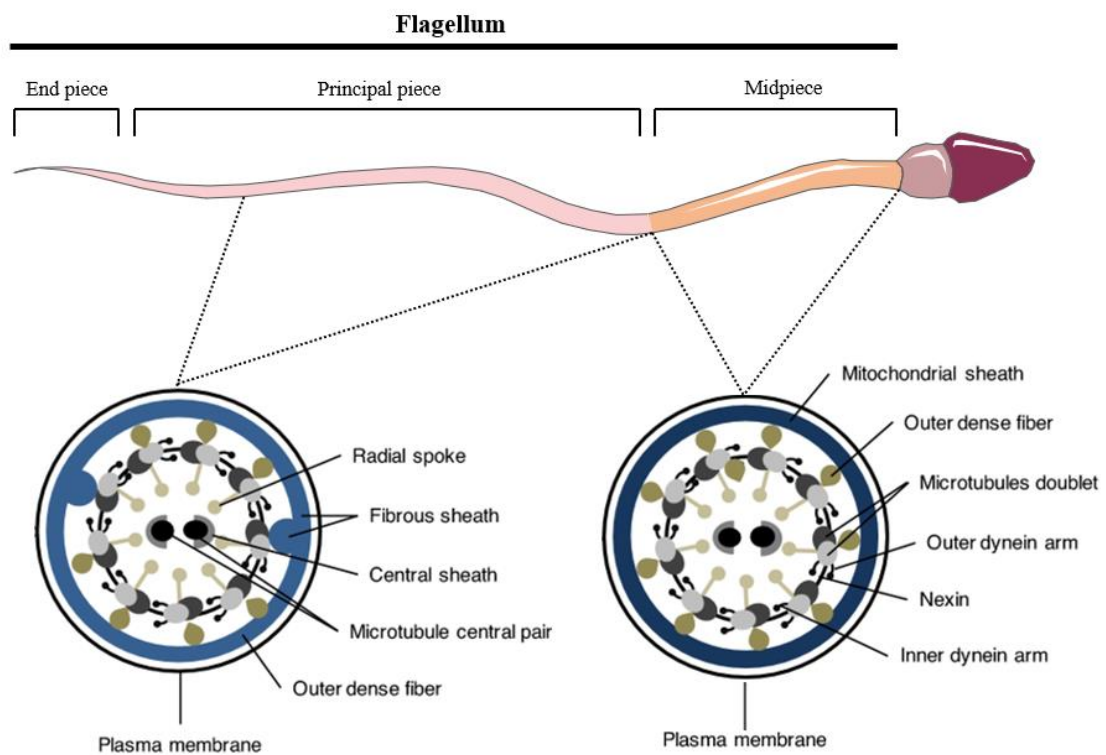


Figure 15. Sperm flagellum structure. Schematic representation of sperm shows the flagellum structure. The structure of the sperm flagellum differs between the midpiece and the principal piece. The outer dense fiber (ODF) in the midpiece is surrounded by the plasma membrane and mitochondrial sheath while the ODF in the principal piece is surrounded by the plasma membrane and fibrous sheath. The ODF in two opposing microtubules in the principal piece are replaced by longitudinal columns of the fibrous sheath. Adapted from (Freitas, Fardilha, & Vijayaraghavan, 2017).

Sperm motility

The sperm has two types of motility: progressive (symmetrical wave) and hyperactive (asymmetrical wave). The progressive motility can be defined as movement of the sperm in a straight line or in a large circle. This type of motility is gained after epididymal maturation. On the other hand, the hyperactivation motility is gained in the female reproductive tract before fertilization (Darszon, Nishigaki, Beltran, & Treviño, 2011; Zeng, Clark, & Florman, 1995) (Figure 16).

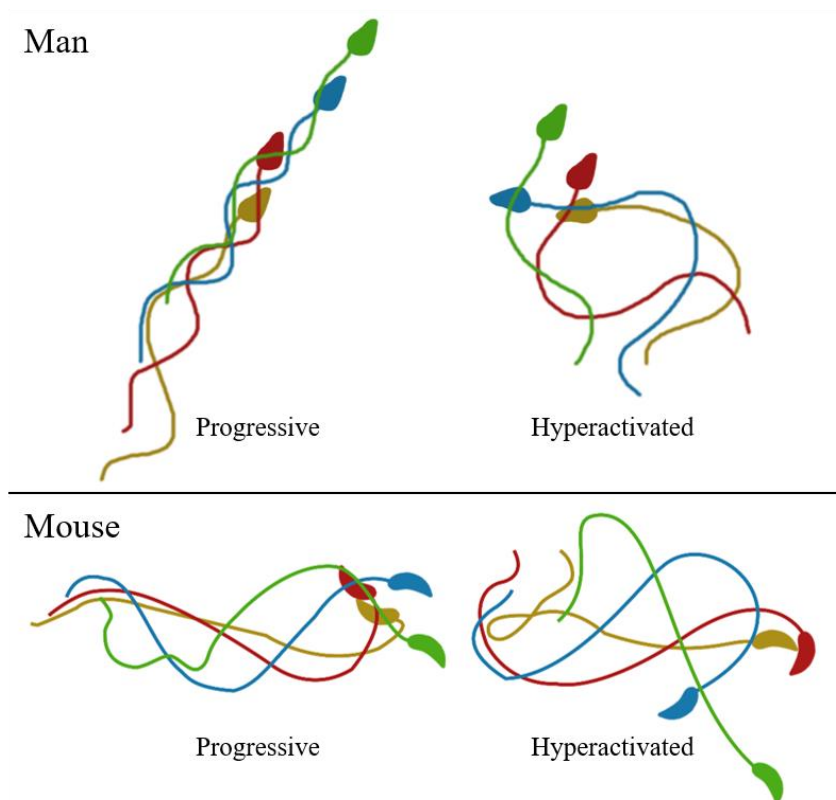


Figure 16. Progressive and hyperactivated motility in mammalian sperm. The progressive motility is observed in the uncapacitated sperm. On the other hand, the sperm incubation under capacitated conditions or sperm recovered from the oviduct results in less symmetrical flagellar bending, which is a characteristic of hyperactivated sperm. Adapted from (Plant & Zeleznik, 2014).

After spermatogenesis, the sperm are released from the seminiferous tubules into the epididymis. The epididymis is composed of three compartments: caput, corpus, and cauda. Each compartment is separated by connective tissue to provide a micro-environment which aids in sperm maturation. During transport from the caput to the cauda epididymis, the sperm gains the fertilization ability. The sperm extracted from the caput show no motility when compared to the forward motility evidenced in caudal sperm. This change in motility is acquired after reshaping of the acrosome, the disappearance of the cytoplasm droplets and certain biochemical changes. These biochemical changes, and the signaling pathways during this transition are not fully understood. The first described protein that was involved in this motility is phosphoprotein phosphatase 1 (PP1). The activity of PP1 protein specifically PP1 γ is high in the immotile caput sperm while it is inactive in the motile caudal sperm (Chakrabarti, Cheng, Puri, Soler, & Vijayaraghavan, 2007).

After ejaculation and while the sperm are traveling in the female reproductive tract, the sperm gain another style of motility during the capacitation which is called hyperactivation. The capacitation is the last step before the acrosomal reaction occurs in mammalian sperm. The capacitation is required to make the sperm competent to fertilize the egg. *In vitro*, capacitation occurs by incubating the sperm in defined media such as human tubal fluid (HTF) media for several hours. The hyperactivation motility of sperm is produced by a high beat amplitude for the sperm flagella. This style of high beat produces a movement pattern of circular trajectories (Darszon *et al.*, 2011; Zeng *et al.*, 1995). Calcium level and bicarbonate presence are the two major factors that play a role

in hyperactivation. The importance of the calcium has been seen in the *Catsper1* knockout mice. *Catsper* also known as the cation channels of sperm, is a special voltage sperm gated calcium channel found in the principle piece of the tail. *Catsper1* null mice are infertile due inability of the sperm to undergo hyperactivation. The addition of bicarbonate to the mature caudal sperm is also known to induce hyperactivation motility through activity of the SLC4A2 bicarbonate transporter. The hyperactivation is also regulated by events that involve cAMP/PKA. The cAMP activates PKA which phosphorylates Ser/Thr residues on several unidentified proteins. This change in the phosphorylation is thought to be involved in hyperactivation motility (Arnoult *et al.*, 1999; Arnoult, Zeng, & Florman, 1996).

1.4 Protein Phosphatase in gametogenesis

The reversible phosphorylation is involved in all cellular functions such as transcription, translation, cell division, metabolism, signal transduction, apoptosis, intracellular communication, migration/motility, *etc.* This process involves the addition of phosphate by protein kinase (phosphorylation) or removing the phosphate by protein phosphatase (dephosphorylation) to an existing protein. The phosphorylation of the protein can either activate or deactivate the protein by inducing conformational change in the structure. The most common site for phosphorylation is the serine residue. The phosphorylation also occurs on threonine and tyrosine residues. There are 518 protein kinases and 150 protein phosphatases encoded in the human genome. Out of 150 protein phosphatases, 107 are tyrosine phosphatases (PTP), and fewer than 40 are serine/threonine phosphatases (PSP). The PSP can be subdivided further into phosphoprotein phosphatases (PPP), metal-dependent protein phosphatases (PPM) and aspartate-based phosphatases (FCP/SCP) (Cohen, 2002; Shi, 2009).

Protein Phosphatase 1 is a member of the serine/threonine family of phosphatases. Other members include PP2A, PP2B, PP4, PP5, PP6, and PP7. PP1 isoforms function in cell cycle regulation, apoptosis, and metabolism. In eukaryotic cells, three genes encode four different isoforms of PP1 (Figure 17). The PP1 family is among the most evolutionarily conserved protein groups. Moreover, mammalian PP1 isoforms share around 90% of their amino acid sequences with each other. Their differences are only at the extreme N- and C- termini that play a role in binding to different regulatory subunits

which determine the substrate specificity and localization (Lin, Buckler, Muse, & Walker, 1999; Sasaki et al., 1990).

PPPICA, *PPPICB*, and *PPPICC* encode PP1 α , β , and γ , respectively. There are several splice variants of *PPPICA* and also of *PPPICB*; however, these are not well characterized in mice. *PPPICC* has two well characterized splice variants, known as *PPPICC1* (PP1 γ 1) and *PPPICC2* (PP1 γ 2). PP1 α and PP1 β , both along with PP1 γ 1, are ubiquitously expressed in all tissues. However, PP1 γ 2 is enriched only in meiotic and post-meiotic male germ cells (Bollen & Stalmans, 1992; Chakrabarti, Cheng, *et al.*, 2007; Kitagawa *et al.*, 1990; Mumby & Walter, 1993; Varmuza *et al.*, 1999; Wera & Hemmings, 1995).

The *PPPICC* gene consists of eight exons and seven introns. Exons 1-7 make up the coding region of PP1 γ 1, the remaining intron 7 along with exon 8 become the 3'UTR. In contrast, exons 1-6, part of exon 7, and exon eight make up the coding region of PP1 γ 2. During the splicing event to produce PP1 γ 2, part of exon 7 along with intron 7 are spliced out, and exon 8 becomes the coding sequence of the unique C-terminus tail of PP1 γ 2 (Okano, Heng, Trevisanato, Tyers, & Varmuza, 1997).

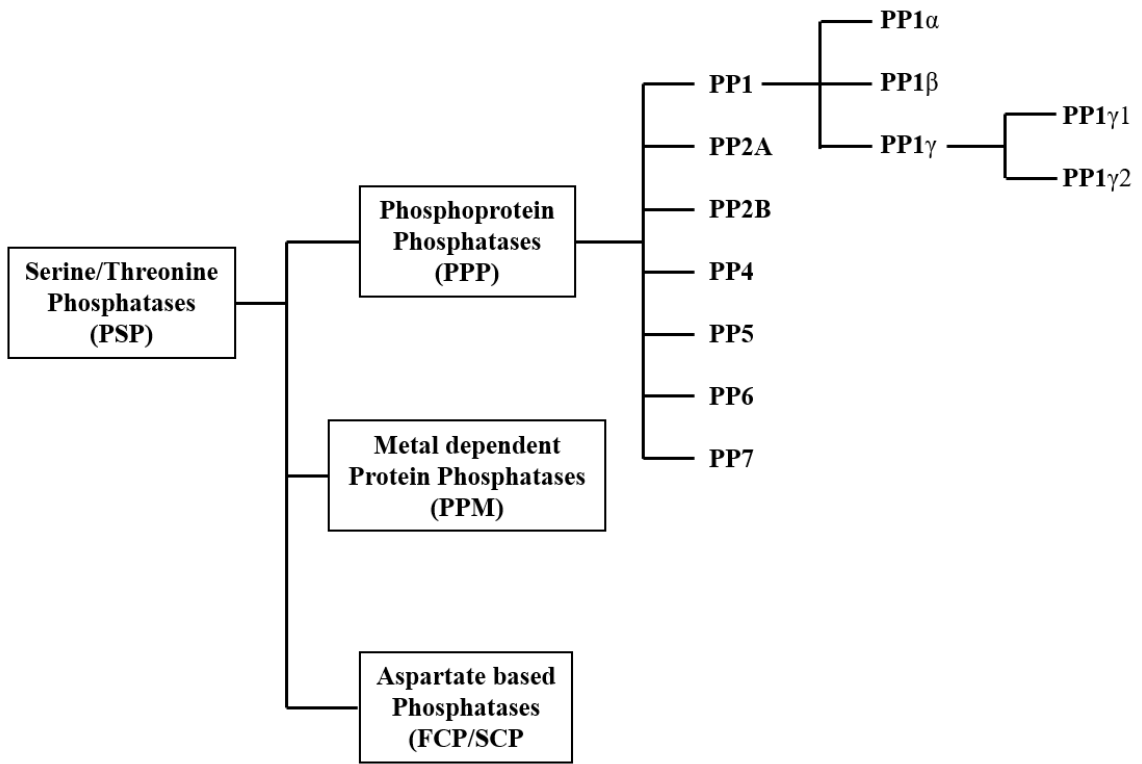


Figure 17. The family of Phosphoprotein Phosphatases (PPP). Seven different subfamilies are known (based on the human genome). All share a common catalytic subunit but are different in the extreme N and C terminal ends of the protein. PPP4, PPP5, and PPP6 are encoded by one gene, while the others are encoded by more than one gene and most all have alternatively-spliced versions.

The role of PP1 in oocyte maturation

The specific roles of PP1 and other phosphatases in oocyte maturation are not entirely defined. Evidence, mostly from inhibitor studies, with some more recent manipulations of the genes, suggests the dephosphorylation of proteins by these phosphatases is necessary at several unique steps in meiosis. For example, a recent study indicates the elimination of both isoforms of PP2A in the mouse oocytes has no effect on the growth of oocytes in ovarian follicles, or in the initial resumption of meiosis induced by hormones, suggesting that PP2A is not a potential candidate for the resumption of meiosis in prophase I arrested oocytes. However, oocytes lacking the two isoforms of PP2A failed to complete Meiosis I correctly due to chromosome misalignment and abnormal spindle assembly resulting in infertility (Tang *et al.*, 2016).

PP1 is known to be inhibited by heat-stable inhibitors such as I-1 and I-2. In addition, Okadaic acid (OA) is a toxin that has been used to study the role of PP1 and PP2A in the oocyte. OA is used to inhibit PP1, PP2A, PP4, PP5, and PP7 activity at different concentrations (Swingle, Ni, & Honkanen, 2007).

Various studies on the role of PP1 are complicated by the experimental design in which inhibitors are used that may have nonspecific effects or by experimental designs in which MPF is at least partially inhibited to study downstream events. For example PP1 activity is implicated in maintaining the integrity of the nuclear envelope in germinal vesicle-intact oocytes since treatment with the PPI inhibitor have a greater rate of GVBD (Smith *et al.*, 1998; Swain, Wang, Saunders, Dunn, & Smith, 2003). However, these experiments generally utilize roscovitine, an inhibitor of CDK1 at the same time, making

it difficult to determine the role of PP1 in the initial steps of prophase 1 arrest, specifically in interacting with CDC25B.

The role of protein phosphatases in meiotic arrest remains somewhat elusive and unclear. The interaction of PP1 with CDC25B has not been completely defined. The experiments outlined in Aim 1, will examine the role of PP1 phosphatase in the initial aspects of oocyte maturation.

1.5 YWHA or 14-3-3 Proteins in gametogenesis

YWHA or 14-3-3 proteins are acidic proteins that show a ubiquitous expression in different eukaryotic cells. The protein 14-3-3 is named after its DEAE cellulose chromatography fraction number and starch gel electrophoresis migration position. It was identified first as a brain abundant protein (Moore & Perez, 1967). Later, this protein was found to inhibit PKC and activate the enzyme tyrosine hydroxylase (Ichimura *et al.*, 1988; Isobe *et al.*, 1992; Toker, Ellis, Sellers, & Aitken, 1990). YWHA has the ability to bind to many functional signaling proteins, including phosphatases, kinases, and transmembrane receptors. The regulation of 14-3-3 is involved in growth and development, including cell cycle regulation, apoptosis, and cancer (Aitken, 2006; Mackintosh, 2004; Morrison, 2009; van Hemert, de Steensma, & van Heusden, 2001). There are seven isoforms encoded by seven different genes (beta, epsilon, gamma, eta, tau/theta, zeta, and sigma). The crystal structures study of various human 14-3-3 isoforms reveals striking structural similarities. In some cases, the ability of one isoform to compensate for the loss of another has been demonstrated (Acevedo, Tsigkari, Grammenoudi, & Skoulakis, 2007; Gardino, Smerdon, & Yaffe, 2006; Ichimura *et al.*,

2004; Schoenwaelder *et al.*, 2017; van Hemert *et al.*, 2001). Most of the binding partners for 14-3-3 are in the phosphorylated form. However, some of them are not. This protein exists as functional homodimers or heterodimers with a monomeric size of 30kDa (Aitken, 2011). The binding motif for 14-3-3 protein was first identified by (Muslin, Tanner, Allen, & Shaw, 1996) as RSXpSXP. Later on, by using 39 phosphor-serine oriented peptide libraries, RXY/FXpSXP sequence was reported as an additional binding motif (Yaffe *et al.*, 1997). The protein 14-3-3 has a great many functions such as activating and inhibiting proteins, changing localization, or affecting the phosphorylation status of other proteins (Bridges & Moorhead, 2005). All isoforms were found to exist in mice ovaries, oocytes, and eggs (De, Marcinkiewicz, Vijayaraghavan, & Kline, 2012). Also, the presence of some isoforms was noticed in testis and sperm. However, the role of this protein in spermatogenesis is still not clear.

Role of 14-3-3 in oocyte maturation

Roles for the 14-3-3 proteins in oocyte maturation have not been entirely defined. In the egg of the frog, *Xenopus laevis*, an isoform of 14-3-3 is known to bind to and inactivate CDC25 (Kumagai, Yakowec, & Dunphy, 1998). There is evidence to suggest that 14-3-3 eta is required for the normal assembly of the first meiotic spindle. The protein 14-3-3 eta isoform localizes in the meiotic spindle. Knocking down the expression of 14-3-3 eta in the oocyte using translation-blocking morpholino oligonucleotides leads to deformation or absence of the spindle (De & Kline, 2013). The 14-3-3 protein was demonstrated to bind to α and β tubulin in mitotic cells (Meek, Lane, & Piwnica-Worms, 2004; Pozuelo Rubio *et al.*, 2004). In the meiotic spindle, 14-3-3 eta

appears to associate with tubulin. Evidence for the co-localization of 14-3-3 eta with α tubulin was demonstrated using the *in situ* Proximity Ligation Assay (PLA), though further work is needed to examine if other proteins might be interacting with 14-3-3 eta and tubulin in a complex (De & Kline, 2013).

In the fertilized mouse egg, it has been reported that 14-3-3 epsilon binds to CDC25B and regulates mitosis (Cui *et al.*, 2014). There is one report to suggest that 14-3-3 epsilon prevents oocyte maturation when bound to CDC25B in oocytes; however, these data relied solely on partial knockdown of 14-3-3 epsilon mRNA with siRNA and the results are somewhat unclear (Meng *et al.*, 2013). Preliminary data suggest that 14-3-3 eta may be required for maintenance of prophase I arrest. Partial knockdown of 14-3-3 eta by injection of specific translation-blocking morpholinos promoted oocyte maturation (De, 2014).

While 14-3-3 proteins are implicated in binding to CDC25B and maintaining meiotic arrest, the role of these proteins and which isoforms are involved is unresolved. The experiments outlined in this project will attempt to define the roles of 14-3-3 eta and 14-3-3 epsilon in oocyte maturation.

Role of 14-3-3 in Spermatogenesis

Changes in protein phosphorylation mediate sperm motility, capacitation, acrosomal reaction, and sperm-egg fusion. 14-3-3 proteins are present in mammalian testes and sperm. For example, 14-3-3 zeta binds to phosphorylated PP1 γ 2 as well as many other proteins in bovine sperm (Puri, Myers, Kline, & Vijayaraghavan, 2008). The 14-3-3 isoforms, beta, theta, and epsilon are expressed in rat testis. The 14-3-3 isoforms theta and epsilon are expressed in testicular germ cells however the expression of 14-3-3 beta isoform is restricted to Sertoli cells and Leydig cells in rat testis (Chaudhary & Skinner, 2000; Graf, Brobeil, Sturm, Steger, & Wimmer, 2011; Wong, Sun, Li, Lee, & Cheng, 2009).

While it is known that 14-3-3 proteins are expressed in testis and sperm, the expression and role for each of the seven isoforms have not been characterized yet. The experiments outlined for Aim 3 will examine the roles of 14-3-3 eta and 14-3-3 epsilon in mouse testis and sperm.

The aims for my thesis are:

Aim 1: To identify the possible roles of PP1 in oocyte maturation

Aim 2: To define the role of 14-3-3 eta and 14-3-3 epsilon in oocyte maturation

Aim 3: To study the role of 14-3-3 eta and epsilon in spermatogenesis

CHAPTER 2

Materials and Methods

2.1 Materials and Methods for Aim 1 and 2

Collection of oocytes and eggs

All mice wild type (WT), global and conditional Knockouts (KO) used in the following experiments were housed and used at Kent State University. The protocols for experiments were approved by Kent State University Institutional Animal Care and Use Committee (IACUC) in accordance to the NIH and National Research Council's publication "Guide for Care and Use of Laboratory Animals".

To obtain oocytes, female mice were injected with 5 IU eCG to stimulate follicle growth and, 44-48 hours later, the ovaries were removed and repeatedly punctured with a 26-gauge needle to rupture follicles. Cumulus cell-enclosed oocytes were isolated, and the cumulus cells were removed by repeated pipetting through a small-bore pipette. Fully-grown oocytes with intact nuclei (germinal vesicles) were cultured in MEM α , supplemented with pyruvate and an antibiotic/antimycotic, and containing 0.1 mg/mL dibutyryl cAMP (dbcAMP; Sigma-Aldrich) or 0.1 mg/mL 3-Isobutyl-1-methylxanthine (IBMX; Sigma-Aldrich), each of which prevents cAMP breakdown and spontaneous oocyte maturation. Mature, metaphase II-arrested eggs were obtained from mice 13-14 hours following superovulation by injection of 5 IU hCG which was preceded by a priming injection of 5 IU eCG injection 48 hours earlier. The cumulus mass and egg were

left intact for *in vitro* fertilization or the cumulus cells were removed with 0.3 mg/ml hyaluronidase. In some cases, *zonae pellucidae* of oocytes and eggs thus collected were removed by a brief treatment in acidic Tyrode's solution (Sigma-Aldrich). Oocytes and eggs from outbred mice [ICR (CD-1), Harlan Laboratories, and now Envigo] and inbred mice [C57BL/6J, JAX mice, Jackson Laboratory] were used in these studies as well as transgenic animals, outlined below.

Oocyte and egg lysates

After oocytes and eggs collections, the cells were moved into homogenizing buffer (BH+) that contained Tris-HCL 20 mM pH 7.0, EGTA 1 mM and EDTA 1 mM pH 8.0, MS-SAFE Protease and Phosphatase Inhibitor (Sigma-Aldrich # MSSAFE). Laemmli sample buffer (5X, Tris-HCL pH 6.8-7.0, Glycerol 50%, SDS 5%, Bromophenol Blue 0.05% and DTT 250 mM) was then added and the lysate was boiled for five minutes at 95⁰ C.

Ovary lysate

Ovaries from both PP1 γ KO mice and CD-1 WT were collected and homogenized in HB+ adjusted to a ratio of 100 mg tissue/ml HB+. The suspension then centrifuged at 16,000 xg for 15 minutes at 4^o C. The supernatant then moved and saved for western blotting, Co-Immunoprecipitation (Co-IP) and pulldown techniques.

Messenger RNA extraction

Ovaries, oocytes and eggs from CD-1 mice were used for mRNA expression analysis. Messenger RNA from oocytes and eggs were isolated from 50 μ l pools of 30 cells lysates using the Dynabeads mRNA DIRECT™ kit (ThermoFisher) following the manufacturer's directions. The mRNA was then eluted off the Oligo (dT)₂₅ beads with 10 mM Tris-HCl.

For isolation of mRNA from ovaries, 100 mg of CD1 mouse ovary was homogenized in 1 ml cold Tri reagent (Sigma-Aldrich). The sample was then incubated with 200 μ l of chloroform for 15 minutes on ice before centrifugation at 12,000 xg for 15 minutes at 4° C. The top layer that has RNA was then collected. Isopropanol (500 μ l) was added to the mRNA and incubated at room temperature for 10 minutes. The sample was then centrifuged at 10,000 xg for 10 min at 4° C. The supernatant was then collected. One milliliter of 75% ethanol was added and vortexed gently. The mixture was then centrifuged at 7,500 xg for 7 minutes at 4° C. The supernatant was discarded, and the pellet was semi dried. The pellet was then resuspended in approximately 50 μ l of Nuclease-Free Water (Promega). Finally, the RNA concentration for ovaries, oocytes and eggs were measured by using a Nanodrop spectrophotometer (ND-1000; Nanodrop technologies).

Complementary DNA were prepared using the QuantiTect Reverse Transcription kit (Qiagen) following the manufacturer's instructions. Two reaction mixtures of cDNA were made from mRNA extraction and 2 μ l of the cDNA was used for each PCR reaction tube.

Primers were designed for each PP1 γ isoform transcript using the NCBI Primer-BLAST program and were designed to span exon-exon junctions. The forward PP1 γ 1 primer spanning the junction of exons 5-6 while the reverse primer spanning the 3' end of exon 7 which is not present in PP1 γ 2. On other hand, PP1 γ 2 transcript forward and reverse primers spanning the junction of exons 7-8 and 3'UTR respectively.

The PCR products were then run on a 2% agarose gel stained with GelRed Nucleic Acid Stain (Phenix) and visualized during exposure to UV light.

Table 1. Primers used to detect presence of each PP1 γ isoform by RT-PCR

Gene	Forward Primer	Reverse Primer	Product Size
<i>PPP1CC</i> 1	5'-CCC ATC AGG TGG TTG AAG- 3'	5'-CTT GCT TTG TGA TCA TAC CC- 3'	222 bp
<i>PPP1CC</i> 2	5'-CCA CCA CGG GTT GGA TCA G-3'	5'-GTA TAA ACC GGT GGA CGG CA-3'	175 bp

Microcystin Pull down

Microcystin-agarose beads (MC-agarose; Upstate Biotechnology, Lake Placid, NY) were washed twice with equal amount of HB+ buffer. Ovarian protein lysate was then added to the beads and incubated for 4 hours at 4° C with shaking. The mixture was centrifuged at 12,000 xg for 5 minutes and the flow-through (FT) was then collected from the supernatant stored at -20° C for later western blot analysis. The proteins bound to MC-agarose were washed once with TTBS (0.2 M Tris [pH 7.4], 1.5 M NaCl, 0.1% thimerosol and 0.5 % Tween 20) and three times with HB+ buffer. The bound was then analyzed by Western blot following boiling of the pellet with Laemmli sample buffer.

Single cell sequencing for 14-3-3 and PP1 γ isoforms mRNA

Single oocytes were isolated in PBS and processed by SingulOmics (New York) for RNA sequencing and data analysis. The computational pipeline for expression quantification was primarily based on STAR aligner and Cufflinks software tool. Reads from RNA-seq were subjected to quality control using FastQC (version 0.11.4), quality trimming using Trim_Galore (version 0.4.1) and aligned to mouse reference genome (GRCM38.91) using STAR (version 020201; options: `-outSAMAttrIHstart0--outSAMstrandField intronMotif--outFilterIntronMotifs RemoveNoncanonical--alignIntronMin 20--alignIntronMax 1000000-outFilterMultimapNmax 1`). Duplicated reads were discovered using Picard tools (version 1.119) and removed. Gene annotations (gtf file; version GRCM38.91) were obtained from Ensembl. FPKM values of genes were estimated using cufflinks (version 2.2.1). FPKM values give some qualitative and quantitative estimate of gene expression. Data was obtained for oocytes collected from females of the wild type CD-1. Oocytes were also obtained from the oocyte-specific knockouts of *Ywhae* and *Ywhah*, and the oocyte-specific double knockout for *Ywhae* and *Ywhah*. Additionally, we examined an oocyte from a female in which the *PPP1CC* gene is globally inactivated in mice with a CD-1 background.

Immunofluorescence Microscopy

To study the characterization and the distribution of PP1 isoforms in mouse oocytes and eggs, CD-1 WT mice were sacrificed to obtain either oocytes or eggs. The cells were then incubated in 4% paraformaldehyde (PFA, EM grade) in PBS for 30 minutes at room temperature. The cells were permeabilized with 1% TritonX-100

(Sigma-Aldrich) for 10 minutes to promote antibody penetration. The cells were washed in PBS-PVA 3 times for 7 minutes followed by incubation with blocking buffer (5% normal Goat serum) for 45 minutes. The cells were then incubated overnight with one of the following antibodies [PP1 α : Rabbit polyclonal anti Pp1 α (YenZym) 1:500 dilution; PP1 β : Rabbit monoclonal anti Pp1 β (EPITOMICS #2029-1) 1:500 dilution; PP1 γ 1: Rabbit polyclonal anti Pp1 γ 1 (YenZym) 1:500 dilution; PP1 γ 2: Rabbit polyclonal anti Pp1 γ 2 (YenZym) 1:1000 dilution; PP2A: Rabbit monoclonal anti PP2A (Cell Signaling #2290P) 1:500 dilution; α -Tubulin: Rat monoclonal anti α -tubulin (Santa Cruz Biotechnology #SC-69970) 1:200 dilution]. The following day, the cells were washed 3 times with 1% blocking buffer for 10 minutes and incubated with the following secondary antibodies (Goat anti Rabbit CY3 and Donkey anti Rat FITC) for 90 minutes. The cells washed again four times with 1% blocking buffer for 15 minutes. In the last wash, the cells were incubated with Hoechst, a nuclear stain (Molecular probe Hoechst H3570; Invitrogen). , The cells were transferred to drops of PBS containing antifade (SlowFade antifade kit s2828; Invitrogen) under mineral oil (Mineral Oil O121-1; Fisher Scientific) and imaged by confocal microscopy (FluoView 1000 Confocal microscope, Olympus).

Co-Immunoprecipitation (Co-IP)

Lysates from ovarian tissue were prepared as described above. One ml of the supernatant was incubated with 20 μ l of Pp1 α antibody 0.86 μ g/ μ l (YenZym) overnight on a rotor at 4 $^{\circ}$ C. The next day the antibody-protein complexes were isolated by binding to a 50 μ l suspension of magnetic Dynabeads Protein G (Invitrogen # 10003D) which had

been washed with HB+ for 10 minutes at room temperature. The samples were incubated with the magnetic beads for 6 hours at 4° C with rotation. Using magnetic racks, the magnetic beads were separated from the remaining sample. The supernatants were removed and saved as flow-through. The beads were then washed 5 times with TTBS, resuspended with 2X SDS reducing sample buffer (6% SDS, 25 mM Tris-HCL pH6.5, 50 mM DTT, 10% glycerol and bromophenol blue) and boiled for 10 minutes. The beads were separated using the magnetic rack again and the supernatant were saved as bound. Input (the original untreated ovarian lysate), flow-through and bound were analyzed by western blot.

His-tag pulldown

Recombinant proteins PP1 γ 1 and PP1 γ 2 containing 6x- histidine tag were added to a 50 μ l suspension of Dynabeads His-tag isolation and pulldown magnetic beads (Invitrogen 10103D) for 30 minutes at room temperature. 500 μ l of the ovarian lysate was incubated with the His-tag protein/beads complex for 2 hours with rotation. The beads then were separated from the lysates by using a magnetic rack. The supernatants were collected and saved as flow-through. The beads then washed 3 times with TTBS. Finally, the bound proteins were eluted with 300mM Imidazole solution. The beads were separated using the magnetic rack again and the supernatant were saved as bound. Input (the original untreated ovarian lysate), flow through and bound fractions were analyzed later by western blotting.

Western Blot

Protein lysates were separated in a 12% polyacrylamide gel and the proteins were transferred by electrophoresis to a PVDF membrane (Amersham Hybond P 0.2 PVDF 10600021) and blocked with 5% nonfat dry milk in TTBS. The blots were incubated with primary antibody overnight at 4° C [PP1 γ 1: Rabbit polyclonal anti-Pp1 γ 1 (YenZym, 1:1000 dilution); PP1 γ 2: anti-Pp1 γ 2 c-terminal (YenZym, 1:5000 dilution); PP1 α : Rabbit polyclonal anti Pp1 α (YenZym 1:1000 dilution); CDC25b: Goat polyclonal anti-Cdc25b (R&D 1:1000 dilution). PP1 antibody (E-9): Mouse monoclonal anti Pp1 (E9) antibody (Santa Cruz 1:1000 dilution); beta-tubulin: Rabbit monoclonal anti β -tubulin antibody (Abcam #ab52901) 1:5000 dilution]. The blots were washed with TTBS twice for 15 minutes each and incubated with the appropriate secondary antibody conjugated to horseradish peroxidase for at least one hour at room temperature. The blots were then washed with TTBS four times for 10 minutes. Finally, the blots were developed with Amersham ECL Prime Western Blotting Detection Reagent (Amersham, RPN2232) and imaged.

Conditional and global knockouts for *Ywhah* and *Ywhae* isoforms

We generated a mouse line in which exon 2 of the mouse *Ywhah* gene was flanked by LoxP sites. The conditional knockout mouse line was produced by a commercial company (Cyagen Biosciences, Santa Clara, CA) using standard ES cell based gene targeting, Exon 2 of the mouse *Ywhah* gene was selected as the conditional knockout region. The targeting vector, 5'homology arm, 3'homology arm and CKO regions were amplified from BAC DNA and confirmed by end sequencing. The targeting

vector was electroporated into C57BL/6 ES cells. Clones were screened by PCR and selected clones by Southern blot. ES cells were injected into B6-albino mice blastocysts and the chimera produced breed for germline transmission. Progeny containing the floxed gene were mated with C57BL/6J mice to obtain a colony on this strain. Mice homozygous for the LoxP in the *Ywhah* gene were mated with ZP3-Cre (C57BL/6-Tg (Zp3-cre)), The Jackson Laboratory) or ACTB-Cre mice (B6N.FVB-*Tmem163*^{Tg(ACTB-cre)}^{2Mrt}/CjDswJ, , The Jackson Laboratory). Progeny of these mating pairs were examined by PCR to show disruption of the gene and/or protein analysis to show loss of protein. These mice were used for *in vivo* breeding, oocyte analyses, oocyte maturation and in some cases, for *in vitro* fertilization studies.

We also obtained a mouse line with LoxP sites inserted in the *Ywhae* gene from Dr. K. Toyo-Oka (Drexel University). These mice contain LoxP sites to remove exons 3 and 4 of the *Ywhae* gene with Cre recombinase and have been successfully used to study the role of YWHAE protein in the developing brain (Toyo-Oka *et al.*, 2003; Toyo-Oka *et al.*, 2014). Mice were maintained in the floxed condition in 129/SvEv mice and animals homozygous for the LoxP in the *Ywhae* gene were mated with ZP3-Cre or ACTB-Cre mice. We also cross bred both LoxP *Ywhah* and *Ywhae* lines to get a homozygous mouse for both genes and mated those mice with the ZP3-Cre line to knockout both proteins.

Unique primers were used in PCR to confirm disruption of the *Ywhah* and *Ywhae* genes (see Table 2) using DNA from ear-punches or, in some cases, from oocytes. The *Ywhah* LoxP primer distinguished the mice that carried the flanked gene from the wild type. The size for the flanked gene is 292 bp, while the wild type gene is 226 bp.

Heterozygous LoxP animals expressed two different bands with two different sizes: one for the wild type and another for the flanked gene. Absence of any band indicated disruption of the gene. In addition, primers external to the gene knockout region were used to confirm the knockout condition, producing a band at 390 bp. The *Ywhae* LoxP primer distinguished the mice that carry the flanked gene from the wild type condition. The band-size for the flanked gene is 536 bp, while the wild type gene is 450 bp. The heterozygous condition would express two different bands at two different sizes: one for the wild type while the other for the flanked gene. Absence of any band indicated disruption of the gene. In addition, primers external to the gene knockout region were used to confirm the knockout condition, producing a band at 664 bp. A generic Cre primer set detected the sequence of the Cre that was found in both ZP3 and ACTB lines. The band at 100 bp confirms the presence of the Cre.

Table 2. Primers used to detect LoxP and *Ywhah* in female mice

PCR product	PCR primers	Fragment size (bp)
<i>Ywhah</i> LoxP	Forward: 5'- TAATTGTGAGCCACCCGAAATGA -3' Reverse: 5'- GCCAACGACCAATGCCAATTATAG -3'	WT: 226 Floxed: 292
<i>Ywhah</i> knockout	Forward: 5'- CCTGATCTAGGATAGCTAGGGCTACATAG -3' Reverse: 5'- AGTATACCTTTTGGAGACAGGATCTATTATAGCC -3'	Deletion gives band at: 390
<i>Ywhae</i> LoxP	Forward: 5'- GCATGTGTTTTGTCTGTCAGAGGAC -3' Reverse: 5'- AGGTACCAAAACAGTAAGCCATCTCCCTA -3'	WT: 450 Floxed: 536
<i>Ywhae</i> knockout	Forward: 5'- TTCTTTTGTAGAAATTGGGGAAGGTCATGG -3' Reverse: 5'- AGGTACCAAAACAGTAAGCCATCTCCCTA -3'	Deletion gives band at: 664
Generic Cre	Forward: 5'- GCG GTC TGG CAG TAA AAA CTA TC -3' Reverse: 5'- GTG AAA CAG CAT TGC TGT CAC TT -3'	Cre Positive: 100

Homozygous WT, homozygous LoxP with no Cre and LoxP/WT with no Cre, are effectively wild type females, which served as control animals in some cases (generally litter mates) along with true wild-type animals. LoxP/WT with Cre positive, -/WT, -/LoxP with Cre negative and WT/LoxP with ZP3-Cre positive were taken as heterozygous females. The ZP3 conditional knockout expressed -/LoxP with ZP3-Cre positive in ear-punch while the oocytes do not express the gene. The global knockout females were homozygous for the knockout (-/-) in all cells, as identified by the primers listed above.

Western blotting for knockout mice

In several cases, we confirmed the knockout condition in ovary or oocyte cell lysates using specific antibodies in Western blots. Cell lysates were prepared from oocytes, eggs and 2-cell embryos in HB+. Laemmli sample buffer was then added and the lysate was boiled for five minutes at 95⁰ C. Cell lysates were separated in a 12% polyacrylamide gel and the proteins were transferred by electrophoresis to a PVDF membrane and blocked with 5% nonfat dry milk in TTBS. The blots were incubated with primary antibody overnight at 4⁰ C [YWHAH: mouse monoclonal anti-YWHAH (Novus Biological, NBP1-92691, 1:5000 dilution) or goat anti-YWHAH (R&D Systems AF4420, 1:1000 dilution); YWHAE: anti-YWHAE (Santa Cruz, sc-23957, 1:1000 dilution); Rabbit monoclonal anti β -tubulin antibody (Abcam #ab52901) 1:5000 dilution]. The blots were then washed with TTBS twice for 15 minutes each, and incubated with the appropriate secondary antibody conjugated to horseradish peroxidase for at least one hour at room temperature. The blots were then washed with TTBS twice for 15 minutes each and twice for 5 minutes each. Finally, the blots were developed with Amersham ECL Prime Western Blotting Detection Reagent and imaged.

In Vitro Fertilization (IVF)

Sperm were collected by puncture and snipping of each *cauda epididymis* and *vas deferens* of three- to five-month old wild-type male mice in a 1000 μ l drop of HTF media (Millipore: EmbryoMax[®] Human Tubal Fluid) and cultured at 37⁰ C under 5% CO₂ in a humidified incubator for 10 minutes to allow the sperm to swim out. The tissues were removed from the drop after 10 minutes and sperm were maintained in the incubator for

45 minutes to allow for capacitation. Eggs were obtained from two to three months old wild type and *Ywhae* oocyte-specific knockout females following superovulation induced by intraperitoneal injection of 5 IU of eCG (Sigma-Aldrich) and 46-50 hours later, injection of 5 IU of hCG (Sigma-Aldrich). Oocyte/cumulus complexes were removed from the ampullae 13-15 hours after hCG injection and transferred to a 135 μ l drop of HTF covered with mineral oil. After capacitation, 15 μ l of the sperm suspension was added to the 135 μ l drop of containing oocyte/cumulus complexes. The dish was incubated at 37° C in 5% CO₂ for 4 hours. The eggs were then washed by pipetting into fresh media (removing dissociated cumulus cells) and incubated overnight in a 300 μ l drop of HTF medium at 37° C and 5% CO₂. The following day, the number of two-cell embryos were counted. Some two-cell embryos were cultured to blastocyst stage.

2.2 Materials and Methods for Aim 3

Sperm isolation and count

Mice aged between 8-16 weeks were sacrificed and each *cauda epididymis* and *vas deferens* was isolated in 1ml Phosphate Buffer Saline (PBS). Using a 45-mm gauge needle, the *cauda epididymis* was punctured. The sperm also were squeezed out from the *vas deferens*. The epididymis was then left at 37° C for 10-15 minutes to let the sperm to swim out. The sperm were then transferred into microcentrifuge tubes by using a large bore pipette tips. For sperm counts, 10 µl of sperm suspension was diluted 1:10 in water and 10 µl diluted sperm was then transferred to a Neubauer hemocytometer for counting.

Differential Interference Contrast (DIC) microscopy

The sperm suspension was centrifuged at 750 xg for 10 minutes at 4 °C. The supernatant was removed and the pellet was suspended with 4% paraformaldehyde (PFA) (EM grade) in 1X PBS for 30 minutes at 4 °C. The fixed sperm were then mounted on slides that were covered with poly-L-lysine (Sigma P-8920). Sperm were then observed on an Olympus ix81 microscope (Olympus) using differential interference contrast.

Sperm and testis extracts for western blot analysis

The sperm suspension after the counting was centrifuged at 750 xg for 10 minutes at 4° C. The PBS was then removed and 1% SDS was added to obtain a sperm count of $1 \times 10^7/\mu\text{l}$). The suspension was then boiled for 5 minutes at 95 °C. After boiling, the suspension was centrifuged at 16000 xg for 15 minutes at room temperature. The supernatant was saved at -20 °C until used for western blot analysis.

The testis were isolated and washed with PBS. The tissue was then homogenized in homogenizing buffer (HB+) that contains Tris-HCL 20 mM pH 7.0, EGTA 1 mM and EDTA 1 mM pH 8.0, MS-SAFE Protease and Phosphatase Inhibitor (Sigma-Aldrich # MSSAFE). One ml of HB+ buffer was used for 100 mg of tissue. The homogenate was then centrifuged at 16000 xg for 15 minutes at 4 °C and the supernatant stored at -20 C until use.

Western Blot

Testis or sperm extracts were boiled for 5 minutes with Laemmli sample buffer (5X, Tris-HCL pH 6.8-7.0, Glycerol 50%, SDS 5%, Bromophenol Blue 0.05% and DTT 250 mM). The proteins were separated on either 10% or 12% SDS-PAGE and transferred to PVDF membranes. The membrane was then incubated with 5% nonfat dry milk diluted in Tris-Tween Buffer Saline (TTBS) (0.2 M Tris, pH 7.4, 1.5 M NaCl, 0.1% thimerosal and 0.5% Tween 20) for 45 minutes. Followed by incubation with different antibodies. The following antibodies were diluted in 1% nonfat dry milk diluted in TTBS [14-3-3 η : Rabbit anti-14-3-3 η (Millipore Sigma AB9736, 1:1000 dilution); 14-3-3 ϵ : anti-14-3-3 ϵ (Santa Cruz, sc-23957, 1:1000 dilution); phospho-GSK3 α/β : Rabbit monoclonal anti p-GSK3 α/β (Ser21/9) antibody (Cell Signaling Technology) 1:1000 dilution; phospho-T320 PP α : Rabbit monoclonal anti p-T320 Pp1 α antibody (Abcam #EP1512Y) 1:1000 dilution; PP1 γ 2: anti-Pp1 γ 2 c-terminal (YenZym, 1:5000 dilution); beta-tubulin: Rabbit monoclonal anti β -tubulin antibody (Abcam #ab52901) 1:5000 dilution; beta-actin: Mouse monoclonal anti β -actin antibody AC-15 (GeneTex# 26276) 1:2000 dilution; Anti phospho-(Ser) 14-3-3 binding motif: Rabbit polyclonal anti p-Ser 14-3-3 binding motif

antibody (Cell Signaling Technology #9601S) 1:1000 dilution]. Following primary antibody incubation the blot was washed four times with TTBS for 5 minutes and incubated with an appropriate horseradish peroxidase-conjugated secondary antibody for 90 minutes at room temperature. The blot was then washed four times with TTBS for 10 minutes and developed with enhanced chemiluminescence (Thermo Scientific Super Signal West Pico ECL).

Immunofluorescence labeling of sperm

Sperm were extracted in PBS and moved into microcentrifuge tubes. The suspension was then centrifuged at 750 xg for 10 minutes at 4 °C. The supernatant was removed and the pellet was diluted with 4% PFA in PBS for 30 minutes at 4 °C for fixation. The suspension was then centrifuged at 1000 xg for 5 minutes and the 4% PFA was removed as a supernatant. The pellet was then washed two times with PBS and recentrifuged. After the second wash, the fixed sperm were mounted on poly-L-lysine coated coverslips. The coverslips were then covered with 0.2% Triton-X for 10 minutes for permeabilization and washed two times later with PBS for 5 minutes. The coverslips were then covered with either 5% goat or donkey serum for 45 minutes at room temperature. The cover slips were incubated overnight at 4° C with the following antibodies diluted in the 1% blocking buffer [pan 14-3-3: Rabbit polyclonal anti 14-3-3 (YenZym) 1:1000 dilution; 14-3-3ε: Goat anti 14-3-3ε (R&D #AF4419) 1:500 dilution]. For the negative control sample, the incubation with the primary antibodies was omitted. The samples were then washed three times with PBS for 5 minutes and incubated with the secondary antibodies (Donkey anti goat CY3 and goat anti rabbit CY3) for 90

minutes at room temperature. The coverslips were then washed three times with PBS for 10 minutes. Before adding the mounting media, the coverslips covered with Hoechst diluted in 1% blocking buffer for 10 minutes and washed later with PBS. The sperm was then imaged and examined by confocal microscopy.

Testis sections for histochemistry

The testes were extracted and washed with PBS. The tissue was then incubated overnight in Bouin's fixative solution at 4° C. The tissue then washed two times with 70% ethanol for 5 minutes. Using Shanton Citadel 2000 tissue processor (Thermos Fisher Scientific), the fixed tissues were dehydrated through a graded series of increasing ethanol (70%, 80%, 90% and 100%) and permeabilized through two changes of Citrosolve. The processed tissue was removed and embedded in paraffin wax. The samples were at a thickness of 10 µm and sections were transferred to poly-L-lysine-coated slides.

Immunofluorescence labelling of testis sections

Testis sections were deparaffinized using two changes of Citrosolve for 5 minutes and rehydrated through a decreased graded series changes of ethanol (100%, 90%, 80% and 70%). The slides were then boiled in antigen retriever solution (Sigma Citrate Buffer Antigen Retriever C9999) three times for 1 minute with resting time of 2 minutes. The slides were rest at room temperature for 30 minutes in the antigen retrieval solution. The slides then washed with deionized water for 5 minutes. The slides were then covered with 5% blocking buffer (Goat serum diluted in PBS) at room temperature for 45 minutes. The sections were incubated overnight with the mouse monoclonal anti-14-3-3ε (Santa Cruz,

sc-23957, 1:500 dilution) diluted in 1% blocking buffer at 4°C. For the negative control, the incubation with the primary antibody step was omitted. The slides were then washed 3 times with PBS for 5 minutes and the sections were incubated with the secondary antibodies (Goat anti mouse CY3) for 90 minutes at room temperature. The slides were washed four times with PBS for 10 minutes and in the last wash the Hoechst stain was added. The sections were mounted and the images were obtained by using the FluoView 1000 Confocal microscope.

The sections were also stained with Periodic Acid-Schiff staining kit (Leica Biosystems) following the manufacturer's protocol. The sections were counterstained with Gill II hematoxylin for 3 minutes then rinsed with tap water for 5 minutes. The sections later were dehydrated and mounted with xylene based mounting media.

RNA isolation and Quantitative PCR

Wild type mice of different ages (10 days, 15 days, 20 days, 25 days and 12 weeks) were used to obtain testis RNA. Total RNA was isolated by using Trizol reagent (Sigma), phenol-chloroform extraction (Amersco), and isopropanol precipitation. The RNA pellet was then washed with 75% ethanol and dissolved in DEPC-treated water. The QuantiTect Reverse Transcription Kit (Qiagen) was used for cDNA preparation from extracted RNA.

The quantitative PCR was performed by using Rotor-Gene Q series. An average of threshold cycles were measured from triplicate reactions for SYBER green (QuantiTect SYBER green RT-PCR kit) qRT-PCR. *Gapdh*, a housekeeping gene was used as an internal control. The qPCR thermal cycle included an initial denaturation at 95° C for 5

minutes. The amplification was repeated 35 cycles (94°C 30 seconds, 57°C for 45 seconds and 72°C for 45 seconds). The *Ywhae* primer set was designed by using Primer-Blast software and to span exon-exon junctions. The primers (forward 5'-GCCATTTTTCCTGCTCGGAC-3' and reverse 5'-CCACCATTTTCGTCGTATCGC-3') produced the predicted 172 bp sequence on 1% agarose gel. The average of Ct values of each sample was analyzed by dCt method.

Mouse Models and Genotyping

The procedure for obtaining the inserted LoxP mice for *Ywhah* and *Ywhae* genes mouse lines is described above (Materials and Methods for Aim 1 and 2). The homozygous mice containing LoxP sequences were bred with either ACTB-Cre (B6N.FVB-*Tmem163*^{Tg(ACTB-cre)2Mrt}/CjDswJ, The Jackson Laboratory) mice for global knockout or Stra8-iCre (008208 STOCK Tg (Stra8-icre) 1Reb/J, The Jackson Laboratory) mice for testis specific knockout. Stra8-iCre is driven by the Stimulated by Retinoic Acid gene8 (Stra8) promoter and is expressed specifically during spermatogenesis (Sadate-Ngatchou, Payne, Dearth, & Braun, 2008). On the other hand, ACTB-Cre is driven by the human beta actin gene promoter and is expressed in all cells of the embryo by the blastocyst stage (Lewandoski, Meyers, & Martin, 1997).

Using mice ear punches, DNA was isolated and used in PCR to confirm the disruption of *Ywhah* and *Ywhae* genes. For each mouse, we used three different primers. The LoxP primers were used to distinguish the WT from the mice that has floxed gene. The Knock out primers were designed as an external primers that show band only in case

of allele deletion. The generic Cre primers were used to detect the presence of ACTB-Cre while the Stra8 Cre primers were used with progeny from Stra8-iCre cross breeding.

Table 3. Primers used to detect LoxP and *Ywha* genes in male mice

PCR primers	Primers Sequence	Size (bp)
<i>Ywhah</i> LoxP	Forward: 5'- TAATTGTGAGCCACCCGAAATGA -3' Reverse: 5'- GCCAACGACCAATGCCAATTATAG -3'	WT:226 Floxed:292
<i>Ywhah</i> KO	Forward: 5'- CCTGATCTAGGATAGCTAGGGCTACATAG -3' Reverse: 5'- AGTATACCTTTTGGAGACAGGATCTATTATAGCC -3'	Deletion gives band at: 390
<i>Ywhae</i> LoxP	Forward: 5'- GCATGTGTTTGTCTGTCAGAGGAC -3' Reverse: 5'- AGGTACCAAAAACAGTAAGCCATCTCCCTA -3'	WT:450 Floxed:536
<i>Ywhae</i> KO	Forward: 5'- TTCTTTTGTAGAAATTGGGGAAGGTCATGG -3' Reverse: 5'- AGGTACCAAAAACAGTAAGCCATCTCCCTA -3'	Deletion gives band at: 664
Generic Cre	Forward: 5'- GCG GTC TGG CAG TAA AAA CTA TC -3' Reverse: 5'- GTG AAA CAG CAT TGC TGT CAC TT -3'	Cre Positive: 100
Stra8 iCre	Forward: 5'- GTGCAAGCTGAACAACAGGA-3' Reverse: 5'- AGGGACACAGCATTGGAGTC -3'	Cre Positive: 179

Wild type males that served as control animals (litter mates) were genotyped as one of the following (homozygous WT, Homozygous LoxP with no Cre and LoxP/WT with no Cre) while the Heterozygous genotyped as follow (LoxP/WT stra8 cre positive, WT/-, Loxp/- with no Cre). The global knockout males were genotypes as a homozygous for the KO (-/-), which should show no band with the LoxP primers, while the conditional knockout were genotyped as Loxp/- with Stra8-iCre positive.

Fertility testing

Transgenic male mice were bred with littermate WT females over a period of 8 weeks. After mating, the following morning females were checked for a vaginal plug to determine if copulation had occurred. The number of pups in each litter were recorded.

In Vitro Fertilization (IVF)

For female super ovulation, 2-3 month wild type females were primed intraperitoneally (IP) with 5 IU equine chorionic gonadotropin (eCG) followed 52 hours later with an injection of, 5 IU of human chronic gonadotropin (hCG). Sperm were obtained from the *cauda epididymis* and *vas deferens* of both 14-3-3 epsilon conditional knockout and litter mate WT mice in 1ml HTF media. The sperm were capacitated at 37° C in an atmosphere of 5% CO₂ for 1 hour. Oocyte/cumulus complexes were collected 13-15 hours after hCG injection and transferred to a 285 µl drop of HTF covered with mineral oil. After capacitation, 15 µl of the sperm suspension was added to the drop of containing oocyte/cumulus complexes and the cells were incubated for 4 hours at 37° and 5% CO₂. Eggs were then removed from the fertilization dish washed twice into a new dish containing 200µl of HTF. This dish was then incubated overnight at 37 and 5% CO₂. The next morning, cells were examined and the number of 2-cell stage embryos were counted.

Sperm motility

After capacitation, sperm motility was analyzed by a Computer Assisted Sperm Motility Analyzer (CASA). At least five random fields were chosen for each sample and analyzed using the following settings: 90 frames acquired at 60 frames/sec; minimum

contrast of 30; minimum cell size at 4 pixels; default cell size at 13 pixels; static cell intensity of 60; low size gate of 0.17; high size gate of 2.26; low-intensity gate of 0.35; high-intensity gate of 1.84; minimum static elongation gate of 0; maximum static elongation gate of 90; minimum average path velocity (VAP) of 50 μ /sec; minimum path straightness (STR) of 50%; VAP cut off of 10 μ /sec; and straight line velocity cut off of 0 μ /sec.

Mitochondrial Potential Assay

The *cauda epididymis* and *vas deferens* sperm were extracted in 1 ml of HTF media and capacitated as described. After capacitation, 500 μ l of sperm suspension was mixed with 100 nM of cyanine dye DiIC1(5) (MitoProbe™) and incubated at 37 °C and 5% CO₂ for 15 minutes. Cyanine dye DiIC1(5) is known to penetrate the living cells and primarily accumulate in the mitochondria with active membrane potential. The accumulation and the intensity of the stain are reduced when the eukaryotic cells are treated with reagents that disrupt the mitochondrial membrane potential (Shapiro, Natale, & Kamensky, 1979). The sperm suspensions were then analyzed by using Flow cytometry (BD Biosciences, San Jose, CA) with 633 nm excitation.

ATP Assay

Sperm from the *cauda epididymis* was isolated in HTF media as described above. The Sperm aliquots, 30 μ l each, were diluted with 270 μ l of boiling Tris-EDTA buffer (0.1 M Tris-HCL and 4 mM EDTA; pH 7.75) as described (Goodson et al., 2012). The suspensions were then boiled for 5 minutes and frozen in a dry ice acetone mixture. Samples were then thawed and centrifuged at 15000 xg for 5 minutes at 4 °C and the

supernatant was diluted 1:10 using the Tris-EDTA buffer. ATP quantification was performed by using Bioluminescence Assay Kit CLS II (Roche Applied Science) with 100 μ l of the diluted samples. Luminescence was measured in a Turner Biosystems 20/20 luminometer.

GSK3 Activity Assay

Sperm suspensions were centrifuged at 700 $\times g$ for 10 minutes at 4 °C and the pellets were resuspended in 1X RIPA buffer supplemented with 0.1% β -mercaptoethanol, 10 mM benzamidine, 1 mM phenyl-methylsulfonyl fluoride (PMSF), 0.1 mM N-tosyl-L-lysyl chloromethyl ketone (TPCK), 1 mM sodium orthovanadate, 1 nM calyculin A, and incubated on ice for 30 minutes and then centrifuged at 16000 $\times g$ at 4 °C for 20 minutes. The supernatants were collected and used for GSK3 assay. The amount of $^{32}\text{PO}_4$ transferred from [^{32}P] γ -adenosine triphosphate to phosphor-glycogen synthase peptide (GSK3 substrate, Millipore) was the measure of GSK3 activity. The assay buffer contained 200 mM HEPES, 50 mM MgCl_2 , 8 μM DTT, 5 mM sodium β -glycerophosphate, 0.4 mM ATP and 4 μCi of $\gamma\text{-P}^{32}$ ATP. In a microcentrifuge tube, 5 μ l of the assay buffer was added to 5 μ l of the extract and GS2 peptide: **YRRAAVPPSPSLSRHSSPHQ-pS-EDEEE** (1 mg/ml). The mixture was incubated at 30 °C water bath for 15 minutes. The reaction was then stopped by cooling down on ice for 10 minutes. The mixture was then applied onto a phosphocellulose cation exchanger (P18; Whatman Inc, Clifton, NJ) paper cutt into 1.5 cm X 1.5 cm. the paper was then washed with 0.1% (vol/vol) phosphoric acid three times for 5 minutes and then placed into scintillation vials with 2 ml of distilled water and counted with scintillation

counter. Each reaction was set in triplicate. The presence of 1 mM LiCl was used to inhibit GSK3 activity (Ryves, Fryer, Dale, & Harwood, 1998). The lithium sensitive activity as considered to be due to GSK3. The GSK3 activity was calculated with the following formula: **Activity units/10⁷cells = (lithium-sensitive cpm) x (Reaction vol/spot vol) / (specific activity of P 32 ATP) x reaction time**

Co-immunoprecipitation (CO-IP)

Testis extracts were pre-cleaned with protein G-sepharose 4 Fast Flow beads (GE Healthcare), incubated for 2 hours at 4 °C and then washed three times with HB+ by centrifugation at 8000 xg for 2 minutes. The beads were then incubated overnight at 4 °C with gentle rocking with primary antibodies [goat polyclonal 14-3-3ε (R&D #AF4419); mouse monoclonal 14-3-3ε (Santa Cruz #SC23957) and rabbit PP1γ2 (YenZym) antibody]. Serum (goat, mouse and rabbit serum) was used as a negative controls. The beads were then washed two times with homogenizing buffer. The pre-cleared extracts/lysates were added to the beads/antibodies and incubated for four hours at 4° C, and then washed 5 times with TTBS and resuspended with 2XSDS reducing sample buffer boiled for 10 minutes. The beads were centrifuged at 10000 xg for 10 minutes and the supernatants were used for western blot analysis.

Statistics

Statistical analyses were performed by using GraphPad Prism 6.03 (GraphPad Software Inc.). The statistically significant differences in all cases between samples were considered significant for p-values ≤ 0.05.

CHAPTER 3

Aim 1 and 2

3.1 Aim 1: To identify the possible roles of PP1 in oocyte maturation

3.1.1 Rationale

PP1 α , PP1 β , or PP1 γ may play a central role by affecting a number of steps in meiosis, including the resumption of meiosis in prophase 1 arrested oocytes. However, the interaction of PP1 with CDC25B is not clear, although evidence suggests that PP1 dephosphorylates CDC25B (Margolis *et al.*, 2006, 2003; Peng *et al.*, 1997). The isoform responsible for this in mammalian oocytes is not known. Previous studies have implicated PP1 in regulation of oocyte meiosis; however, there has never been an examination of the two alternatively spliced isoforms of PP1 γ , PP1 γ 1 and PP1 γ 2. The following results described below show, for the first time, that both splice isoforms of PP1 γ are present in the mouse ovarian, oocytes and eggs. Therefore, any study of the interactions of PP1 with CDC25B should include both isoforms.

We have obtained a *PPP1CC* (PP1 γ), knockout mouse line. The male of this strain is completely infertile due to impaired spermatogenesis. The females of this line appear to be normally fertile. This line has been described previously and is well studied (Chakrabarti, Kline, *et al.*, 2007; Sinha, Puri, Nairn, & Vijayaraghavan, 2013). We used WT CD-1 mice and genetically modified PP1 γ KO mice to clarify the role of PP1 in mouse oocytes and eggs.

3.1.2 **Result**

Presence of PP1 γ 1 and 2 transcripts in mouse oocytes and eggs

PP1 γ 1 and PP1 γ 2 have been previously shown to be transcribed (as mRNA) but not translated (as protein) in mouse eggs and oocytes (Smith, Sadhu, Mathies, & Wolf, 1998). Here, by using the RT-PCR we confirm the presence of both PP1 γ 1 and PP1 γ 2 transcripts in mouse ovaries, oocytes and eggs. The protocol for the mRNA isolation included a step to eliminate a potential DNA contamination; and the primers for each isoform was designed to cross the exon junction to ensure mRNA amplification. The message for both isoforms was detected in the ovaries, oocytes and eggs of outbred CD1 mice (Figure 18).

Single oocytes from both CD1 and PP1 γ knockout mice were used also to examine the presence of the message by using single cell sequencing. Reads from RNA-seq were annotated to Ensembl. FPKM (fragments per kilobase of exon model per million reads mapped), the normalized estimation of gene expression is based on the RNA-seq data, was estimated using Cufflinks. Message for both isoforms of PP1 γ 1 and PP1 γ 2 were detected and the single cell sequencing data confirms the results of the RT-PCR.

As a side, recent study shows two isoforms of CDC25B are expressed in somatic cells by alternative splicing (Kang, Bang, Choi, & Han, 2017). The role of these two isoforms in oocytes maturation is not known. However, the two isoforms are expressed in the WT oocytes (Table 4). It should be noted that the single cell sequencing data is only from one cell for each. Nevertheless, the presence of message for two isoforms of PP1 γ 1

and 2 is indicated. The presence of multiple isoform message for CDC25B has not been confirmed in oocytes and the potential protein function for these isoforms of CDC25B in oocytes needs further examination.

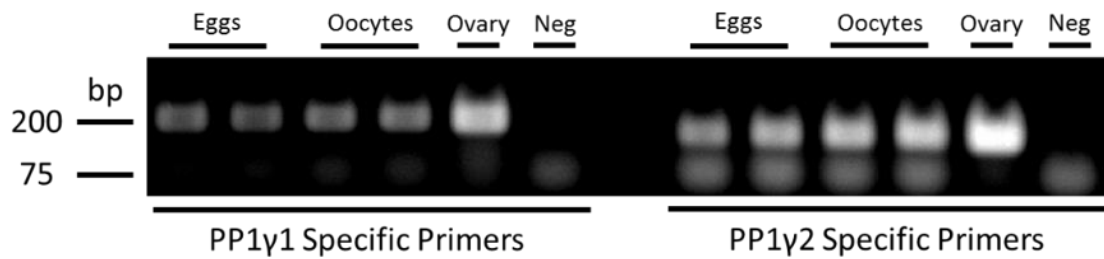


Figure 18. PP1γ1 and PP1γ2 mRNA expression using RT-PCR technique. PCR of cDNA from mRNA from wild type eggs, oocytes, and ovaries shows the presence of both PP1γ1 and PP1γ2 mRNA. The 222 bp band corresponds to PP1γ1 (forward primer at the exon 5-6 junction and reverse primer in exon 7 in a region that is not present in PP1γ2), and the smaller 175 bp band corresponds to PP1γ2 (forward primer at the exon 7-8 junction, not found in PP1γ1, and the reverse in the 3'UTR).

Table 4. Expression of Ppp1c and Cdc25 isoforms mRNA in single cell

	<i>PPP1CA</i> PP1 α	<i>PPP1CB</i> PP1 β	<i>PPP1CC1</i> PP1 γ 1	<i>PPP1CC2</i> PP1 γ 2	<i>CDC25A</i>	<i>CDC25B1</i>	<i>CDC25B2</i>	<i>CDC25C</i>
CD-1 WT	101.80	2.89	2.10	27.92	9.79	10.37	1.59	9.30
PP1 γ KO	91.99	4.44	0.67	1.02	1.98	0.00	3.99	2.36

FPKM values for *PPP1C* isoform transcripts and *CDC25* in single oocytes from an ICR

(CD-1 wild type female and from a female in which the PP1 γ gene is globally inactivated. Ensembl transcript IDs (mouse version GRCM38.p6): *PPP1CC1*, ENSMUST00000102528; *PPP1CC2*, ENSMUST00000086294; *CDC25A*, ENSMUST00000094324; *CDC25B1*, ENSMUST00000028804, *CDC25B2*, ENSMUST00000079857; *CDC25C*, ENSMUST00000060710.

PP1 γ 2 c-terminal Antibody validation experiment using ovarian tissue

Alternative splicing of PP1 γ mRNA produces PP1 γ 1 and PP1 γ 2 proteins. This processing is specific to mammals and occurs predominantly in the post meiotic germ cells of the testis. Here, the presence of two protein variants in oocytes and eggs is shown labelling with two specific antibodies. The PP1 γ 1 and 2 antibodies have been shown to differentiate the two isoforms. The PP1 γ 1 antibody was generated against a peptide corresponding to the 13 amino acids at the carboxy terminus of PP1 γ 1 as the antigen. PP1 γ 2 antibody was prepared using a synthetic peptide corresponding to the 22 amino acids at the carboxy terminus of PP1 γ 2 as the antigen (Chakrabarti, Kline, *et al.*, 2007; Cheng *et al.*, 2009). As shown in figure 19, the specificity was confirmed using recombinant proteins. His-tagged PP1 γ 1 and 2 recombinant proteins separated by gel electrophoresis, and probed in a Western blot with both PP1 γ 1 and PP1 γ 2 c-terminus antibodies. PP1 γ 1 antibody binds strongly to His-PP1 γ 1 and weakly to His-PP1 γ 2. On the other hand, PP1 γ 2 antibody binds only to the His-PP1 γ 2 recombinant protein, which indicates specificity for this protein.

Additionally, ovaries lysates from both PP1 γ KO and CD1 WT mice were incubated with microcystin agarose beads overnight to perform a pull down experiment. The microcystin is a toxin produced by cyanobacteria that binds to the catalytic subunits of both PP1 and PP2A (Puri *et al.*, 2008; Swingle *et al.*, 2007). Ovary lysate from one animal for each group (PP1 γ KO and WT) was prepared. Incubating the ovarian lysate with the microcystin pulls down PP1 and PP2A from the lysate. Therefore, we can detect

whether the ovaries lysate has PP1 γ 2 or not after incubating the bound fraction with the specific antibody.

The blot for wild type lysate was incubated first with anti PP1(E-9) antibody that detects the catalytic core of PP1 isoforms to test the success of the technique. PP1, PP2A and PP2B share the same catalytic core (280 amino acids) and differ only in the N- and C-termini (Fardilha *et al.*, 2013). Ovarian PP1 isoforms bind to microcystin beads (Figure 20). Moreover, blots of ovarian lysates from both PP1 γ KO and WT mice incubated with the PP1 γ 2 c-terminal antibody confirm the specificity of the PP1 γ 2 antibody. Even though the ovarian lysate from PP1 γ KO mice contains other PP1 isoforms, the blot shows no expression for PP1 γ 2 protein. At the same time, the WT ovarian lysate blot shows the presence of PP1 γ 2 protein (Figure 21).

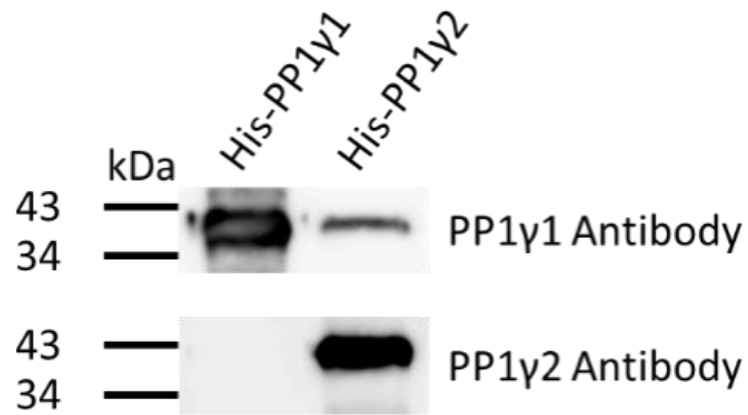


Figure 19. Validation of PP1 γ 1 and PP1 γ 2 antibodies using His-tagged recombinant proteins. His-tagged PP1 γ 1 and PP1 γ 2 were prepared and probed in a western blot with antibodies generated against epitopes specific to P1 γ 1 and PP1 γ 2. The PP1 γ 1 antibody was generated against a peptide corresponding to the 13 amino acids at the carboxy terminus of PP1 γ 1 as the antigen. PP1 γ 2 antibody was prepared using a synthetic peptide corresponding to the 22 amino acids at the carboxy terminus of PP1 γ 2 as the antigen.

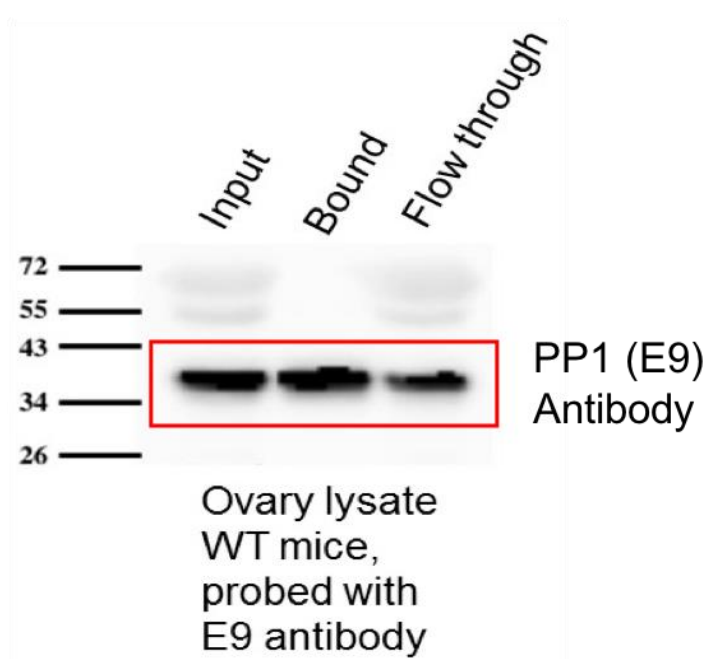


Figure 20. Pull down of PP1 protein from mouse ovaries using microcystin beads. Microcystin beads pulls down PP1 and PP2A proteins from ovaries lysate. PP1 is detected by the anti-PP1(E9) antibody (anti-PP1 catalytic domain) in the input, bound to the microcystin beads (bound) and in the flow through.

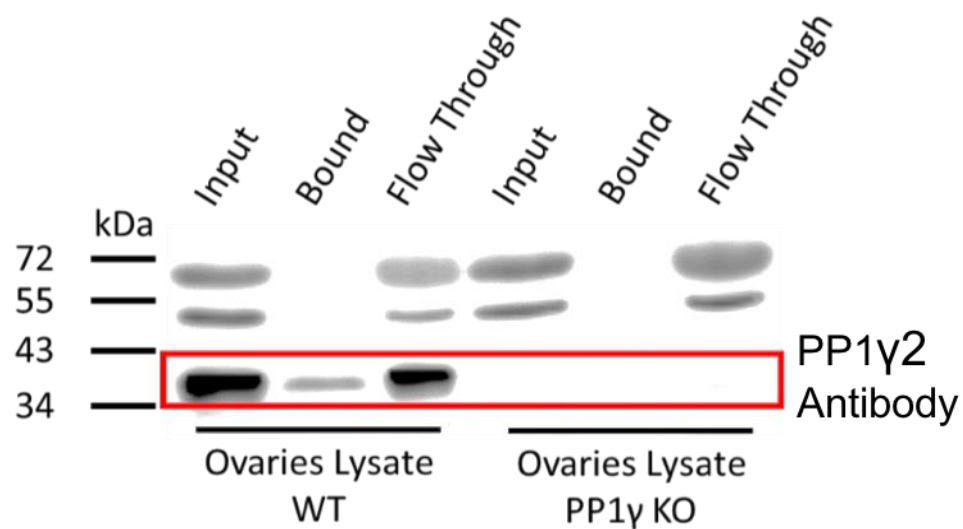


Figure 21. Pull down of PP1 γ 2 protein from mouse ovaries using microcystin beads. Ovaries lysates from both WT and PP1 γ KO mice were incubated with microcystin beads. Microcystin is expected to pull down PP1 and PP2A from the lysates. The blot was probed with PP1 γ 2 c-terminus antibody. The PP1 γ 2 is expressed in wild type ovary lysates (bound lane). The protein is not found in the “input” or “bound” fraction of ovaries from PP1 γ KO mice.

Presence of PP1 γ 1 and PP1 γ 2 proteins in mouse oocytes and eggs

The transcripts for both PP1 γ isoforms were reported in mouse oocytes. Here, the presence of PP1 γ 1 and PP1 γ 2 in mouse oocytes and eggs is shown by using western blotting and immunofluorescence techniques. Ovaries, oocytes and eggs were extracted and collected from CD1 WT mice. Cell lysates of oocytes and eggs were loaded for electrophoresis equally according to the number of cells. The ovaries lysate was prepared according to the following ratio (100 mg ovaries / 1ml of HB+). PP1 γ 1 and 2 were expressed in ovary, oocyte and egg lysates (Figure 22).

As shown by the immunofluorescence technique, both PP1 γ 1 and PP1 γ 2 tend to be expressed in both cytoplasm and nucleus compartments of oocytes. In eggs, PP1 γ 2 shows a co-localization with the spindle in mouse eggs. However, labelling at spindle appears to be an artifact of this particular antibody in immunofluorescence experiments (see below for additional comment). In contrast, PP1 γ 1 tend to be localized near to the spindle (Figure 23).

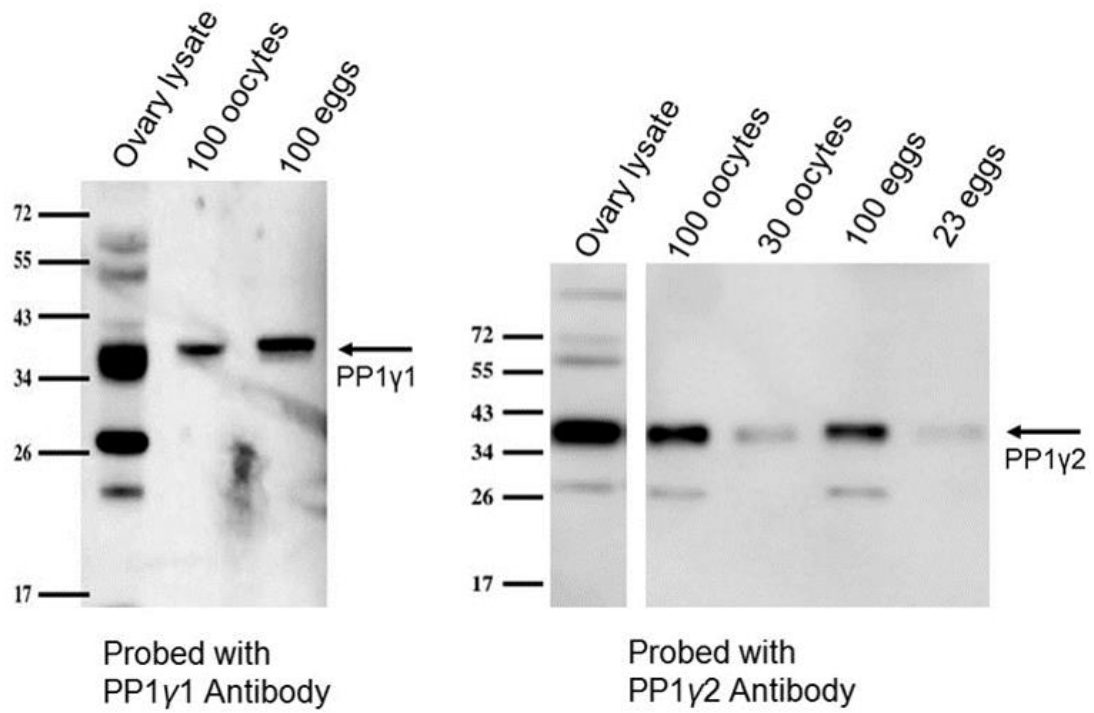


Figure 22. Western blot analysis of lysates probed with anti-PP1γ2 antibody. Lanes show a band at 37 kDa, corresponding to PP1γ1 (left panel) and a 39 kDa band corresponding to PP1γ2 (right panel).

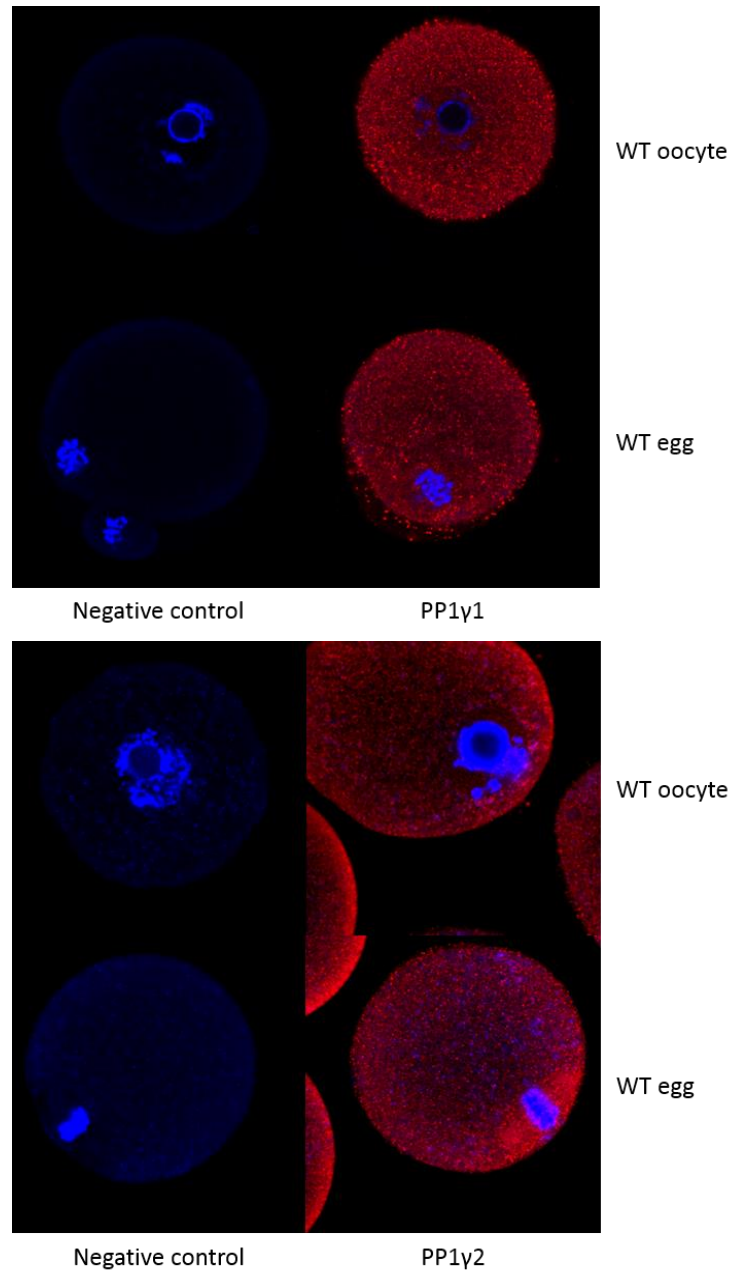


Figure 23. PP1 γ 1 and 2 localization in mouse oocytes and eggs. Upper panel shows immunofluorescence distribution of PP1 γ 1 in oocytes and eggs using PP1 γ 1 specific antibody in red and Hoechst in (Blue). Lower panel shows immunofluorescence distribution of PP1 γ 2 in oocytes and eggs using PP1 γ 2 specific antibody (Red). DNA stained with Hoechst (Blue). Images represent two experiments where six oocytes and eggs were examined with each antibody.

Characterization of all PP1 and PP2A isoforms in PP1 γ KO and WT mice eggs

The immunofluorescence experiments in addition to the western blotting show an expression of both PP1 γ 1 and 2 in mouse oocytes and eggs. PP1 γ KO mice show an infertility phenotype only in males. PP1 γ KO male testis are lacking of sperm due to germ cells arrest at the spermatocytes stage (Varmuza *et al.*, 1999). The absence of any defect in female fertility with the PP1 γ KO mice suggests that either there is no role of PP1 γ , or another PP1 isoform may substitute for its absence in the gene knockout. The expression of all PP1 isoforms in addition to the PP2A in PP1 γ KO and WT eggs was examined by using immunofluorescence. The expression of PP1 α appears to be increased based on the stronger immunofluorescence and a strong clumping pattern in oocytes of PP1 γ KO mice. The data suggest a relationship between the presence of PP1 γ protein and PP1 α abundance since PP1 α was more striking in abundance and altered in distribution in egg of the PP1 γ gene knockout; however, we as yet, there is no direct evidence for linked upregulation and compensation. PP1 β is weakly detected in both PP1 γ KO and WT eggs (Figure 24).

As mentioned above in reference to Figure 23, PP1 γ 1 and PP1 γ 2 antibodies show non-specific binding in the PP1 γ KO eggs when using the immunofluorescence. The accumulation of PP1 γ 2 on the spindle is not real since it also appears in the PP1 γ KO eggs. PP2A in the WT eggs tend to have accumulation in the cortex in the hemisphere containing the spindle (Figure 24). For further examination, and to confirm whether PP1 proteins co-localized with the spindle or not, eggs from WT mice were stained with PP1(E9) antibody that binds to the catalytic core of PP1 and PP2A. The

immunofluorescence images show no accumulation of PP1 in the spindle. Therefore, the co-localization of PP1 γ 2 with the spindle is an artifact, and the PP1 γ 2 antibody shows non-specific binding when it is used in immunofluorescence (Figure 25).

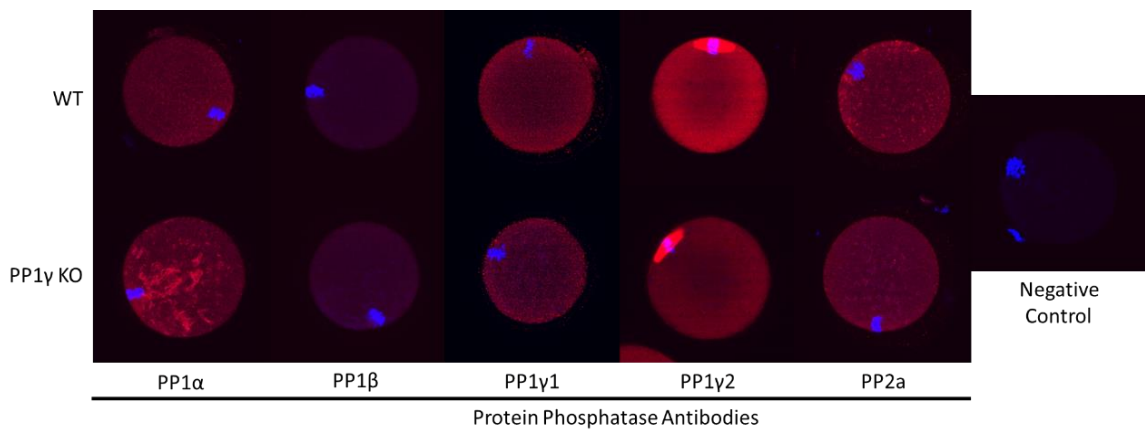


Figure 24. Expression of PP1 isoforms and PP2A proteins in mouse eggs shown by immunofluorescence using isoform specific antibodies. WT = eggs obtained from CD1 mouse. PP1 γ KO = eggs obtained from the *PPP1CC* knockout mouse. Negative = a typical image of a cell incubated with secondary fluorescent antibody alone (no primary). The expression level among the different proteins can't be compared directly because the binding properties are not likely to be similar for different antibodies. Images represent two experiments where six eggs were examined with each antibody.

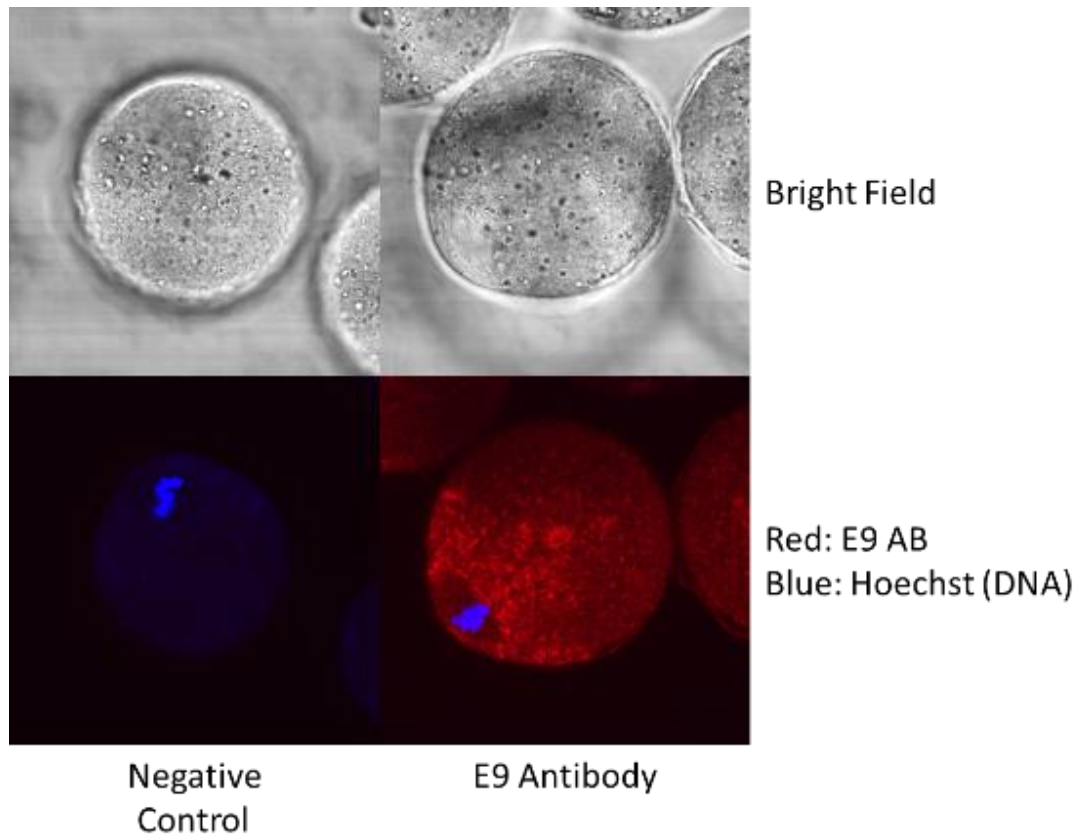


Figure 25. Expression of PP1 isoforms and PP2A proteins in mouse eggs shown by immunofluorescence using PP1 (E9) antibody. Eggs from WT mouse were incubated with anti-PP1(E9) antibody conjugated with Alexa Fluor 647. PP1 isoforms show no accumulation of proteins at the spindle. Images represent one experiment where seven eggs were examined.

PP1 α expression is upregulated in PP1 γ KO oocytes and eggs

Western blotting shows an overexpression of PP1 α protein in ovaries, oocytes and eggs of PP1 γ KO mice (Figure 26). Additionally, immunofluorescence images of oocytes and eggs show a uniform expression of PP1 α in WT eggs and oocytes; however, the expression of PP1 α in PP1 γ KO oocyte seems to be more localized to the nucleus and accumulated near to the spindle with pattern of larger clumps in the PP1 γ KO eggs (Figure 27). The fluorescent intensity was measured for PP1 α expression in both PP1 γ KO and WT oocytes (Figure 28). The intensity of PP1 α inside the KO nucleus is significantly higher than the expression in WT (p value = 0.0025). However, there was no significant difference between the expression of PP1 α in the PP1 γ KO and WT oocyte cytoplasm (p value = 0.0756). This overexpression of PP1 α in the PP1 γ KO mice suggests an overlapping role of PP1 γ 1/ PP1 γ 2 and PP1 α during oocytes development.

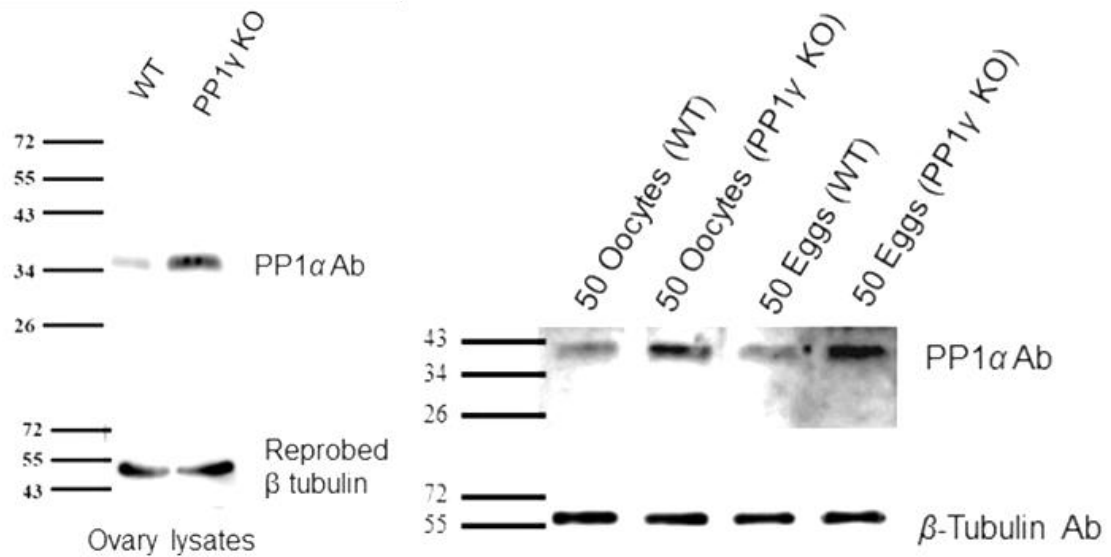


Figure 26. Expression of PP1 α in both PP1 γ KO and WT ovaries, oocytes and eggs. Western blot of ovary lysates from wild type mice compared to PP1 γ KO mice probed with anti-PP1 α antibody suggests an increase of PP1 α in the PP1 γ KO mouse ovaries (left panel) oocytes and eggs (right panel). Lysates were prepared from WT and PP1 γ KO ovaries by the same method and equal volumes were loaded on the gel. The blot was then incubated with β -tubulin antibody to validate the equal loading of the samples. Lysates of oocytes and eggs were prepared using equal numbers of cells.

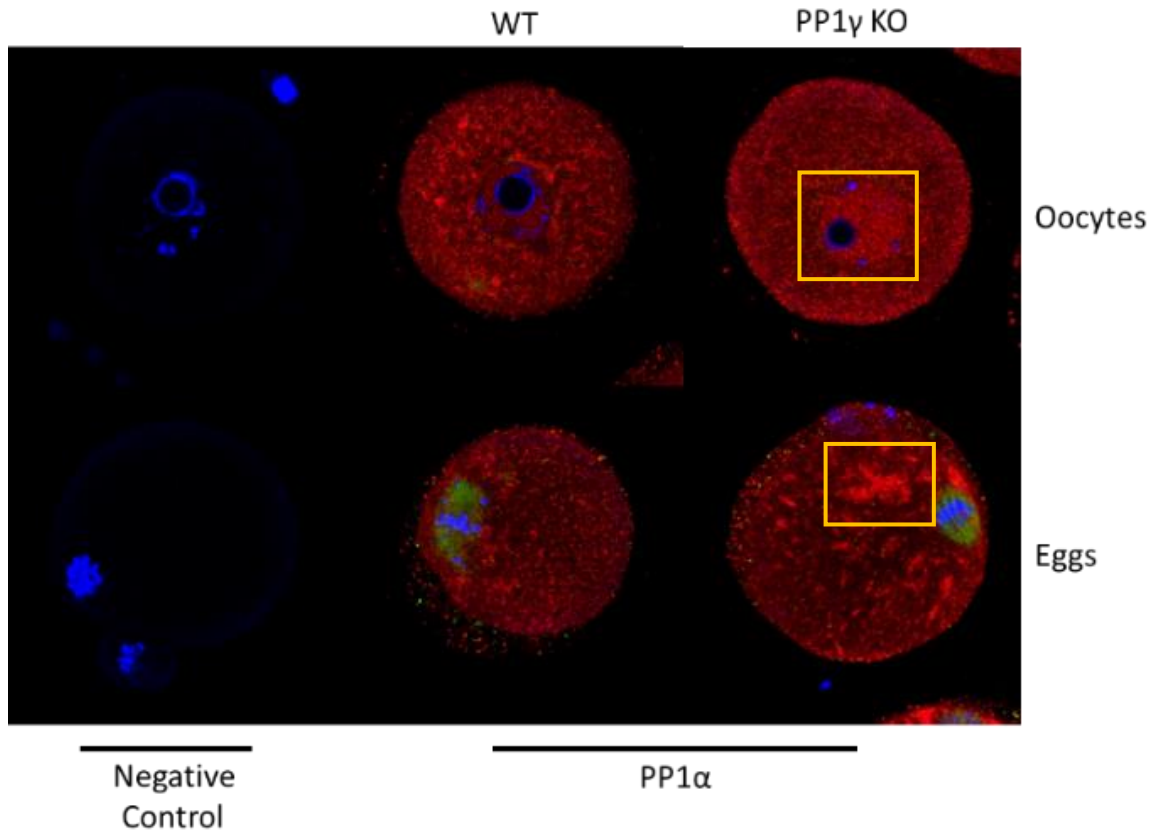


Figure 27. Expression of PP1 α isoform in mouse eggs shown by immunofluorescence using PP1 α antibody. WT = oocytes and eggs obtained from CD1 mouse. PP1 γ KO = oocyte and eggs obtained from the PP1 γ KO mouse. Negative control = a typical image of a cell incubated with secondary fluorescent antibody alone (no primary). PP1 α appears to increase in amount and accumulate more in the nucleus in PP1 γ KO oocytes (yellow-boxed area) and also increase throughout the cytoplasm of the egg (for example in the yellow-boxed areas). Images represent two experiments where six oocytes and eggs were examined.

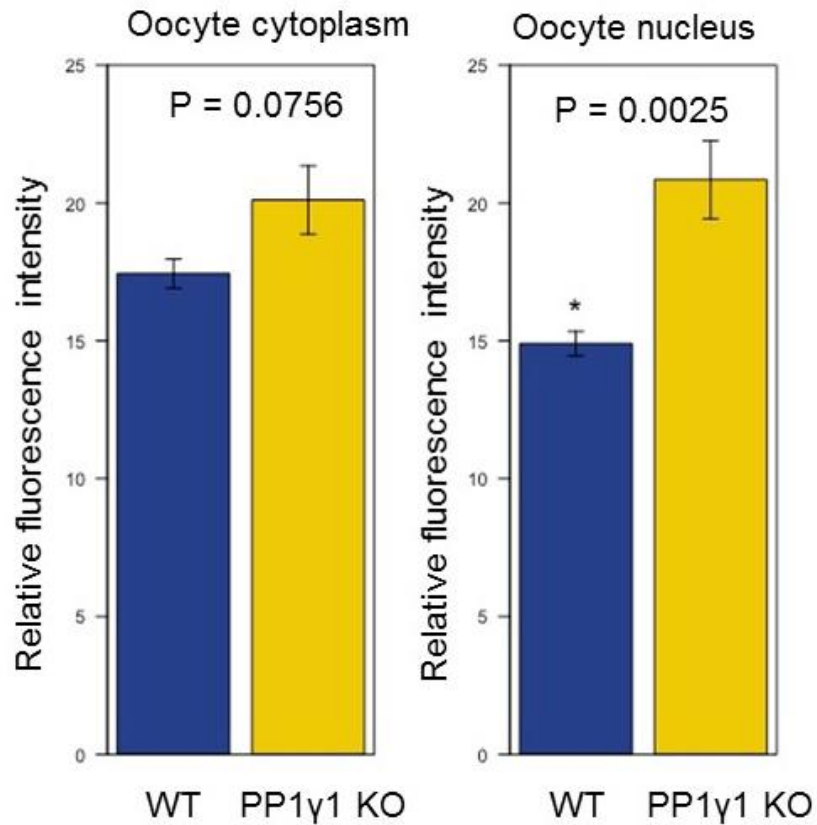


Figure 28. Fluorescent intensity of PP1 α expression in both PP1 γ KO and WT oocytes. Oocytes and eggs from both wild type and PP1 γ KO mice were fixed and incubated with anti-PP1 α antibody. With the same confocal imaging parameters, the arbitrary fluorescence intensity within the cytoplasm and the nucleus in oocytes was measured using ImageJ software and the significant difference between the intensities were examined by t-test. For the initial experiments shown here, the values were determined from six oocytes in each case.

Binding of PP1 γ 1 to CDC25B in WT mice

Phosphorylation and dephosphorylation events regulate many intracellular activities. CDC25 is a phosphatase that is responsible for removing a phosphate group from CDK1. This activates it and helps the somatic cells enter mitosis. During interphase, CDC25 binds to YWHA in the cytoplasm in a phosphorylated form. This phosphorylation inhibits the activity of CDC25 (Kim *et al.*, 2016; Margolis *et al.*, 2006). It's been reported that PP1 has the ability to interact with and dephosphorylate CDC25 in both mitosis and *Xenopus* oocyte meiosis (Izumi, Walker, & Maller, 1992; Perdiguero & Nebreda, 2004; Rebelo *et al.*, 2015). CDC25B also, known to be a phosphatase that is responsible for activation of CDK1 in mammalian oocytes. However, the phosphatase that is responsible for the dephosphorylation of CDC25B is still not known in mammalian oocytes. PP1 activity is implicated in maintaining the integrity of the nuclear envelope in germinal vesicle-intact oocytes because treatment with a PPI inhibitor results in a greater rate of GVBD (Smith *et al.*, 1998; Swain, Wang, Saunders, Dunn, & Smith, 2003). The role of protein phosphatases in meiotic arrest remains somewhat elusive and the interaction of PP1 with CDC25B has not been completely defined. Previously, the protein-protein interaction between CDC25B and PP1 was not detectible since previous work did not show the expression of PP1 γ in mouse oocytes (Margolis *et al.*, 2003; Smith, Sadhu, Mathies, & Wolf, 1998; Swain *et al.*, 2003; Wang *et al.*, 2004).

Because we have specific antibodies for PP1 γ 1 and PP1 γ 2, we were able to detect these isoforms in mouse oocytes and eggs. Here, we used His-PP1 γ 1 and His-PP1 γ 2 recombinant proteins for pull down techniques. Pulling down the binding proteins using His-PP1 γ 1 and His-PP1 γ 2 show a strong binding of CDC25B to His-PP1 γ 1 and weak binding to His-PP1 γ 2 in ovaries lysates (Figure 29). Since the PP1 γ KO females show normal fertility, another isoform might play a role in the regulation of CDC25B.

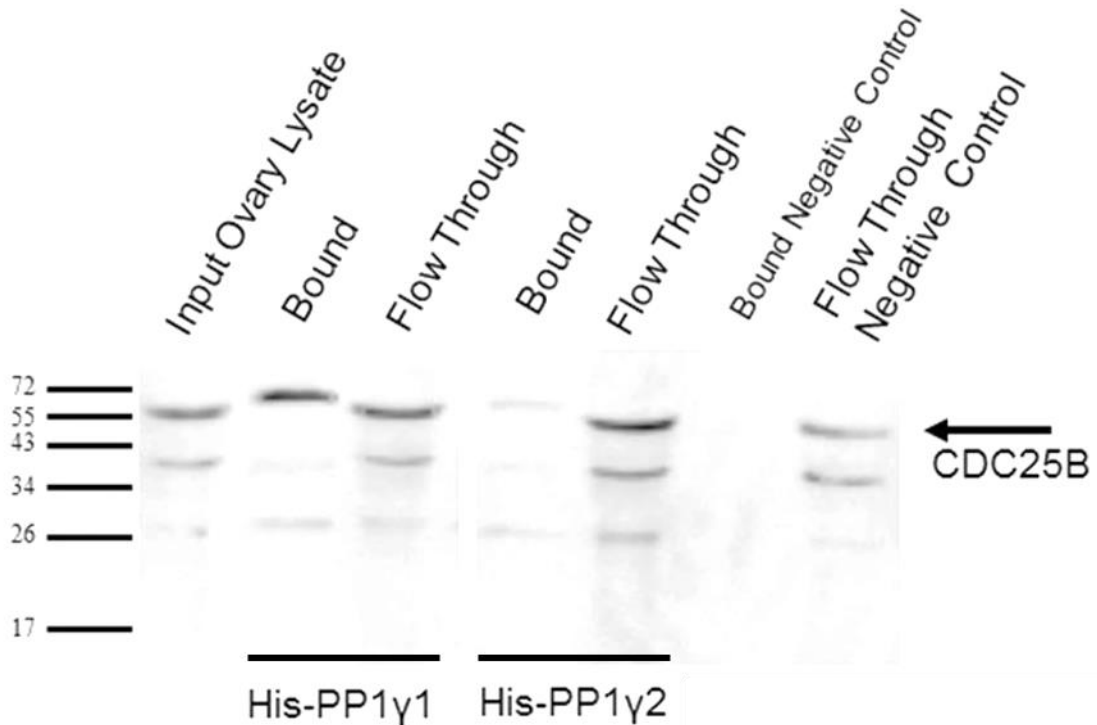


Figure 29. Pull down of CDC25B protein from WT ovaries by using His-tagged PP1 γ 1 and PP1 γ 2 recombinant proteins. Western blot of input, bound and flow through fractions of WT ovary using His-PP1 γ 1 and His-PP1 γ 2 probed with anti-CDC25B antibody. PP1 γ 1 binds strongly to CDC25B while the PP1 γ 2 shows weak binding.

PP1 α binds to CDC25b in the absence of PP1 γ

Using immunocytochemistry and western blot techniques, we show that PP1 α overexpressed in PP1 γ KO mice ovaries, oocytes and eggs. The different localization pattern for PP1 α in the presence and absence of PP1 γ might suggest different binding partners for PP1 α in both cases. In other words, PP1 α might bind to different binding partners in the absence of PP1 γ to compensate for its loss.

A co-immunoprecipitation assay was performed by incubating the PP1 α antibody with ovary lysates from both WT and PP1 γ KO mice ovaries. The Co-IP is a straightforward experiment to study protein-protein interaction. G-sepharose magnetic beads, which are used in the Co-IP, have a high affinity to the fragment of crystallizable (Fc) region of the IgG antibody. Thus, the PP1 α antibody will bind to the beads and precipitate the other binding partners. After the immuno-precipitation, the blot was run on gel electrophoresis and incubated with CDC25B antibody. The bound fraction of the PP1 γ KO ovaries show a strong interaction between PP1 α and CDC25B (Figure 30).

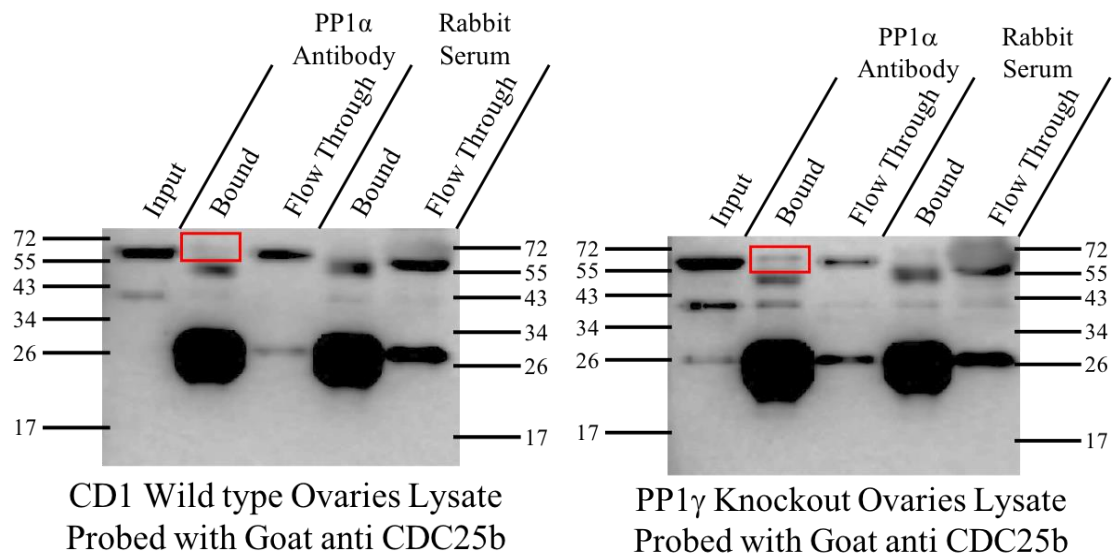


Figure 30. Immunoprecipitation of CDC25B protein from both PP1 γ KO and WT ovaries by using PP1 α antibody. Ovary lysate was incubated with PP1 α antibody which was then bound to Protein G beads. Control, Flow-through and bound fractions were collected and analyzed by Western blot with an antibody specific to CDC25B (red). There is little binding between PP1 α and CDC25B (65 kDa) in lysates from wild type mice (left panel). In the absence of PP1 γ , PP1 α appears to bind CDC25B to a greater degree (right panel).

Summary

Both PP1 γ 1 and PP1 γ 2 proteins are expressed in mouse oocytes and eggs. The role for these protein isoforms in oogenesis is still not entirely clear. However, knocking out both isoforms globally in mice appears to upregulate the protein phosphatase 1 isoform PP1 α . PP1 γ 1 shows strong binding to CDC25b in WT mouse ovaries. In the PP1 γ KO mice, the PP1 α expression is apparently upregulated and PP1 α binds CDC25B more than when PP1 γ proteins are present. The apparent upregulation of PP1 α in the absence of PP1 γ and the role of PP1 α on oogenesis needs further study.

3.1.3 Discussion

Evidence, mostly from inhibitor studies, with some more recent genetic manipulations of the genes, suggest the dephosphorylation of proteins by protein phosphatases is necessary at several unique steps in meiosis. For example, a recent study indicates the elimination of both isoforms of PP2A in the mouse oocytes has no effect on the growth of oocytes in ovarian follicles, or in the initial resumption of meiosis induced by hormone, suggesting that PP2A is not a potential candidate for the resumption of meiosis in prophase I arrested oocytes. However, oocytes lacking the two isoforms of PP2A failed to complete meiosis I correctly due to chromosome misalignment and abnormal spindle assembly resulting in infertility (Tang *et al.*, 2016). Also, elimination of Ppp6C in oocytes will disrupt meiosis II cytokinesis (Hu *et al.*, 2015).

The role of protein phosphorylation during mitotic cell division has been well studied in various cell models. However, it is more challenging to study the exact roles of kinases and phosphatases regulating meiosis due to the absence of stable cell cultures during this stage in both the male and female. A few phosphatases have been shown to have significant roles during mouse oocyte maturation with PP1 α and PP2A being the two most studied. PP1 γ 1 and 2 are differentially spliced variants of the same gene *PPP1CC*. While PP1 γ 1 protein is expressed widely in most of the somatic cells, PP1 γ 2 protein is predominantly expressed in the post-meiotic cells of the testis. It has been reported previously that the mRNA transcripts for PP1 α , PP1 γ 1, PP1 γ 2 and PP2A are present in the fully grown mouse oocytes and the protein levels for both PP1 α and PP2A

were detectible using western blotting and immunohistochemical staining. However, neither PP1 γ 1 nor PP1 γ 2 protein levels were detected previously (Smith *et al.*, 1998). Work on the characterization of PP1 family in mouse oocytes has been limited. Here, by using RT-PCR and single cell sequencing techniques we confirm the presence of both PP1 γ 1 and 2 transcripts in mouse ovaries, oocytes and eggs.

Previously, the protein expression of PP1 γ 1 and PP1 γ 2 proteins were unknown due to the unavailability of specific antibodies. However, we have two specific antibodies for PP1 γ 1 and PP1 γ 2, and we validated the antibodies for western blot by two different methods: 1) the antibodies were tested with his-tagged PP1 γ 1 or 2 recombinant proteins, and 2) the antibodies were tested after using microcystin beads to pull down PP1 isoforms.

Cell cycle progression is controlled by many factors including the phosphorylation and dephosphorylation cascades. The role of kinases, phosphatases and regulatory proteins in meiotic resumption are not clear and still under investigation. In *Xenopus* oocytes, the PP1 protein plays a crucial role in oocyte meiotic arrest by binding to dephosphorylated Cdc25b (Margolis *et al.*, 2003; Peng *et al.*, 1997). In mammalian oocytes, it has been suggested that PP1 has a role in oocyte maturation since okadaic acid, which is a phosphoprotein phosphatase inhibitor, releases the oocytes from the arrest. The specific isoform that may be involved and the interaction of these phosphatases is still not defined.

To clarify the role of each isoform of PP1, the expression of each isoform was characterized. Here, for the first time we show the expression of each isoform in both WT and PP1 γ KO mice eggs. PP1 γ 1 was found to be distributed evenly in the cytoplasm and nucleus of oocytes and eggs. Based on experiments with the PP1 (E9) antibody, which recognizes the catalytic core of the PP1 isoform, PP1 proteins do not appear to be distributed in the spindle. The absence of PP1 γ 2 protein from the egg spindle region was also reported when a fusion protein of EGFP and PP1 γ 2 was expressed in eggs (Gilker, 2018).

PP1 α is known to be overexpressed in PP1 γ KO mice testis (Chakrabarti, Kline, *et al.*, 2007). Here, we show that PP1 α is also upregulated and overexpressed in ovaries, oocytes and eggs of PP1 γ null mice by using western blot. Immunofluorescence shows more accumulation of PP1 α in the nucleus of PP1 γ KO oocytes. In PP1 γ KO eggs, PP1 α expresses highly with a clumping pattern towards the spindle. All PP1 isoforms are expressed in many subcellular compartments within eukaryotic cells with more expression in the nucleus (Lesage *et al.*, 2004; Rebelo *et al.*, 2015; Schindler, 2011). Also, previous reports show that PP1 α proteins accumulates in the nucleus of mouse oocytes (Smith *et al.*, 1998).

The protein phosphatase involved in activating CDC25B which subsequently activates CDK1 is still unknown. Some evidence suggests that PP1 α , PP1 β , or PP1 γ may play a central role by affecting a number of steps in meiosis, including the resumption of meiosis in prophase 1-arrested oocytes. The role of PP1 γ in oogenesis is somewhat

unclear, though the females of PP1 γ null appear to be normally fertile. Here, we show that PP1 γ 1 strongly binds to CDC25B in WT ovaries lysate which means that the CDC25B could be dephosphorylated by this isoform. PP1 α shows no binding to CDC25b in the WT ovaries extract. However, PP1 α is binding to CDC25B in the absence of PP1 γ . This finding suggests that the normal fertility of PP1 γ KO females might be due to the substitution of PP1 α in dephosphorylating the CDC25B complex. If this was the case, we expect to see a failure in oocytes maturation (oocytes stay arrested at Prophase I) from the double *PPP1CA* (PP1 α) and *PPP1CC* (PP1 γ) KO mice if those mice were generated. There is no clear answer for which PP1 isoform is the main player in oocyte maturation. We need more study of the interactions of PP1 isoforms with CDC25B in the mouse oocyte. The expression of PP1 β should be examined as well. The phosphoprotein phosphatase family is composed of PPP2C, PPP3C, PPP4C, PPP5C, PPP6C and PPEF including PPP1C (Korrodi-Gregório, Esteves, & Fardilha, 2014). This will add a possibility for another PPP in oocytes maturation other than PP1 α , β and/or γ .

3.2 Aim 2: To define the role of 14-3-3 eta and 14-3-3 epsilon in oocyte maturation

3.2.1 Rationale

Global 14-3-3 knockouts of different isoforms have not given us any information about oogenesis. The 14-3-3 gamma knockout shows no phenotype, although it is not clear that reproductive potential was examined in detail (Steinacker *et al.*, 2005). With global 14-3-3 epsilon knockout, mice die at birth due to cardiac malformations (Gittenberger-de Groot *et al.*, 2016). The prenatal embryos for the same knockout show hippocampal and cortical defects in the brain (Toyo-Oka *et al.*, 2003). The 14-3-3 zeta knockout also shows neurological defects (Cheah *et al.*, 2012; Kosaka *et al.*, 2012; Toyo-Oka *et al.*, 2014).

The role of 14-3-3 eta and epsilon in oogenesis were determined in this study by using an oocyte-specific conditional knockout and global knockout for 14-3-3 eta and epsilon. We particularly knocked out 14-3-3 eta to examine its role in oocytes meiotic arrest based on preliminary reported from our lab (De, 2014). We also examined knockout of 14-3-3 epsilon to confirm or reject the suggestion by other researchers that 14-3-3 epsilon is responsible for maintaining meiotic arrest. Moreover, it is conceivable that the conflicting results from knockdown experiments for eta and epsilon isoforms may be due to a partial reduction in oocyte maturation, particularly if 14-3-3 heterodimers of eta and epsilon form or if homodimers of each can substitute at least

partially for one another. We also produced mice with simultaneous oocyte-specific knockout of eta and epsilon isoforms of 14-3-3.

One report indicated that only 14-3-3 beta and 14-3-3 epsilon are present in mouse oocytes (Meng *et al.*, 2013). This was surprising since a panel of antibodies had identified more isoforms (De & Kline, 2013) and, for example, transcripts of at least six isoforms of 14-3-3 are present in mouse eggs (Detwiler, 2015; Pan, Ma, Zhu, & Schultz, 2008) and all seven 14-3-3 isoform messages are found in human eggs (Grøndahl *et al.*, 2010; Grøndahl *et al.*, 2013). In this report, we include additional evidence for the presence of 14-3-3 mRNA for seven isoforms of 14-3-3 mouse oocytes by using single cell sequencing technique.

3.2.2 Results

Messenger RNA analysis of 14-3-3 isoform expression in mouse oocytes and eggs

It has been reported that all seven 14-3-3 proteins are expressed in mouse oocytes and eggs based on the use of isoform-specific antibodies (De *et al.*, 2012). To confirm this observation, we examined expression transcripts in mouse oocytes of CD-1 wild-type mice and several knockout models by mRNA sequencing of single oocytes (Table 5). Reads from RNA-seq were annotated to Ensembl. FPKM (fragments per kilobase of exon model per million reads mapped), the normalized estimation of gene expression is based on the RNA-seq data, was estimated using Cufflinks. Message for all seven isoforms of 14-3-3 were detected.

Table 5. Expression of 14-3-3 isoform mRNAs in single oocytes

	<i>Ywhah</i> 14-3-3 (eta)	<i>Ywhae</i> 14-3-3 (epsilon)	<i>Ywhaq</i> 14-3-3 (tau/theta)	<i>Ywhaz</i> 14-3-3 (zeta)	<i>Ywhab</i> 14-3-3 (beta)	<i>Ywhag</i> 14-3-3 (gamma)	<i>Sfn</i> 14-3-3 (sigma)
Wild type	63.7	365.1	75.1	132.5	58.9	23.4	2.7
<i>Ywhae</i> 14-3-3 (epsilon) CKO	61.7	(13.1)	52.4	96.8	44.5	23.4	4.3
<i>Ywhah</i> 14-3-3 (eta) CKO	(0.6)	323.7	87.3	126.3	47.8	19.5	7.6
<i>Ywhae</i> and <i>Ywhah</i> 14-3-3 (eta/epsilon) double CKO	(0.5)	(18.3)	119.0	97.5	48.1	13.3	7.6

FPKM values for 14-3-3 isoform transcript in a single oocytes of wild type, *Ywhae* (14-3-3 epsilon) oocyte-specific knockout (CKO), *Ywhae* (14-3-3 eta) CKO and a double knockout oocyte-specific *Ywhae* and *Ywhah* (14-3-3 eta/epsilon). Ensembl transcript IDs (mouse version GRCM38.p6): *Ywhah*, ENSMUST00000019109; *Ywhae*, ENSMUST00000067664; *Ywhaq*, ENSMUST00000135088; *Ywhaz*, ENSMUST00000022894; *Ywhab*, ENSMUST00000018470; *Ywhag*, ENSMUST00000055808; *Sfn*, ENSMUSG00000047281.

Inactivation of 14-3-3 eta and epsilon by oocyte-specific and global knockout

To definitively characterize the role of 14-3-3 eta protein in mouse oocytes we produced a line that has LoxP sites flanked in exon 2 in the mouse *Ywhah* (14-3-3 eta) gene (Figure 31) (see Methods). We also obtained mice containing LoxP sites in the *Ywhae* (14-3-3 epsilon) gene to remove exons 3 and 4 of the gene after Cre recombination. These mice were bred with mice expressing Zp3 Cre or ACTB Cre. Expression of Zp3 Cre is driven by the zona pellucida protein 3 (Zp3) promoter and is expressed only in oocyte beginning primary follicles and expression is maintained in oocytes in preantral follicles (Lan, Xu, & Cooney, 2004). Expression of Zp3 Cre in oocytes of mice expressing LoxP sites in a gene will generate an oocyte-specific knockout of the gene. Breeding with ACTB Cre mice can generate a global knockout. ACTB Cre is driven by the human beta actin gene promoter and is expressed in all cells of the embryo by the blastocyst stage (Lewandoski *et al.*, 1997). It is expected then to act on LoxP constructs in early cells of the blastocyst to generate embryos and adults in which gene function is altered in all cells. We utilized PCR and primers for LoxP sites, Cre, and knockout genes to confirm gene disruption as well as antibodies to demonstrate absence of protein in knockout animals (Figure 32 and 33) (see Methods).

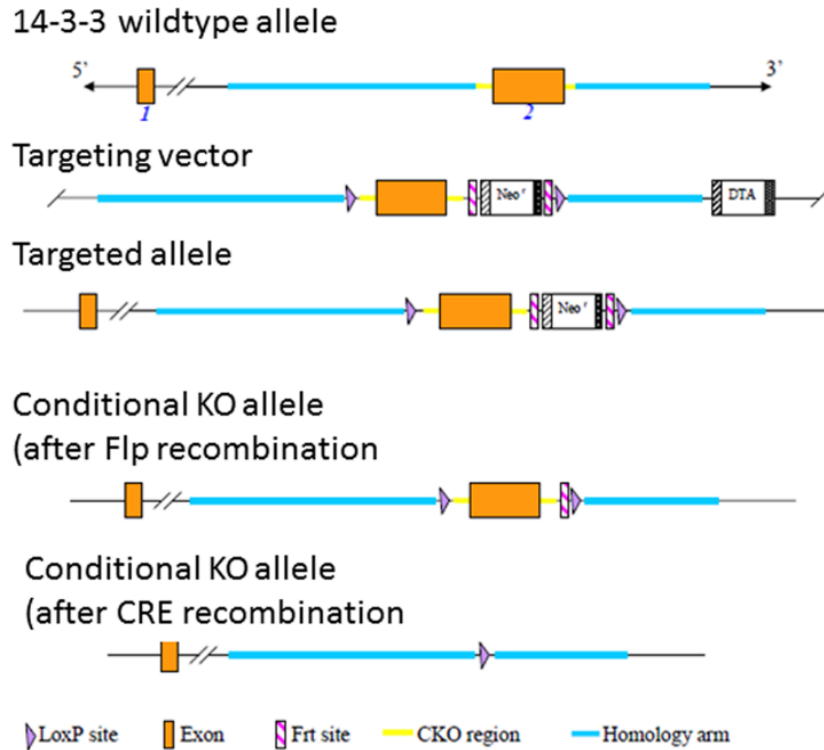


Figure 31. Diagrammatic summary of the production of 14-3-3 eta oocyte-specific conditional knockout. Exons 1 and 2 of the 14-3-3 eta gene are represented by orange boxes. The targeting vector and homology arms are indicated. The vector was electroporated into C57BL/6 ES cells, chimeras were produced, and germ line transmission in C57BL/6J was confirmed. Exon 2 is removed following Cre recombination (see Methods)

Oocyte-specific 14-3-3 eta or 14-3-3 epsilon inactivation does not alter *in vivo* breeding

In vivo breeding of female 14-3-3 eta or 14-3-3 epsilon knockout mice indicated that reproductive capacity is not greatly altered with oocyte-specific inactivation of the genes when breeding of pairs were maintained for at least two months. Female mice with oocyte-specific knockout of 14-3-3 eta or 14-3-3 epsilon were mated with wildtype male mice and these mice produced litters with similar numbers of pups compared to those mice containing only the floxed alleles for 14-3-3 eta or epsilon or female mice containing only the transgene for the Zp3 or ACTB Cre recombinase with no modification of the 14-3-3 genes. The females were genotyped to confirm the knockout condition, and, in some cases, absence of the gene was also confirmed by Western blot (Figure 32 and 33).

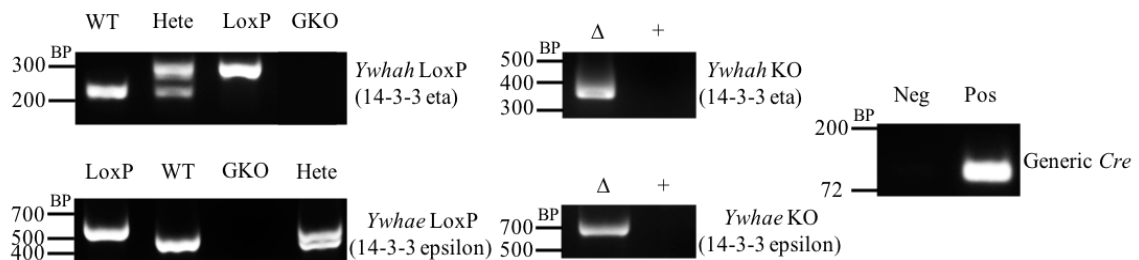


Figure 32. Whole animal genotyping identifies those females with global and oocyte specific gene deletion. 14-3-3 eta and epsilon LoxP primers indicate the presence of LoxP on the 14-3-3 genes, if the upper band is present. The lower band indicates WT and absence of a band indicates a possible gene deletion (-/-). The 14-3-3 eta and epsilon KO primers indicate a deletion (Δ) of one or both alleles if a band is present. The presence of a LoxP band using the 14-3-3 eta and epsilon LoxP primers, a band in the KO primers and a band in the Generic Cre from Zp3 line indicates a oocyte specific knockout (-/LoxP) since the second LoxP will be deleted later in the ovaries. On the other hand, the presence of both LoxP and WT bands with no Cre (LoxP/WT) Cre negative indicates a full functional gene and a WT phenotype in this mouse.

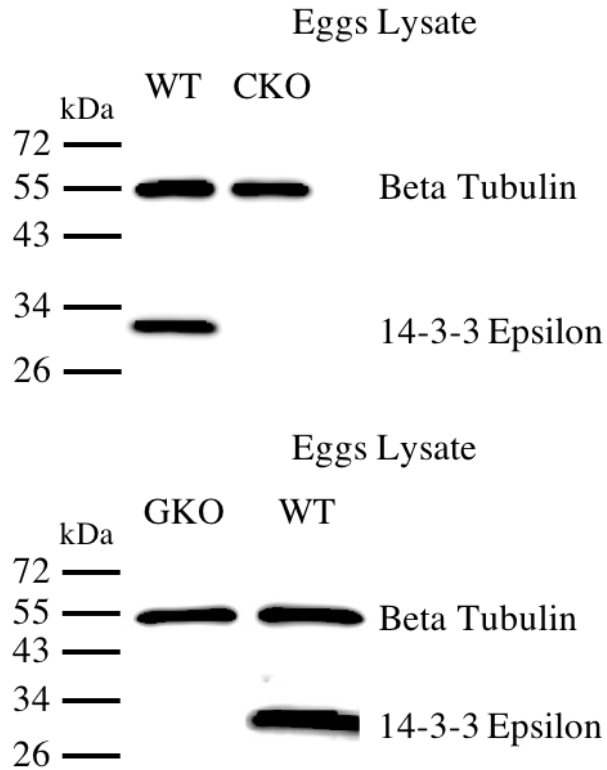


Figure 33. Validation of 14-3-3 epsilon ablation in both 14-3-3 epsilon CKO and GKO eggs by western blot. Representative Western blot of cell lysates of eggs collected from wild-type females, lysates of oocyte-specific knockout of 14-3-3 epsilon (upper panel) and lysates of eggs collected from the global knockout of 14-3-3 epsilon (lower panel). The blots are probed with antibodies for 14-3-3 epsilon or tubulin (loading control). 14-3-3 epsilon protein was not detected in the knockout eggs.

Females with oocyte-specific inactivation of 14-3-3 eta or epsilon are fertile and litter sizes fall in the normal range when compared to litter sizes of females in which 14-3-3 eta or epsilon genes are not inactivated. It should be noted variation in litter number is common and depends on the characteristics of the female and male in the breeding pairs and other factors. The litter sizes of females with global inactivation of 14-3-3 eta in all tissues, including the ovary, are like those of the oocyte-specific knockout animals and are similar to the litter sizes of females in which the gene is not inactivated. In contrast however, no offspring were produced when the gene for 14-3-3 epsilon was globally inactivated in all tissues, including the ovary (Figure 34). As described below, oocytes from both oocyte-specific and global 14-3-3 epsilon knockout mice appear to mature normally. In addition, eggs collected from females with oocyte-specific 14-3-3 epsilon inactivation can be fertilized *in vitro* to produce two-cell embryos without adverse effect on the first meiotic division. Inhibition of *in vivo* breeding in the global 14-3-3 epsilon but not the oocyte-specific, knockout mouse suggests that 14-3-3 epsilon may be required in somatic cells in other tissues affecting reproductive potential.

The *in vivo* breeding data suggests that normal offspring are produced despite oocyte-specific inactivation of the genes for 14-3-3 eta or epsilon. To further examine the characteristics of oocytes from these knockout animals we collected oocytes as usual and matured them *in vitro* to determine if there was any difference in the number of germinal vesicle-intact oocytes collected or any difference in the extent of maturation *in vitro*. Absence of 14-3-3 eta or epsilon protein in oocytes does not appear to affect the number of germinal vesicle-intact oocytes isolated from females primed with eCG and cultured in

3-Isobutyl-1-methylxanthine (IBMX) to prevent spontaneous maturation. The oocytes are of typical size and normal morphology. The extent of *in vitro* maturation was not altered when oocytes were allowed to mature in media without IBMX. For each female, oocytes cultured overnight in IBMX-free media were classified as having intact GVs or having undergone GVBD indicating oocyte maturation (Figure 35-37). One way ANOVAs were run to examine the significant difference between groups, where the P value of less than 0.05 is considered to indicate a significant difference. Absence of either isoform, 14-3-3 eta or epsilon, or both of them in a double 14-3-3 eta/epsilon knockout mice does not appear to alter oocyte quality or *in vitro* maturation to any degree. The P value for each group were as follow: 14-3-3 eta (p value = 0.3992); 14-3-3 epsilon (p value = 0.6993) and 14-3-3 eta/epsilon (p value = 0.4211) (Figure 38).

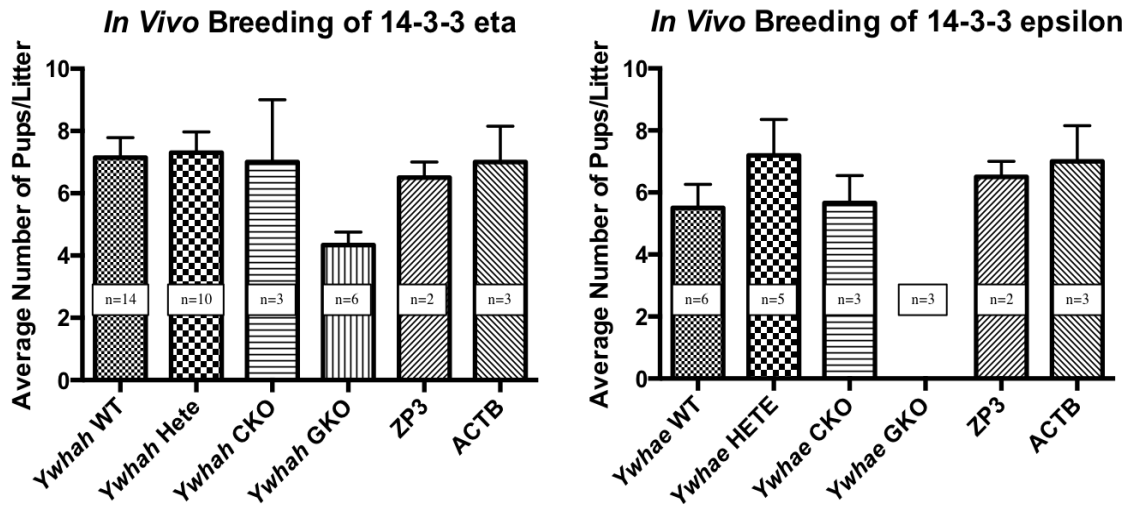


Figure 34. *In vivo* breeding for 14-3-3 eta and epsilon KO females. The fertility 14-3-3 eta and epsilon CKO and GKO were tested by *in vivo* breeding of transgenic females with WT males. The average number of pups born for the first two litters were recorded for breeding pairs (n) for each categories. The 14-3-3 eta GKO and CKO females appear to be fertile, in addition to the 14-3-3 epsilon CKO females. However, females with global 14-3-3 ϵ deletion produced no pups during the experiment. Error bars represents SE.

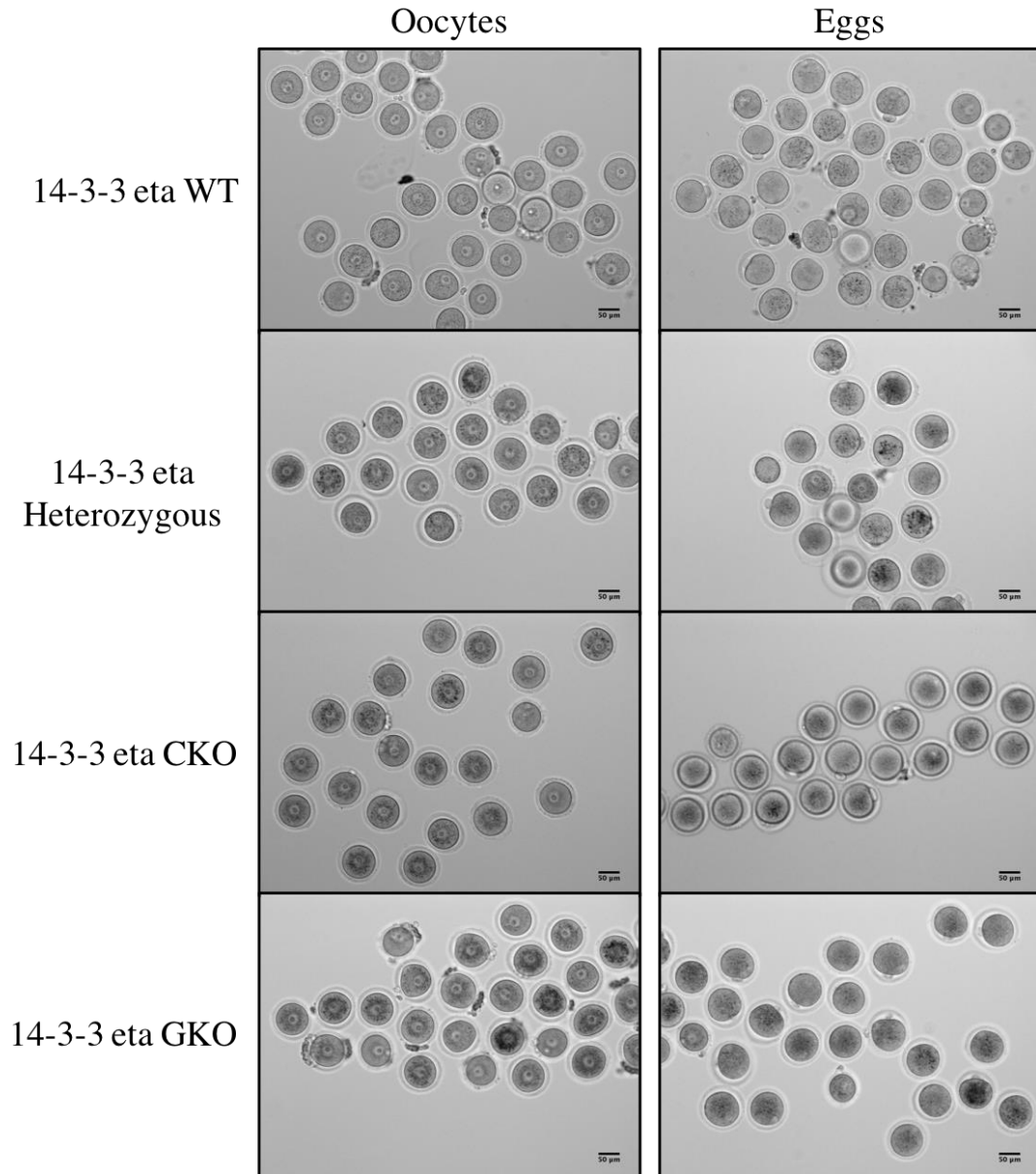


Figure 35. *In vitro* maturation of the 14-3-3 eta CKO and GKO oocytes. Representative images of oocytes collected from 14-3-3 eta CKO and GKO females and the corresponding images of the mature eggs the following day after *in vitro* maturation of oocytes. Oocytes from 14-3-3 eta knockouts females appear normal with intact germinal vesicles. The eggs also appear normal with the presence of first polar body. Scale bars represent 50 μ m.

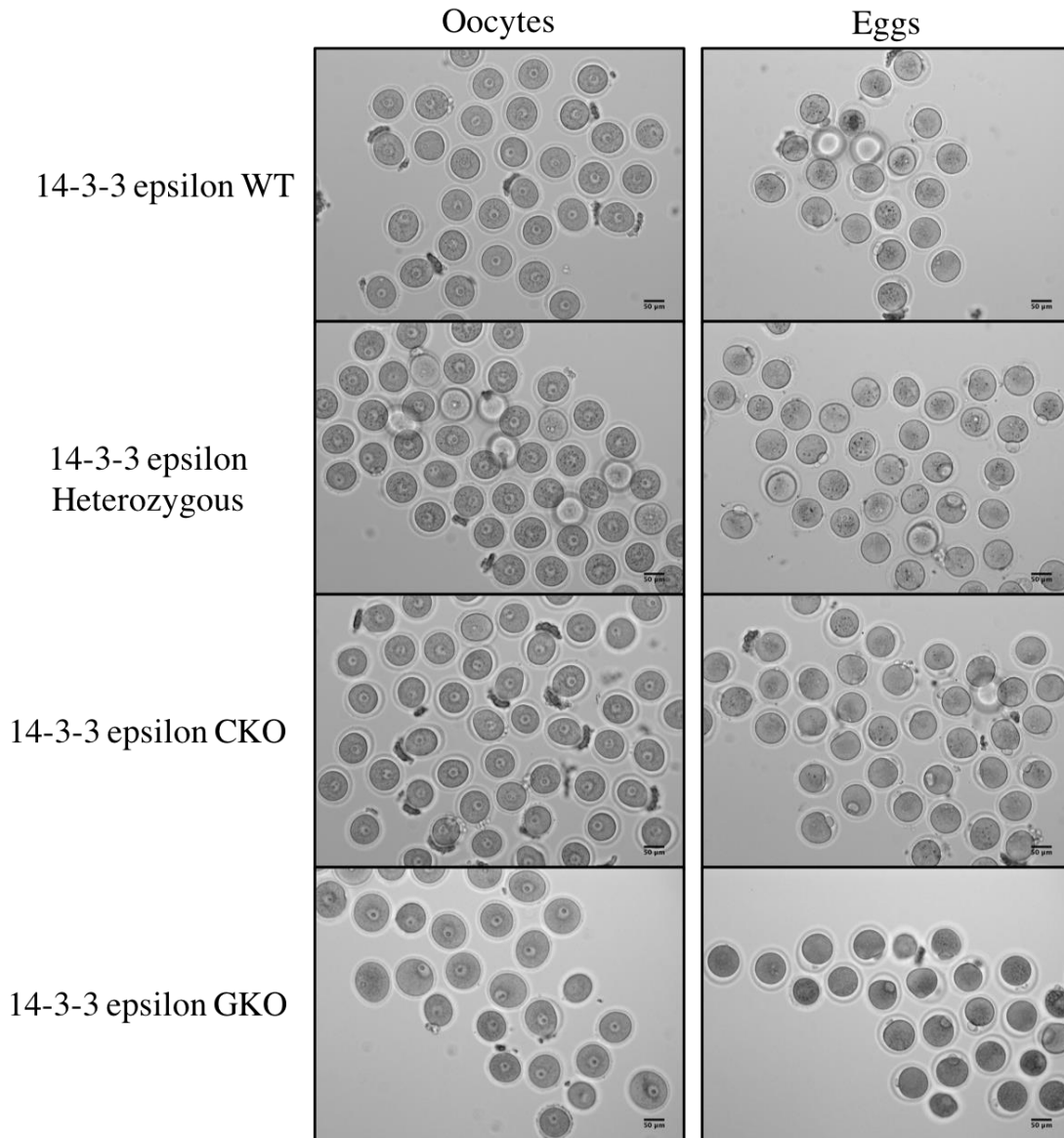


Figure 36. *In vitro* maturation of the 14-3-3 epsilon CKO and GKO oocytes. Representative images of oocytes collected from 14-3-3 epsilon CKO and GKO females and the corresponding images of the mature eggs the following day after *in vitro* maturation of oocytes. Oocytes from 14-3-3 epsilon knockout females appear normal with intact germinal vesicles. The eggs also appear normal with the presence of first polar body. Scale bars represent 50 μ m.

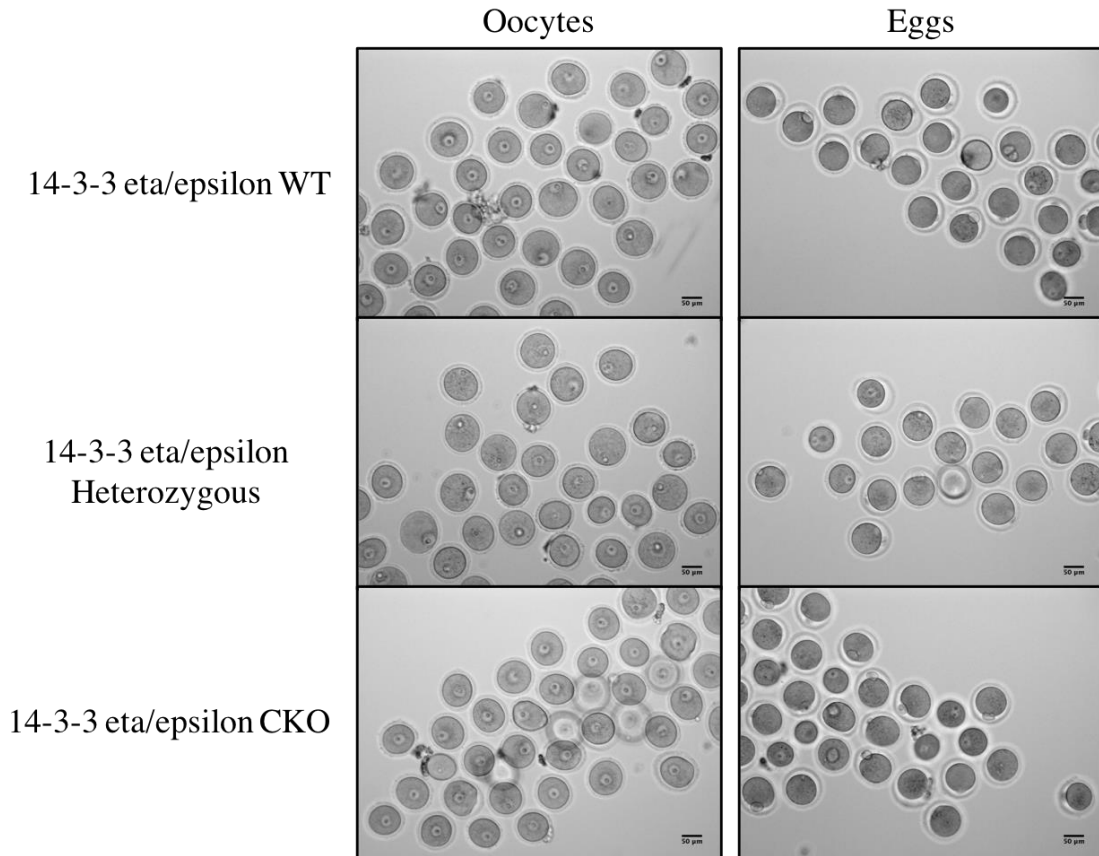


Figure 37. *In vitro* maturation of the 14-3-3 eta/epsilon double CKO oocytes. Representative images of oocytes collected from 14-3-3 eta/epsilon CKO females and the corresponding images of the mature eggs the following day after *in vitro* maturation of oocytes. Oocytes from 14-3-3 eta/epsilon CKO females appear normal with intact germinal vesicles. The eggs also appear normal with the presence of first polar body. Scale bars represent 50 μ m.

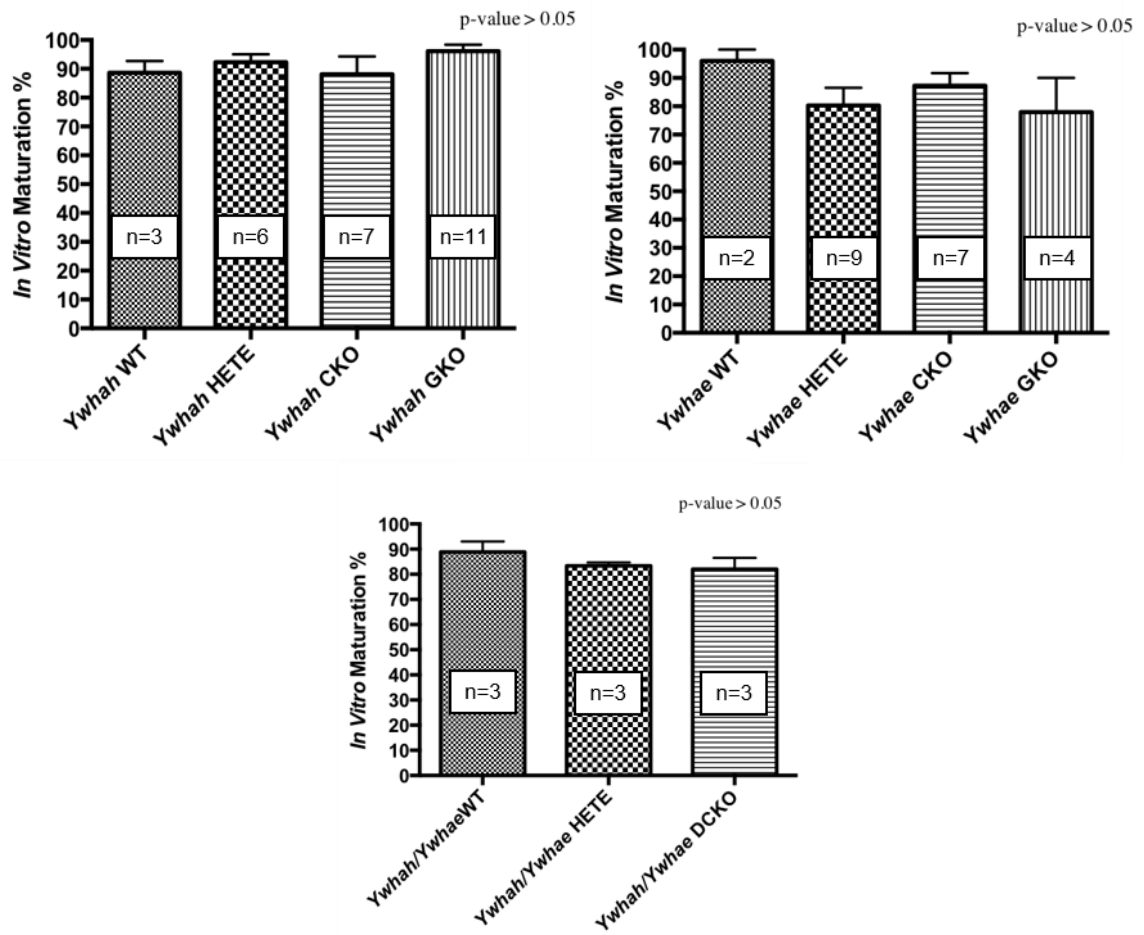


Figure 38. *In vitro* maturation rate of 14-3-3 eta KOs, epsilon KOs and eta/epsilon double CKO. *In vitro* maturation rate of oocytes from females in which either or both 14-3-3 eta and epsilon genes were inactivated in the oocyte, oocytes from females in which one allele of 14-3-3 eta or epsilon was inactivated (heterozygous), or oocytes from wild-type females. Error bars represent SE.

In vitro fertilization of mice with oocyte-specific inactivation of 14-3-3 epsilon is normal

To further examine the role of 14-3-3 epsilon in mouse oocytes we examined the fertilization potential and early development of eggs collected by superovulation from five different oocyte-specific knockout females. The fertilization rates (number of two-cell stage/total number of eggs) for 14-3-3 epsilon WT, Hete and CKO were 45.5%, 42.7% and 44.9% respectively. Eggs from a given 14-3-3 epsilon knockout female were fertilized and developed normally to the two-cell stage, which is comparable to typical *in vitro* fertilization rates of wild-type mice (Figure 39). One way ANOVA analysis was used to test the fertilization rate differences between 14-3-3 epsilon WT, Hete and CKO. There was no significance difference between the groups (p value = 0.6213). In two cases, fertilized eggs from two 14-3-3 epsilon knockout female were continued in cultured and developed to the morula and/or blastocyst stage (Figure 40).

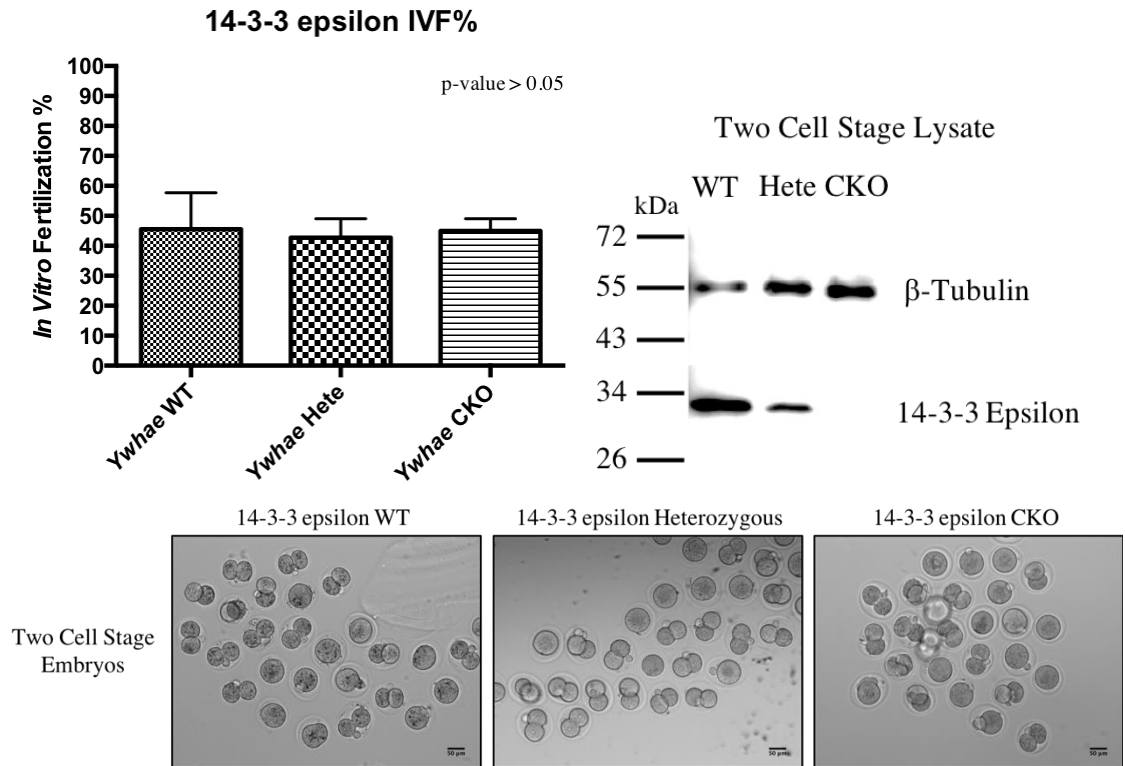


Figure 39. *In vitro* fertilization of eggs from 14-3-3 epsilon knockout females. Upper left panel) Fertilization rate is the percent of eggs that proceeded to the two-cell stage. There was no significant difference between the fertilization rate of 14-3-3 epsilon WT, Hete and CKO (*p* value = 0.6213). Error bars represents SE. Upper right panel) Representative Western blot of 2-cell embryos lysates from fertilized wild-type eggs, heterozygous and from oocyte-specific knockout of 14-3-3 epsilon. The blots are probed with antibodies for 14-3-3 epsilon or tubulin (loading control). The 14-3-3 epsilon protein was not detected in the knockout two-cells embryos. Lower panel) Representative images of fertilized eggs from oocyte-specific 14-3-3 epsilon knockout females, heterozygous and wild-type females. Scale bars represent 50 μ m.

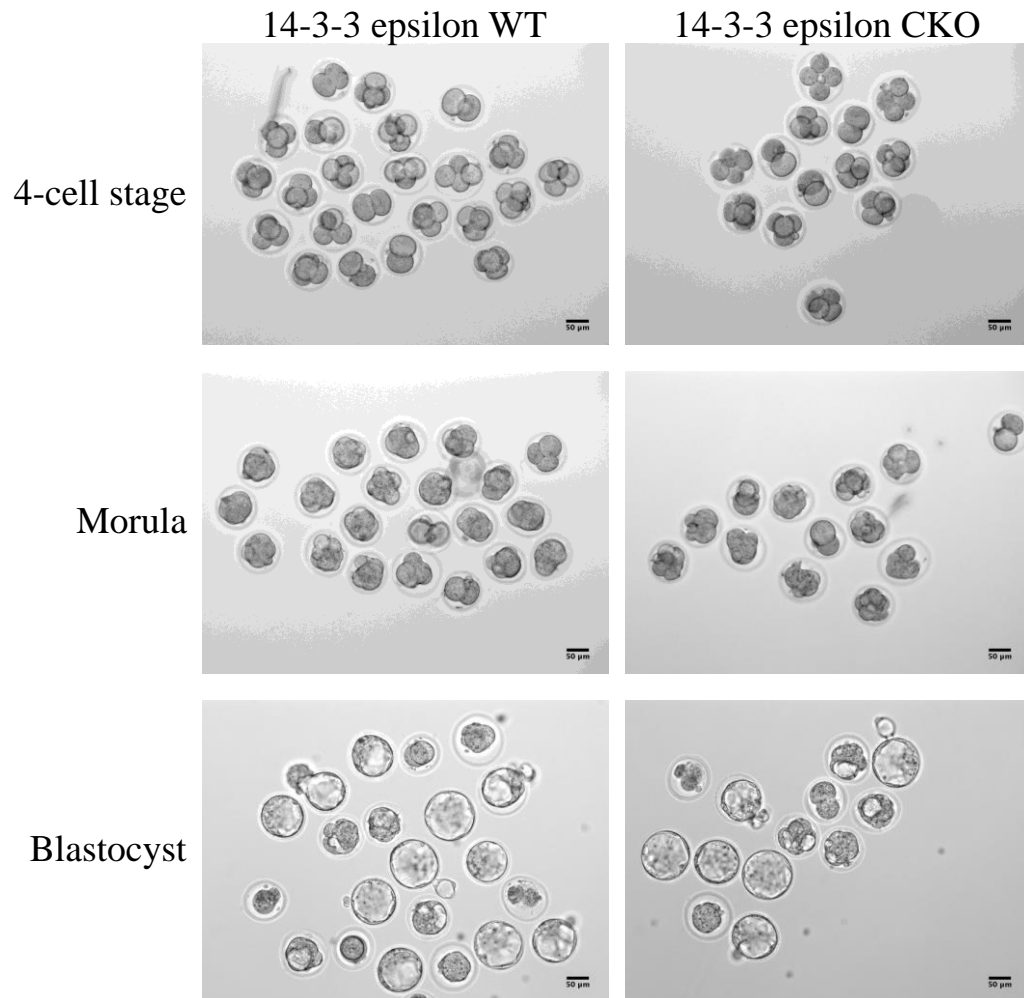


Figure 40. Embryonic development of the 14-3-3 epsilon KO mice. Embryos from two 14-3-3 epsilon knockout females were continued in culture and developed to 4-cell, morula and blastocyst stage.

Summary:

We find that multiple isoforms of 14-3-3 are present in mouse oocytes. While this work and other research suggests that 14-3-3 proteins may bind to and regulate the activity of CDC25B, and possibly other proteins that regulate oocyte maturation, the oocyte-specific gene knockout experiments indicate that 14-3-3 eta or epsilon proteins are not required for normal oogenesis, oocyte maturation and development. The data suggest that one or several of the other isoforms may compensate for the absence of 14-3-3 eta or epsilon proteins within the oocyte and this possibility should be explored. The global inactivation of 14-3-3 eta in female mice does not appear to alter oogenesis, oocyte maturation, and development, while the global inactivation of 14-3-3 epsilon in female mice prevents breeding without affecting oogenesis, oocyte maturation, or *in vitro* fertilization.

3.2.3 Discussion

Multiple 14-3-3 isoform expression in mouse oocytes and eggs

Single cell mRNA sequencing revealed transcripts for all 14-3-3 seven isoforms in ICR (CD-1) mice and in various knockout models. In contrast, one report indicates that only 14-3-3 beta and 14-3-3 epsilon transcripts could be detected in mouse oocytes (Meng *et al.*, 2013). However, several other published reports on mouse egg 14-3-3 message expression agree with our results. Notably, in an expression profiling study of mature mouse eggs (Pan *et al.*, 2008), six 14-3-3 isoforms were detected (*Sfn* was not listed in this report). In a different analysis of maternal mRNA expression in mature eggs (Potireddy, Vassena, Patel, & Latham, 2006) 14-3-3 beta (*Ywhab*), gamma (*Ywhag*), eta (*Ywhah*), tau (*Ywhaq*) and zeta (*Ywhaz*) were noted (others were not mentioned in this report which examined only large changes in expression profiles of late one cell embryos compared to eggs). Of additional interest are two reports on human eggs clearly indicating the all seven isoforms of 14-3-3 message are present in the human egg (Grøndahl *et al.*, 2010; Grøndahl *et al.*, 2013). Taken together, our data on 14-3-3 transcripts and protein expression, along with other published results indicates presence of transcripts and proteins of all seven 14-3-3 isoforms in mouse and human oocytes and eggs. Therefore, it is prudent to consider all 14-3-3 isoforms in any analysis of 14-3-3 functional roles in oocyte maturation, fertilization and early development.

Oocyte-specific 14-3-3 eta or epsilon gene inactivation does not alter *in vivo* breeding or *in vitro* oocyte maturation

If meiotic arrest was solely and completely dependent on 14-3-3 eta or epsilon binding to CDC25B, one might expect that elimination of either of these proteins could lead to premature oocyte maturation, since CDC25B would not be held in the cytoplasm in an inactive state in oocytes within the follicle. We found no evidence that oogenesis was altered when either 14-3-3 eta or epsilon proteins or both were absent. Oocytes obtained from these animals after eCG priming had intact GV's, were normal in size and morphology, and there was no indication of premature meiosis I resumption. Oocytes from these animals underwent normal *in vitro* maturation. Previous work, using antisense morpholino knockdown approaches suggested that 14-3-3 eta plays a role in meiotic spindle formation (De & Kline, 2013). The gene knockout experiments presented here suggest that, if 14-3-3 proteins are required in spindle formation, other isoforms might substitute for 14-3-3 eta. It would be valuable to follow up on this line of research. Breeding and development of pups was normal in the absence of 14-3-3 eta or epsilon in females with oocyte-specific knockout of these genes.

Global inactivation of 14-3-3 eta gene inactivation does not alter *in vivo* breeding or *in vitro* oocyte maturation

As with oocyte-specific 14-3-3 eta inactivation, we found no apparent difference in fertility, oogenesis or *in vitro* maturation of cells obtained from animals with global inactivation of the 14-3-3 eta gene compared to animals containing the gene. This suggests that 14-3-3 eta protein is not required in germ cells or in somatic cells for normal reproduction. We found no obvious abnormal phenotype in 14-3-3 eta knockout females. This indicates that 14-3-3 eta protein is not essential for female reproduction and early embryonic development and, given the importance of 14-3-3 in many cellular events, other isoforms of 14-3-3 might substitute. Normal morphology and presumably normal fertility in female 14-3-3 eta knockout mice has also been recently reported by other investigators who found that absence of 14-3-3 eta protein leads to deafness and hair cell degeneration (Buret, Delprat, & Delettre, 2016).

Global deletion of 14-3-3 epsilon in females prevents breeding without affecting oogenesis, oocyte maturation, or *in vitro* fertilization

No offspring were produced by females when the 14-3-3 epsilon was inactivated in all tissues, including the ovary and oocytes. However, oocytes collected from these mice appear to mature normally *in vitro*. With germ-line deletion of 14-3-3 epsilon in a global knockout, mice die at birth due to cardiac malformations (Gittenberger-de Groot *et al.*, 2016). Deletion of 14-3-3 epsilon in oocytes is apparently compensated by introduction of the normal gene from sperm at fertilization, since apparently normal pups are produced in the oocyte-specific knockout of 14-3-3 epsilon, while in the female

14-3-3 epsilon protein may be required in somatic cells in other tissues of the female, for example in the uterus where implantation might be altered. This observation suggests an important role for 14-3-3 epsilon that will need to be examined. It has been reported that only 14-3-3 epsilon message is expressed in mouse eggs and that knockdown of 14-3-3 epsilon by small interference RNA inhibits first mitosis in some percentage of fertilized mouse eggs (Cui *et al.*, 2014). We find that the oocytes collected from females in which 14-3-3 epsilon is disrupted in oocytes undergo normal *in vitro* maturation, *in vitro* fertilization and early development to the 2-cell stage. Expression of 14-3-3 epsilon does not appear to be required for the first mitotic division nor does absence of the protein interfere with the first mitosis.

Future research

Given the central role of 14-3-3 proteins in regulating the mitotic cell cycle and evidence for regulation of meiosis, additional work is needed to define the roles of the specific isoforms. All 14-3-3 isoforms need examination. Other cell cycle control proteins, in addition CDC25B, will need to be examined in more detail to complete the analysis of 14-3-3 proteins in meiotic regulation. Certainly, a number of cell cycle control proteins interact with 14-3-3, reviewed in (Hermeking & Benzinger, 2006). For example, it is known that 14-3-3 proteins interact with Wee1 in frog egg extracts (Lee, Kumagai, & Dunphy, 2001), in human somatic cells (Meek *et al.*, 2004; Rothblum-Oviatt, Ryan, & Piwnica-Worms, 2001) and with expressed mouse Wee1 protein (Honda, Ohba, & Yasuda, 1997; Y. Wang *et al.*, 2000). Further study will be needed to examine the interaction of 14-3-3 protein with the oocyte-specific WEE2, its activity and the phosphorylation of CDK1.

CHAPTER 4

Aim 3

4.1 Aim 3: To study the role of 14-3-3 eta and epsilon in spermatogenesis

4.1.1 Rationale

The 14-3-3 (YWHA) proteins in mammals consist of seven isoforms encoded by seven independent genes: *Ywhab* (14-3-3 beta), *Ywhae* (14-3-3 epsilon), *Ywhah* (14-3-3 eta), *Ywhag* (14-3-3 gamma), *Ywhaz* (14-3-3 zeta), *Ywhaq* (14-3-3 tau/theta), *Sfn*, (14-3-3 sigma). Multiple isoforms usually exist in many species including plants which contain as many as 15 isoforms. The 14-3-3 proteins are highly conserved and have been shown to bind to various cellular proteins where they complement or supplement intracellular events involving protein-protein interaction or subcellular localization (Dougherty & Morrison, 2004; Carol Mackintosh, 2004). Most of the binding partners of 14-3-3 are phosphorylated; proteins containing phospho-serine and phospho-threonine residues within their RSXpSXP and RX(Y/F)XPSXP amino acid sequence motifs. However, phosphorylation-dependent sites that differ significantly from these motifs have been reported (Aitken *et al.*, 2002) and some interactions of 14-3-3 do exist independent of phosphorylation. The molecular and biochemical effects of 14-3-3 binding are diverse, depending upon the nature of the interacting proteins and the signaling pathways involved. *Ywha* or 14-3-3 proteins have been shown to regulate the localization and

phosphorylation status of proteins and modulate the activity of enzymes (Bridges & Moorhead, 2005). This protein also binds to over 300 proteins regulating a wide variety of cellular pathways such as transcription, translation, splicing, protein trafficking, and cell division. 14-3-3 mediated regulation of cell division is biochemically well defined. YWHA protein is known to play a key regulatory role in both mitosis and meiosis. The 14-3-3 proteins exist as homo- or hetero-dimers with a monomeric molecular mass of approximately 30 kDa (Aitken, 2006).

Previous work identified 14-3-3 proteins in oocytes and in sperm (De *et al.*, 2012; Puri *et al.*, 2008). 14-3-3 proteins also have been identified in Sertoli cells, where they may play a role in adhesion, and also in Leydig cells in testis (Chaudhary & Skinner, 2000). In sperm, 14-3-3 was first identified as a protein phosphatase (PP1 γ 2) binding protein (Puri *et al.*, 2008). A catalytically active form of PP1 γ 2 was found bound to 14-3-3 in sperm. Using TAP-tag and GST-14-3-3 pull down approaches several 14-3-3 binding proteins were identified in testis and sperm (Puri *et al.*, 2011). However, the functions of sperm 14-3-3 however have remained elusive. In this report, we describe the phenotypes in male mice lacking 14-3-3 eta or epsilon. The 14-3-3 epsilon isoform is highly expressed in developing testis with its expression temporally coinciding with the onset of spermatogenesis. Data presented here show that 14-3-3 epsilon is essential for normal spermiogenesis and sperm function whereas loss of the eta isoform is dispensable. Loss of the 14-3-3 epsilon isoform affects sperm morphogenesis and energy metabolism. The phosphorylation status and the catalytic activities of protein phosphatase PP1 γ 2 and glycogen synthase kinase 3 (GSK3) are altered in sperm lacking 14-3-3 epsilon. This is

the first report documenting the essential requirement of one of the seven isoforms, 14-3-3 epsilon, the loss of which cannot be compensated by the other six despite their presence and expression in testis.

4.1.2 Results

14-3-3 eta and 14-3-3 epsilon expression in mouse testis and sperm

It is known that 14-3-3 proteins are present in mammalian testis and sperm (Baker, Hetherington, Reeves, & Aitken, 2008; Puri *et al.*, 2011, 2008), but identification of each of the seven isoforms remains elusive. With the isoform specific antibodies, our western blot analysis showed that 14-3-3 epsilon was present in both testis and sperm lysates whereas signal for 14-3-3 eta was seen only in testis lysates (Figure 41). Next, we examined expression of 14-3-3 epsilon mRNA in post-natal developing mouse testis using qPCR. Figure 42 shows that the expression of 14-3-3 epsilon increased with age coinciding with the onset of spermiogenesis (after 20 days postnatal) and the levels were highest in adult testis. To determine the localization of the protein in testis and sperm in WT mice, testes and sperm were fixed and probed by immunofluorescence with mouse monoclonal antibodies against 14-3-3 epsilon. In sperm, a pan 14-3-3 antibody that detects multiple 14-3-3 isoforms was used to determine localization of the other 14-3-3 isoforms compared to 14-3-3 epsilon. Results with the pan 14-3-3 antibody indicate that 14-3-3 proteins are primarily present in the post-acrosomal and midpiece regions of sperm. In contrast, the 14-3-3 epsilon specific antibody indicated that this isoform was primarily in the midpiece of sperm (Figure 43). In testis, 14-3-3 epsilon was present in

differentiating germ cells but apparently not in spermatogonia which are the first layer of cells within the seminiferous tubule (Figure 44).

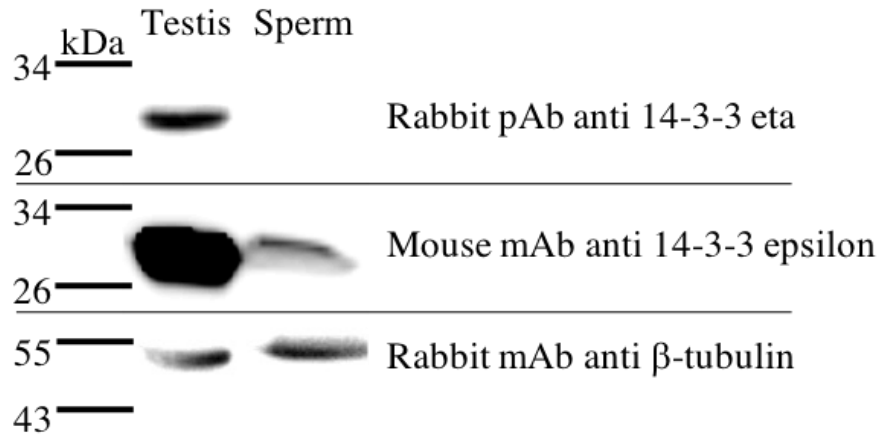


Figure 41. Expression of 14-3-3 eta and epsilon in mouse testis and sperm by using western blot. Western blot analysis of testis and sperm lysates from WT mice shows detection of 14-3-3 eta only in testis lysates while the expression of 14-3-3 epsilon for the same blot was detected in both testis and sperm lysates. The blot later was probed with β -tubulin to show equal sample loading.

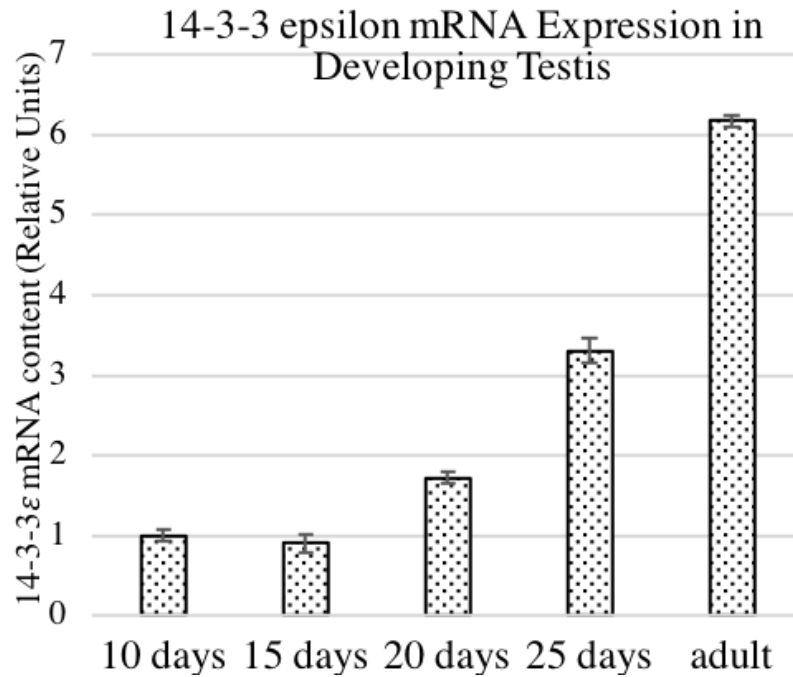


Figure 42. Messenger RNA expression of 14-3-3 epsilon in developing testis by using qPCR. Testes were collected from pups at the postnatal day shown. Messenger RNA was isolated by using TRIZOL reagent. Expression of 14-3-3 epsilon mRNA was quantified with qPCR using specific primers for 14-3-3 epsilon and GAPDH primers as a housekeeping gene. The expression of 14-3-3 epsilon increases with age and the highest expression was found in mature adults. These data are representative a triplicate experiment, and error bars represent Standard of Error (SE).

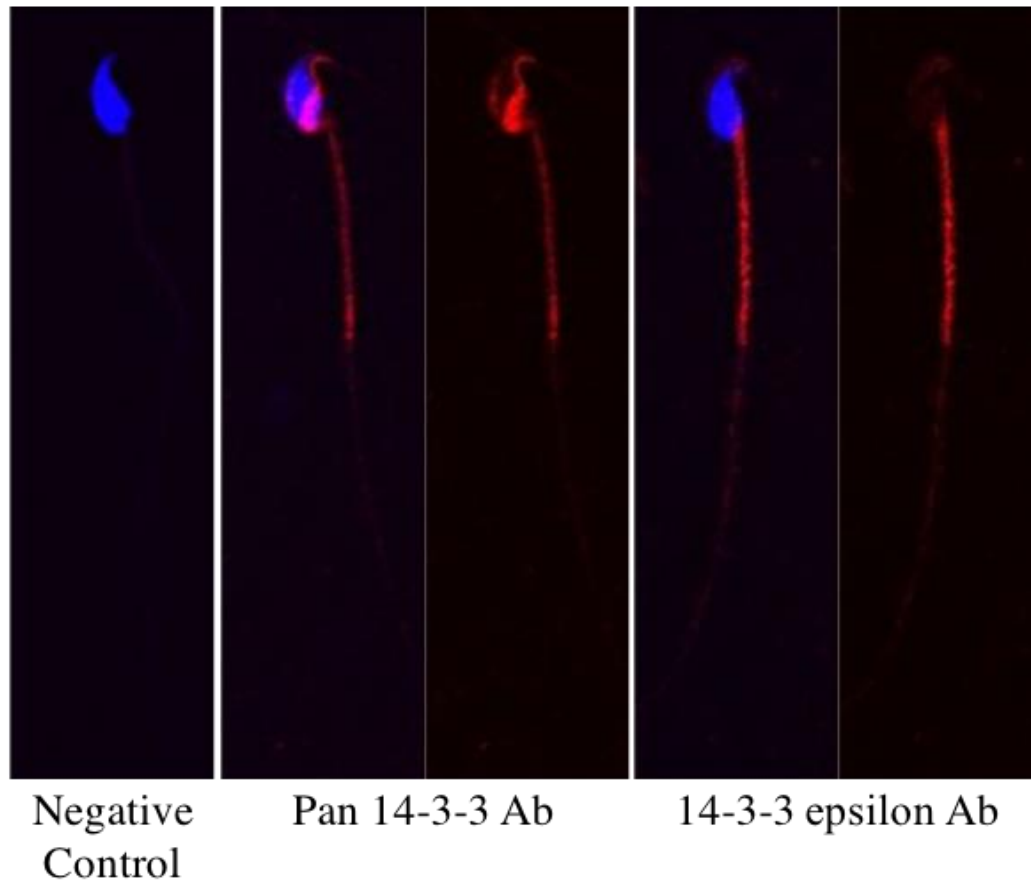


Figure 43. Pan 14-3-3 and 14-3-3 epsilon expression in mouse sperm by using immunofluorescence technique. Sperm was collected from WT mice, fixed with 4% PFA for 45 minutes and stained with either polyclonal goat anti 14-3-3 epsilon or polyclonal rabbit anti Pan 14-3-3 as a primary. The slice then stained with either anti goat antibody CY3 or anti rabbit antibody CY3 counterstained with Hoechst. Cells were imaged using confocal microscopy. Pan 14-3-3 is localized in post-acrosomal regions and midpiece while the 14-3-3 epsilon is only localized in the midpiece of mouse sperm.

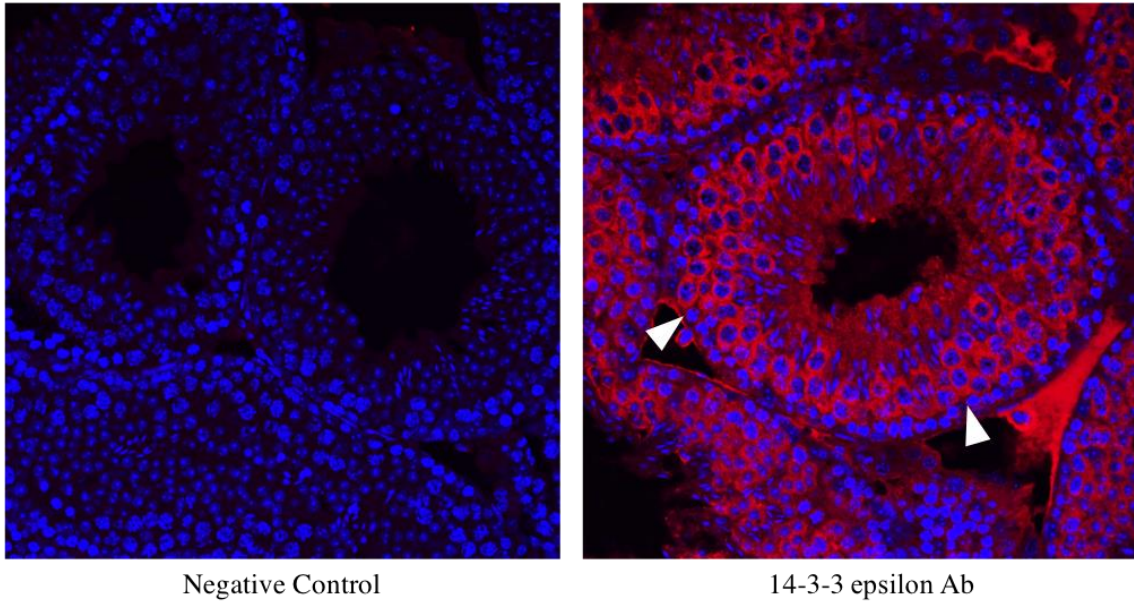


Figure 44. 14-3-3 epsilon expression in mouse seminiferous tubules. Testis from WT mice were fixed in Bouin's fixative solution overnight, processed and sliced into 10 μ m sections. The slice was incubated with mouse monoclonal anti 14-3-3 epsilon antibody followed by secondary anti mouse antibody CY3 and counterstained with Hoechst. 14-3-3 epsilon shows expression in differentiating germ cells but not in the spermatogonia (white arrows) which locates in the first layer of the seminiferous tubules.

Conditional and global knock out 14-3-3 eta and epsilon

In order to characterize the role of 14-3-3 eta and epsilon in mouse testis, we produced mouse lines with a LoxP flanked exon 2 of *Ywhah* or a Loxp flanked exon 3 and 4 of *Ywhae* (Materials and Methods). The floxed mice were crossbred with Stra8-iCre mice to generate testis specific knockout in differentiating germ cells or with ACTB-Cre mice to generate global knockouts. Stra8-iCre is driven by the Stimulated by Retinoic Acid gene8 (Stra8) promoter and is expressed specifically during spermatogenesis (Sadate-Ngatchou *et al.*, 2008). On the other hand, ACTB-Cre is driven by the human beta actin gene promoter and is expressed in all cells of the embryo by the blastocyst stage (Lewandoski *et al.*, 1997).

The genotype of the pups from the knock out mice was confirmed by PCR with three different primers as shown in Figure 45. Protein expression was determined using western blotting. While there was no expression of the 14-3-3 eta in the testis lysate from 14-3-3 eta GKO, but there was an expression of the protein in the CKO testis (Figure 46). The expression was seen in the testis of 14-3-3 eta CKO mice due to the presence of 14-3-3 eta protein in the testicular somatic cells. Similar results were obtained from the 14-3-3 epsilon CKO and GKO in which there is some expression of the 14-3-3 epsilon protein in the CKO compared to the WT testis (Figure 47). The low level of expression seen was due to the presence of 14-3-3 epsilon protein in the testicular somatic cells. The protein was absent in sperm lysates from the 14-3-3 epsilon GKO and CKO mice (Figure 48). Immunofluorescence microscopy analysis further confirmed ablation of the gene in

testis of 14-3-3 epsilon CKO mice; the protein was absent in the seminiferous tubules of the CKO mice (Figure 49).

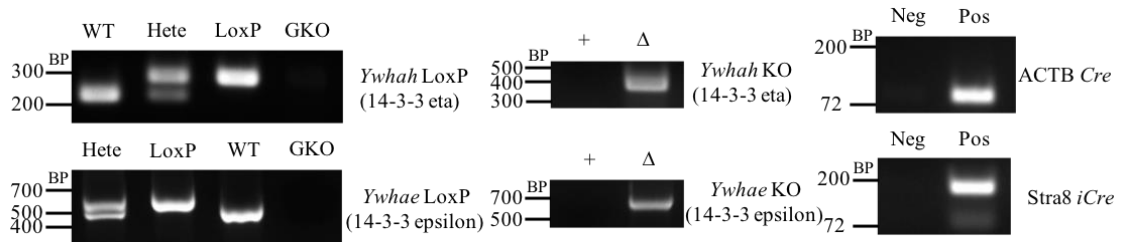


Figure 45. Whole animal genotyping identifies those males with global and testes specific gene deletion. 14-3-3 eta and epsilon LoxP primers indicate the presence of LoxP on the 14-3-3 genes, if the upper band is present. The lower band indicates WT and absence of a band indicates a possible gene deletion (-/-). The 14-3-3 eta and epsilon KO primers indicate a deletion (Δ) of one or both alleles if a band is present. The presence of a LoxP band using the 14-3-3 eta and epsilon LoxP primers, a band in the KO primers and a band in the Stra8 Cre indicates a germ cell-specific knockout (-/LoxP) since the second LoxP will be deleted later in the testis. On the other hand, the presence of both LoxP and WT bands with no Cre (LoxP/WT) Cre negative indicates a full functional gene and a WT phenotype in this mouse.

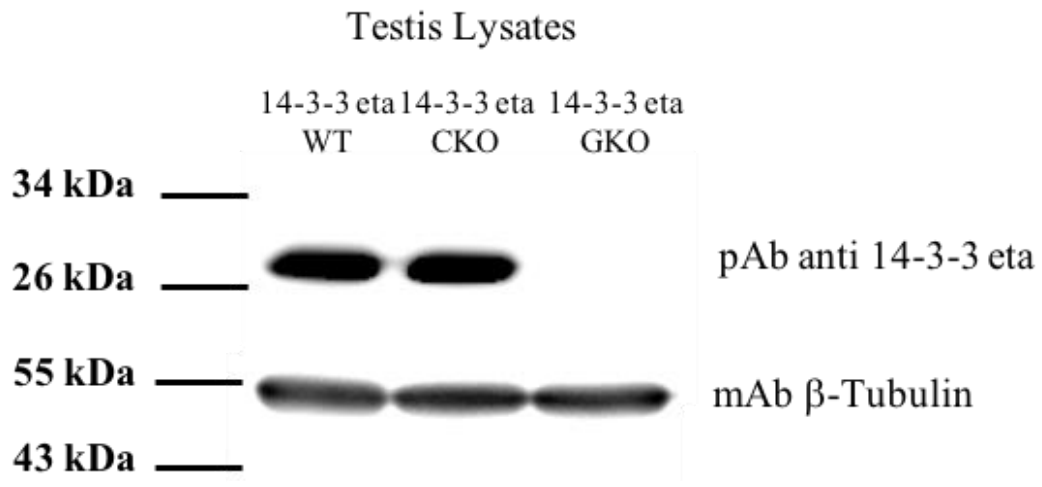


Figure 46. Validation of 14-3-3 eta ablation in both 14-3-3 eta CKO and GKO testis by western blot. The testis lysates from WT, 14-3-3 eta CKO and GKO mice were used in western blot analysis to confirm the success of knocking out the 14-3-3 eta in both global and conditional knockouts. Using rabbit polyclonal anti 14-3-3 eta antibody, the expression of 14-3-3 eta was missing in GKO testis. The expression seen in testis of conditional KO (CKO) mice due to the presence of 14-3-3 eta protein in the testicular somatic cells. The blot was re-probed with a β -tubulin antibody to confirm equal protein loading.

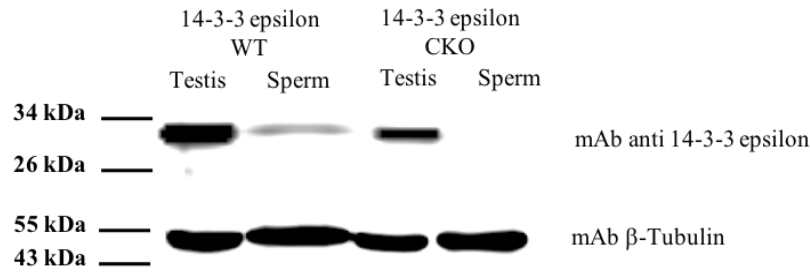


Figure 47. Validation of 14-3-3 epsilon ablation in 14-3-3 epsilon CKO testis and sperm by western blot. The testis lysates from WT, 14-3-3 epsilon CKO mice were used in western blot analysis to confirm the success of knocking out the 14-3-3 epsilon in conditional knockouts. Using anti 14-3-3 epsilon antibody, the expression seen in testis of conditional KO (CKO) mice is due to the presence of 14-3-3 epsilon protein in the testicular somatic cells. The blot was re-probed with a β -tubulin antibody to confirm equal protein loading.

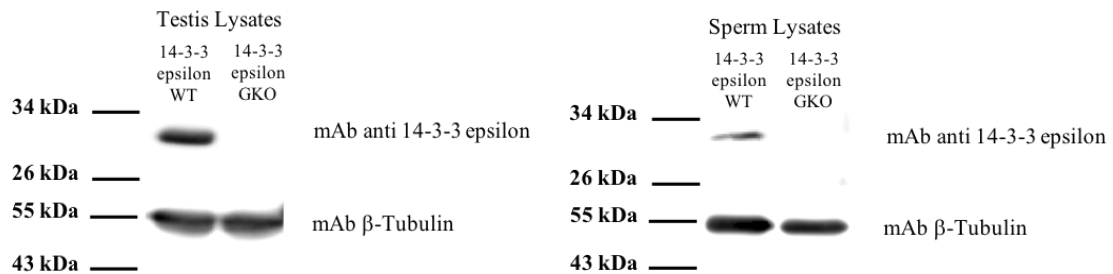


Figure 48. Validation of 14-3-3 epsilon ablation in 14-3-3 epsilon GKO testis and sperm by western blot. Western blot analysis for both testis and sperm lysates of 14-3-3 epsilon GKO were used to confirm the absence of the protein. Testis and sperm lysates from 14-3-3 epsilon GKO show no expression for the 14-3-3 epsilon protein. The blot was re-probed with a β -tubulin antibody to confirm the equal protein loading.

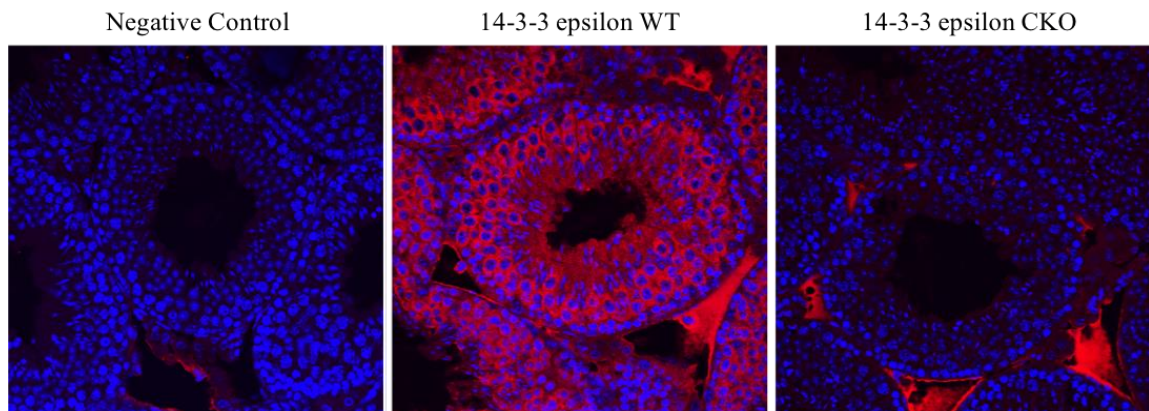


Figure 49. Validation of 14-3-3 epsilon ablation in 14-3-3 epsilon CKO testis by immunofluorescent technique. The testis slices from both WT and 14-3-3 epsilon CKO were incubated with primary antibody against 14-3-3epsilon (mouse mAb 14-3-3 epsilon 8c3 from Santa Cruz) followed by rabbit anti mouse CY3 (Red) and counter stained with Hoechst (Blue, nuclei). Multiple sections were imaged using confocal microscopy. The protein 14-3-3 epsilon is not detected in the seminiferous tubules of 14-3-3 epsilon CKO animals in testes sections that were processed and imaged in parallel with sections from WT mice (n=3).

Fertility of the 14-3-3 eta and 14-3-3 epsilon knockout mice

At least three males from each line were used for fertility testing. All the males were able to mate with the WT females as evidenced by the presence of vaginal plugs. GKO and CKO for 14-3-3 eta male mice were fertile producing pups in litters similar to littermate wild type, ACTB and Stra8 transgenic mice. However, GKO and CKO of 14-3-3 epsilon males were completely infertile; there were no pups produced even after 8 weeks of breeding (Figure 50). *In vitro* fertilization (IVF) was performed with sperm from 14-3-3 epsilon CKO and WT littermate mice and with eggs from WT female mice. The fertility rate (% eggs fertilized, as evidenced by advancement to the two-cell stage) of the 14-3-3 epsilon CKO sperm was 5% compared to 58% with sperm from littermate WT mice. These results indicated that both *in vivo* and *vitro* fertility was impaired in the 14-3-3 epsilon knockout mice (Figure 51).

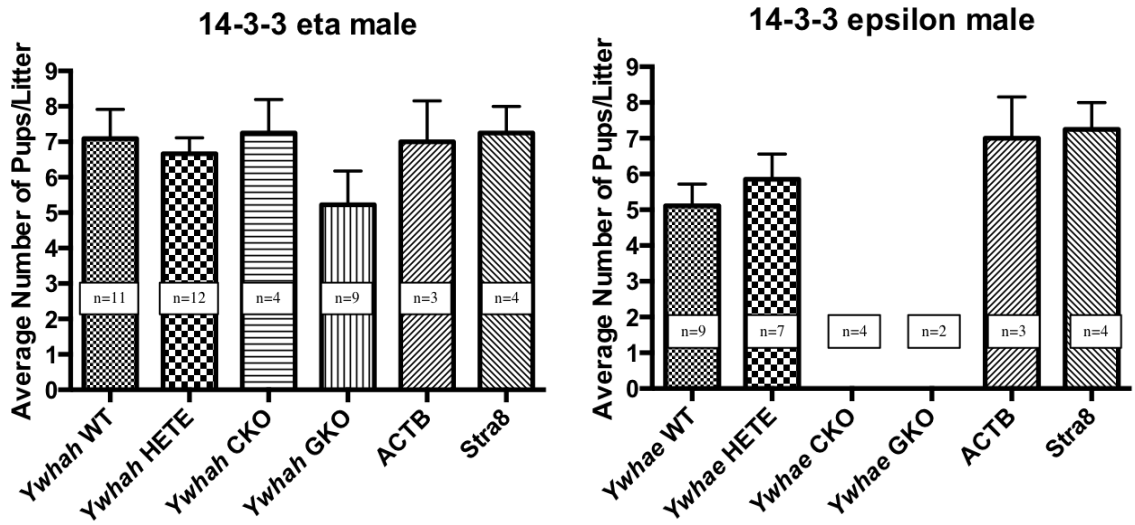


Figure 50. *In vivo* breeding for 14-3-3 eta and epsilon KO males. The fertility of the mice of 14-3-3 eta and epsilon GKO and CKO were tested by *in vivo* breeding of transgenic males with WT females. The average number of pups born for two litters was recorded for breeding pairs (n) for each category. 14-3-3 eta GKO and CKO males appears to be fertile. However, males with the 14-3-3 epsilon deletion produced no pups during the 8 weeks.

Sperm concentration, motility, and ATP levels in 14-3-3 epsilon KO mice

Sperm numbers of the 14-3-3 eta GKO and CKO showed no significant difference compared to littermate WT mice. On the other hand, 14-3-3 epsilon GKO and CKO had significantly lower sperm count than littermate WT mice – sperm numbers were about 30 percent lower ($1-2 \times 10^7/\text{ml}$ in CKO and GKO compared to 3.5 in WT) (Figure 52). Sperm motility was assessed using CASA. Total and progressive motility of 14-3-3 eta GKO and 14-3-3 eta CKO sperm were comparable to motility of WT sperm (Figure 53). Total and progressive motilities of sperm from 14-3-3 epsilon GKO and CKO mice were significantly lower (Figure 54). Velocity parameters: average path velocity (VAP), straight line velocity (VSL) and curvilinear velocity (VCL) were also significantly low (Figure 55).

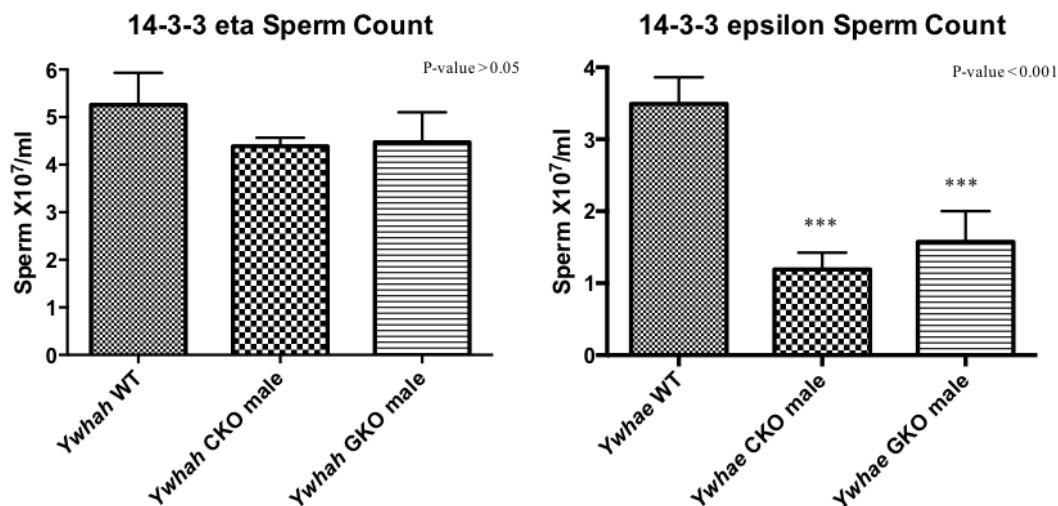


Figure 52. Sperm count of 14-3-3 eta and epsilon KO mice. Sperm from WT, 14-3-3 eta and epsilon KOs were extracted in HTF media. The sperm suspension was then diluted 1:10 and the sperm count was measured by Neubauer hemocytometer. At least three mice were used for the analysis. Prism software was used to perform an ANOVA test. Sperm from 14-3-3 eta GKO and CKO show no significant difference with the WT sperm count (p-value = 0.3765). However, 14-3-3 epsilon GKO and CKO sperm were significantly lower than the WT sperm count (p-value = 0.0005). Error bars in all graphs represent SE.

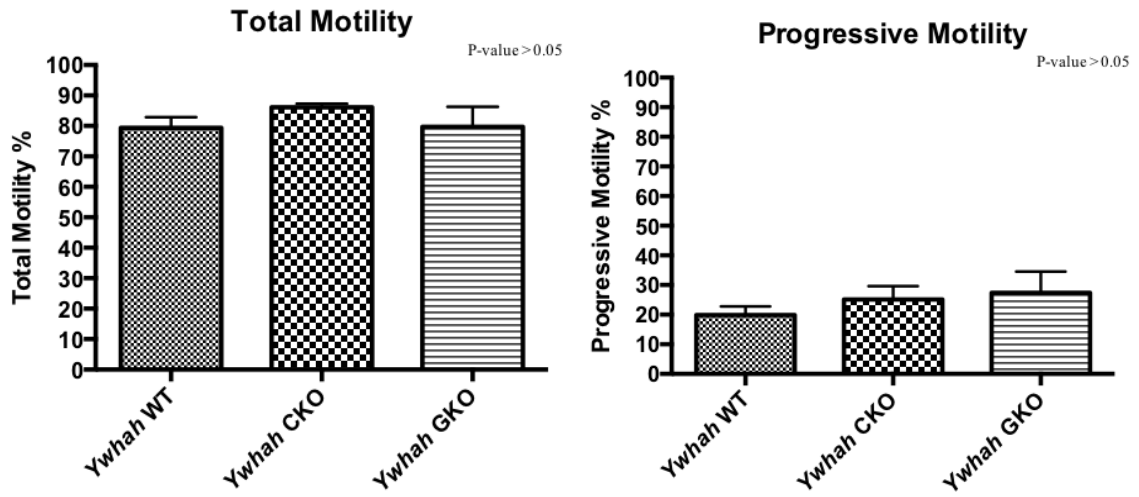


Figure 53. Total and progressive motility of 14-3-3 eta KO sperm. Sperm from WT, 14-3-3 eta CKO and GKO were extracted in HTF media. Using CASA the sperm total and progressive motility were measured for each categories. Five different fields from each mouse were measured and averaged. Three mice were used for each group 14-3-3 eta WT,CKO and GKO. The total and progressive motility for 14-3-3 eta CKO and GKO sperm show no significant difference with WT sperm (p-value = 0.3214 and 0.5207 respectively).

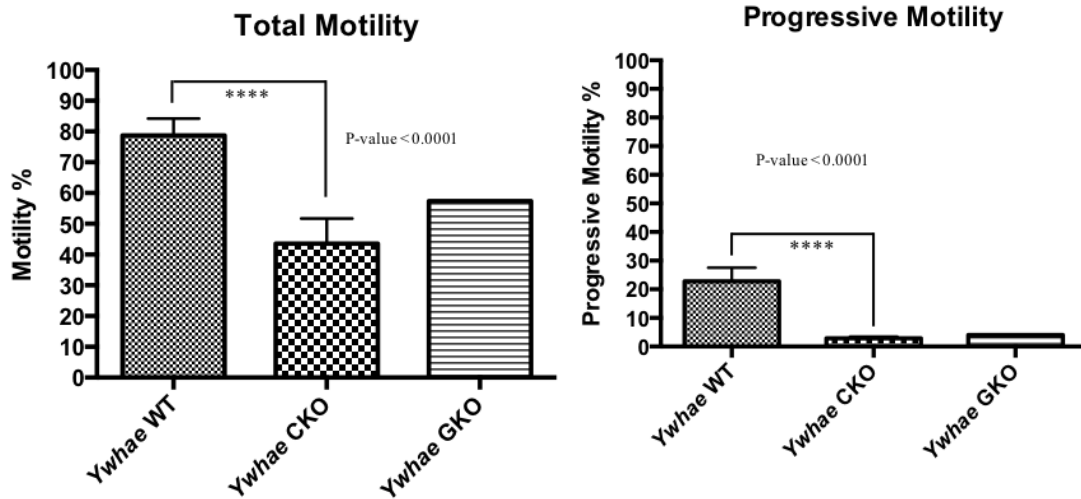


Figure 54. Total and progressive motility of 14-3-3 epsilon KO sperm. Sperm from WT, 14-3-3 epsilon CKO and GKO were extracted in HTF media. Using CASA the sperm total and progressive motility were measured for each categories. Five different fields from each mouse were measured and averaged. The chance of getting an adult 14-3-3 epsilon GKO male is less than 1% due to the embryonic lethality (Toyo-Oka *et al.*, 2003). The motility and the speed parameters sperm (following graphs) were recorded from only one 14-3-3 epsilon GKO mouse. However, the motilities and the speed parameters measurements for the 14-3-3 epsilon WT and CKO were averaged from at least three mice for each category. The t-test shows significantly lower total and progressive motilities for 14-3-3 epsilon CKO compared to the WT with p value < 0.0001. Error bars in all graphs represent SE.

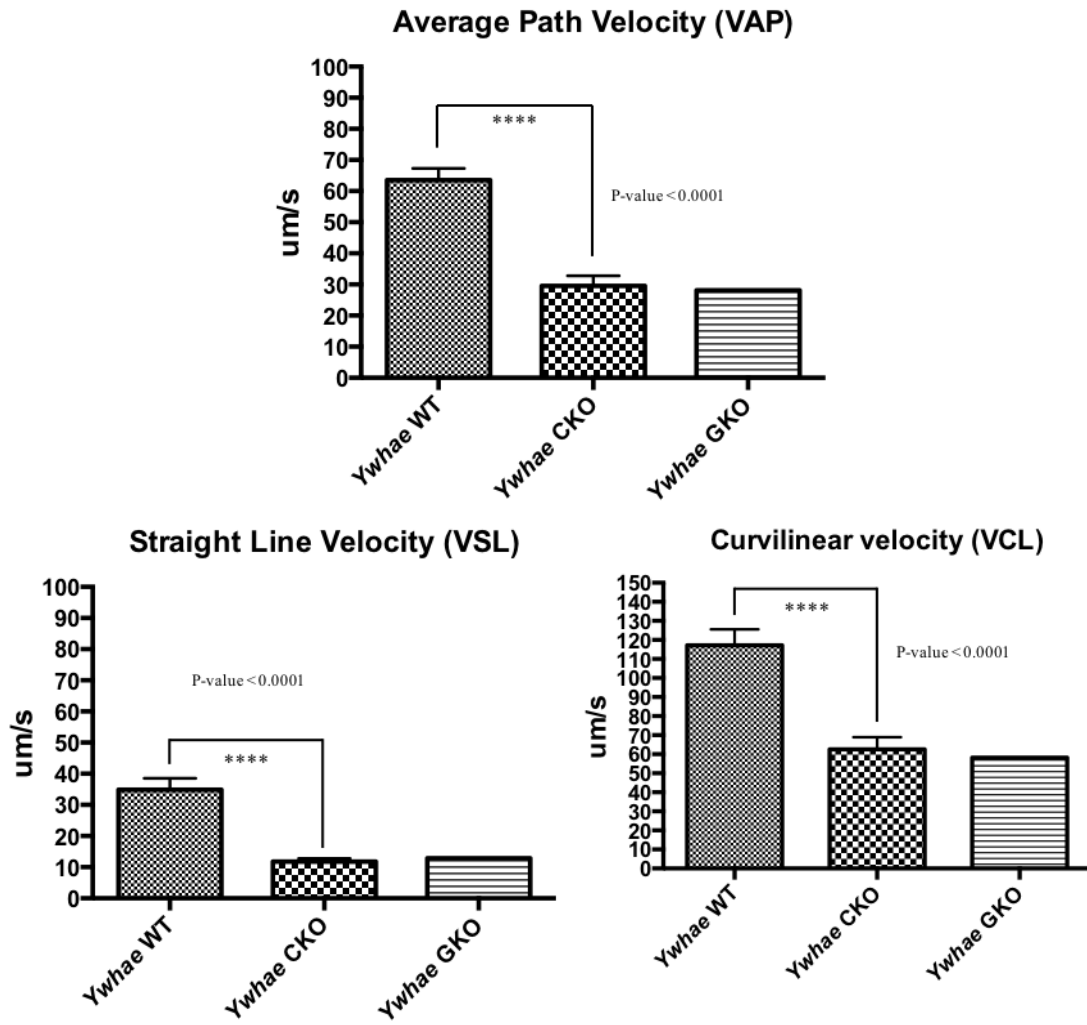


Figure 55. Speed parameters of 14-3-3 epsilon KO sperm. The speed parameters (VAP, VSL and VCL) for 14-3-3 epsilon WT and CKO were measured. 14-3-3 epsilon CKO show a significantly lower speed parameters when it compared to WT with p value < 0.0001. Error bars in all graphs represent SE.

Mitochondrial function and ATP level in sperm from 14-3-3 epsilon knockout mice

Given the reduced motility of sperm from 14-3-3 epsilon KO mice, we examined if general mitochondrial function and ATP production were impaired in sperm from the KO mice. Mitochondrial membrane potential measured using a fluorescent probe was considerably lower in sperm from 14-3-3 epsilon KO mice, suggesting a possible difference in oxidative phosphorylation and mitochondrial function. ATP Levels in sperm lacking 14-3-3 epsilon were significantly diminished – about 50% lower compared to wild type (Figure 56).

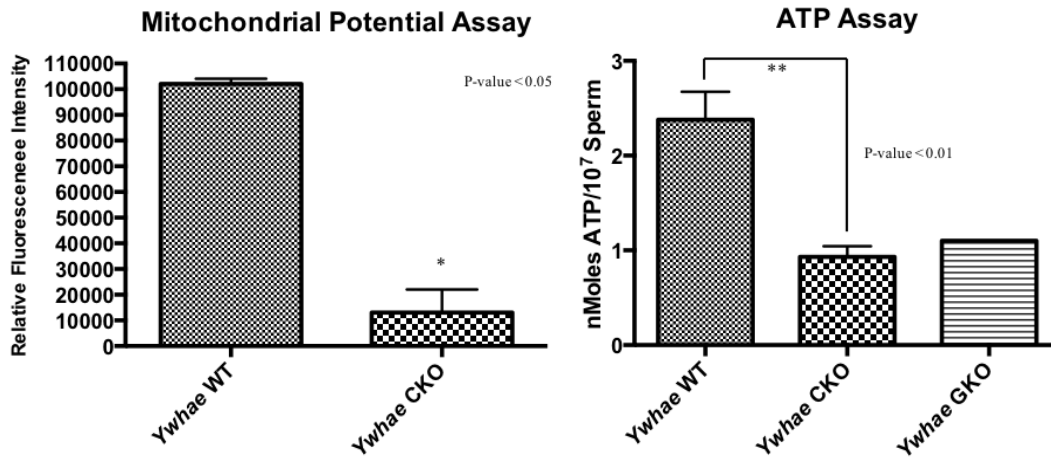


Figure 56. Mitochondrial potential and ATP assay of 14-3-3 epsilon KO sperm. Left panel) Sperm from WT and 14-3-3 epsilon CKO male were extracted in HTF media. The cell suspensions were incubated with the membrane potential sensitive dye MitoProbe™DiIC1(5). The intensities were measured by using flow cytometry. The results suggest that mitochondrial membrane potential is significantly reduced in the absence of 14-3-3 epsilon (p-value = 0.0104). Right panel) Wild type and knock out spermatozoa were collected, and ATP levels were determined by a luciferase assay as described in Materials and Methods. ATP levels in the 14-3-3 epsilon CKO spermatozoa were significantly lower as opposed to that of WT sperm. Values are means ± SEM (n=4); p-value = 0.0038. The ATP levels for 14-3-3 epsilon GKO represents one experiment.

Sperm morphology and spermiation defects in 14-3-3 epsilon KO mice

Sperm from both 14-3-3 epsilon GKO and CKO were fixed and spread on slides to examine their morphology. More than 40% of the sperm from both knockdowns have an abnormally bent heads and the normal sperm from those knockouts were significantly fewer in number compared to the wild type (Figure 57 and 58). Sperm also show other defects such as vacuolated head, amorphous head, bent and irregular mid-piece. Low sperm count, low sperm motility together with morphological abnormalities of sperm could be a manifestation of defects in spermiation. The histology of the testes from 14-3-3 epsilon GKO, 14-3-3 epsilon CKO and WT mice was examined. Periodic Acid Schiff (PAS) stained testis sections show an abnormal localization of sperm near the basement of the seminiferous instead of in the lumen as seen in testis of wild type mice. Elongated spermatids also appear to be disorganized and the heads look abnormal. Some seminiferous tubules show vacuoles due to germ cells sloughing (Figure 59).

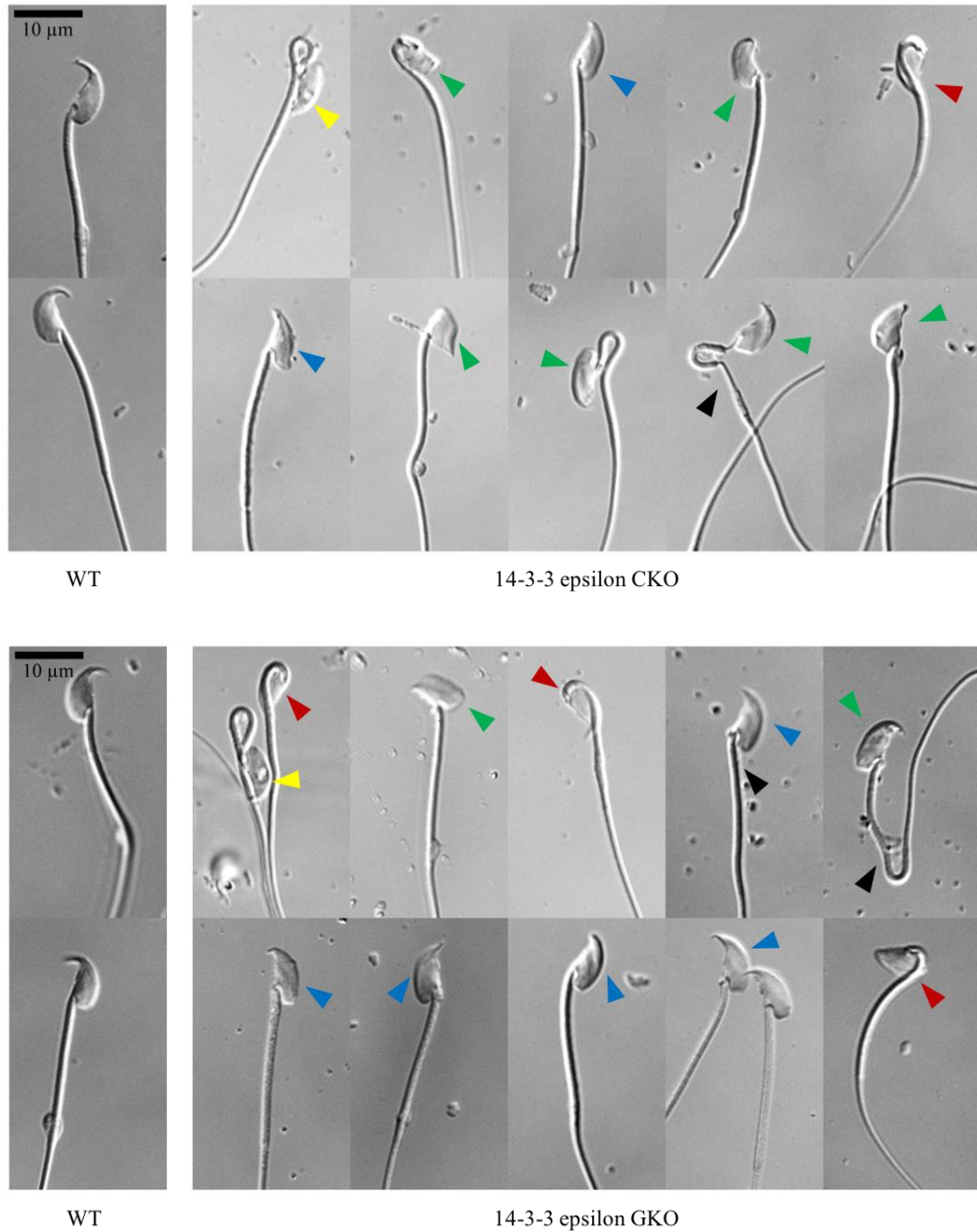


Figure 57. DIC images of 14-3-3 epsilon KO sperm. Both WT and 14-3-3epsilon CKO sperm were extracted in HTF media. The sperm were imaged using DIC optics. Abnormal morphology indicated by arrows as following: vacuolated head (yellow), amorphous head (green), bent head (red), irregular midpiece (black) and hookless sperm head (blue).

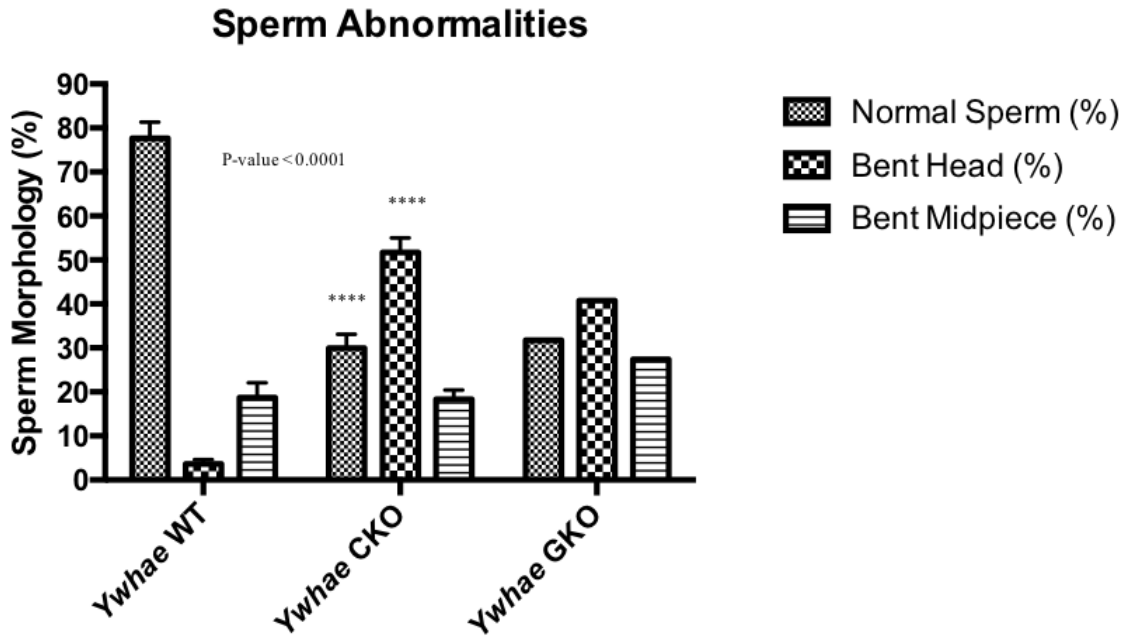


Figure 58. Sperm abnormalities of 14-3-3 epsilon KO sperm. Abnormalities counts were made of sperm apparent from WT (n = 4), 14-3-3 epsilon CKO (n = 4) and 14-3-3 epsilon GKO (n = 1). The abnormal sperm with bent head are significantly higher in the 14-3-3 epsilon CKO sperm (p-value < 0.0001). Error bars represent SE.

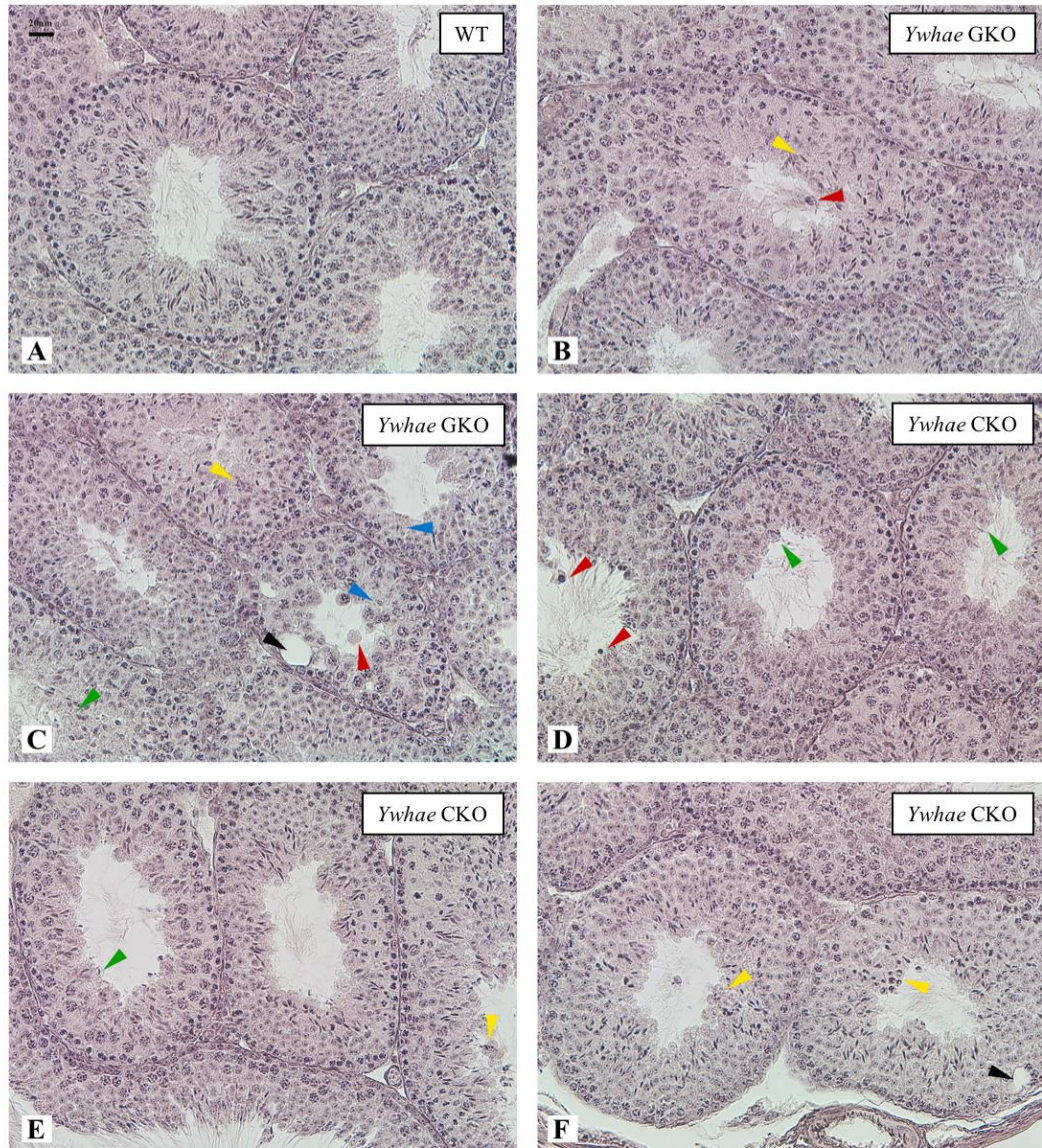


Figure 59. Histological sections of 14-3-3 epsilon KO testis. Testis from WT (A) and 14-3-3 epsilon GKO (B and C) and 14-3-3 epsilon CKO (D, E and F) mice were stained with Periodic Acid Schiff (PAS) stain. Abnormalities in the testes of the knockout mice are indicated by colored arrows as following: Disorganized and abnormal sperm heads (Yellow); Sloughing cells (Red); Loss of elongating spermatids (Blue); Failure of spermiation (Green); Vacuoles where cells have sloughed (Black).

The phosphorylation status and catalytic activities of GSK3 and PP1 γ 2 in sperm lacking 14-3-3 epsilon

It is known that phosphorylation of the protein kinase GSK3 and the protein phosphatase PP1 γ 2 are increased with onset of motility in the *epididymis*. We determined the phosphorylation of these two enzymes in sperm for 14-3-3 epsilon CKO mice. Western blot analysis shows that serine phosphorylation of GSK3 and threonine phosphorylation of PP1 γ 2 are significantly reduced in sperm lacking 14-3-3 epsilon (Figure 60). We also measured GSK3 activity in sperm. GSK3 activity was about two-fold higher in 14-3-3 epsilon CKO compared to WT sperm (Figure 61). Previous work had shown by using a pan antibody that 14-3-3 is a binding partner for sperm PP1 γ 2 (Puri *et al.*, 2011, 2008). Here we sought to determine whether if the sperm 14-3-3 epsilon isoform binds to PP1 γ 2. Two different 14-3-3 epsilon antibodies were able to immunoprecipitate PP1 γ 2 from sperm extracts (Figure 62). This binding data was further confirmed with reciprocal co-immunoprecipitation of 14-3-3 epsilon in sperm extracts with PP1 γ 2 antibodies (Figure 63). Finally, we determined the presence of phosphoproteins detected with antibodies against a phospho-(Ser) motif recognized by 14-3-3. Previous studies using this antibody showed phosphoproteins by 14-3-3 pull-down from sperm extracts and also in extracts from caudal bovine epididymal sperm (Puri *et al.*, 2008). We confirmed the presence of the 14-3-3 phospho (Ser) binding motif containing proteins in extracts of caput and caudal epididymal sperm. The levels of the proteins were higher in mouse caudal compared to caput epididymal sperm similar to data shown with bovine epididymal sperm (Puri *et al.*, 2008). Western blot

signal for 14-3-3 phospho(Ser) binding motif proteins was considerably lower in sperm from 14-3-3 epsilon compared to WT mice even though less higher amounts of extracts from the KO sperm were loaded based on β -actin (Figure 64).

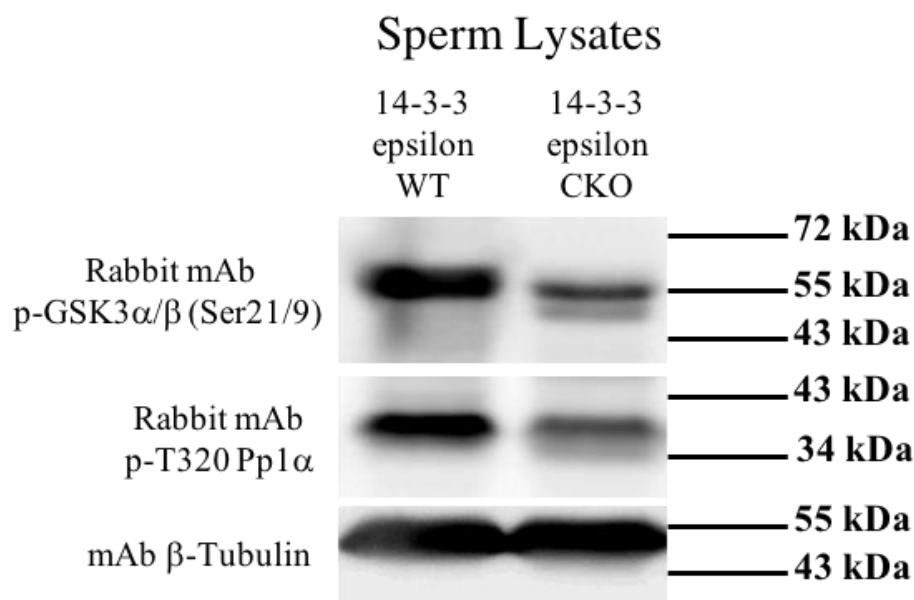


Figure 60. Post-translational modification of GSK3 and PP1 in 14-3-3 epsilon KO sperm. Western blot analysis suggest that expression or post-translational modification of proteins known or likely to be involved in sperm function may be altered in the absence of 14-3-3 epsilon. The 14-3-3 epsilon CKO sperm show a decrease in the phosphorylation of serine and tyrosine for GSK3a/b. The threonine phosphorylation of PP1 also reduced. The blot later was probed with β -tubulin to show equal sample loading.

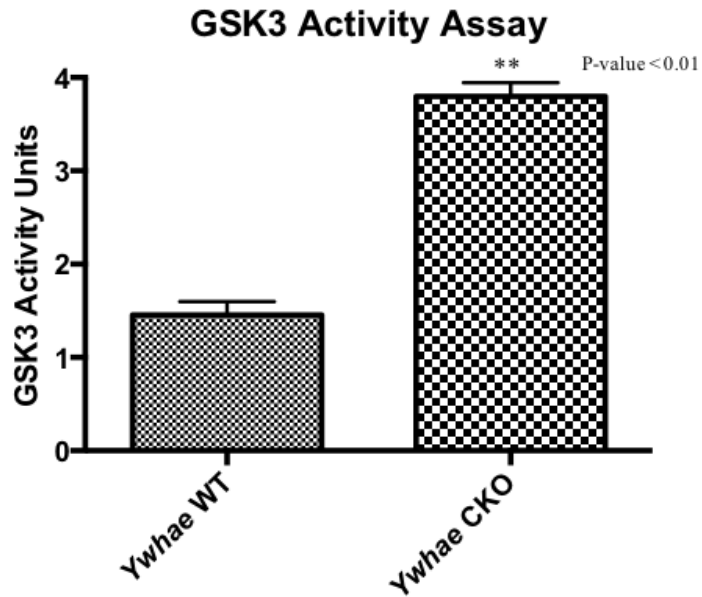


Figure 61. GSK3 activity of 14-3-3 epsilon KO sperm. Catalytic activity of GSK3 was measured using GS2 peptide as a substrate as described in Materials and Methods. Unit activity is defined as nmoles of $^{32}\text{PO}_4^{2-}$ incorporated/min/ 10^7 sperm. Catalytic activity of GSK3 is significantly higher in 14-3-3 epsilon conditional KO compared to wild type sperm. Values are means \pm SEM (n=6); p-value = 0.0077.

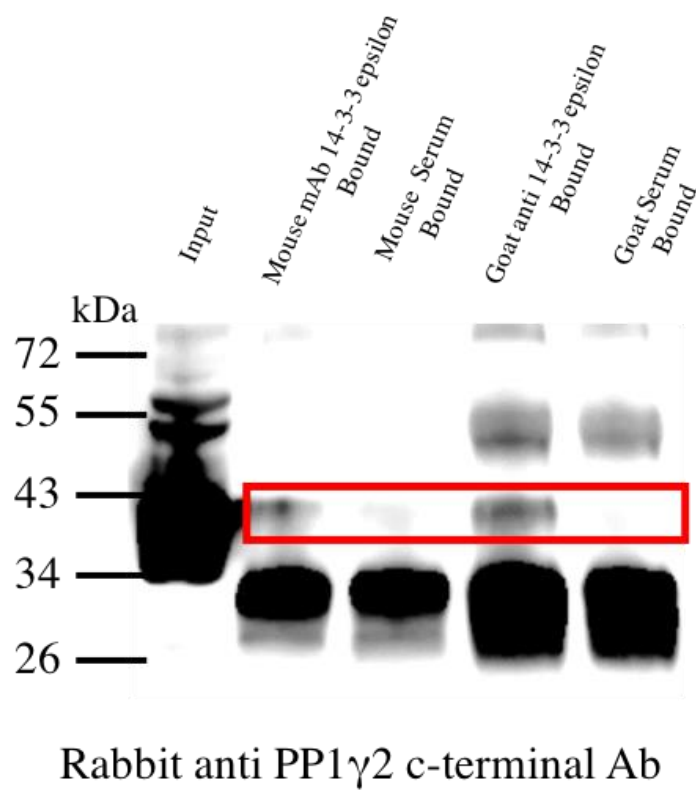


Figure 62. Immunoprecipitation of PP1 γ 2 protein by using two different 14-3-3 epsilon antibodies. Co-immunoprecipitation experiment indicates an interaction of 14-3-3 epsilon with PP1 γ 2 as PP1 γ 2 protein is pulled down by two different antibodies for 14-3-3 epsilon (Mouse monoclonal and Goat polyclonal antibodies).

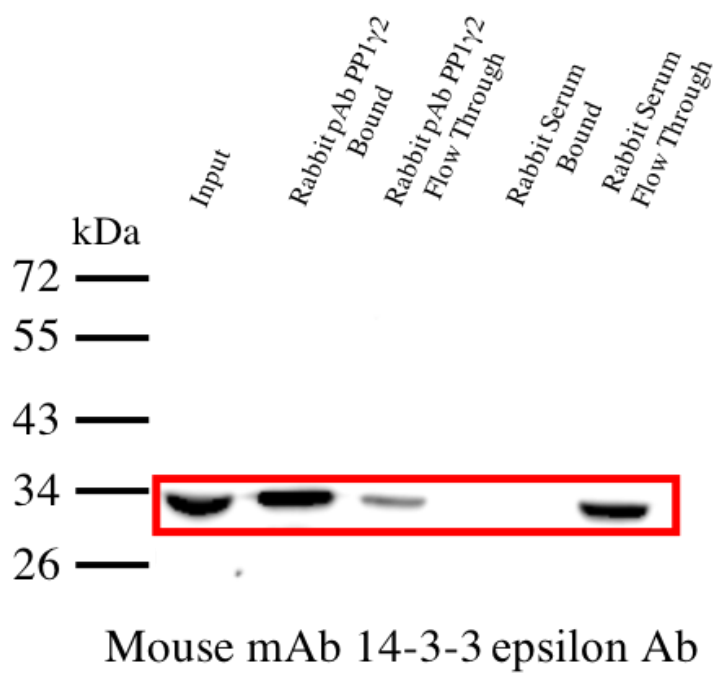


Figure 63. Immunoprecipitation of 14-3-3 epsilon by using PP1 γ 2 antibody. A reciprocal co-immunoprecipitation experiment shows the presence of 14-3-3 epsilon protein when it is pulled down with the PP1 γ 2 c-terminal antibody.

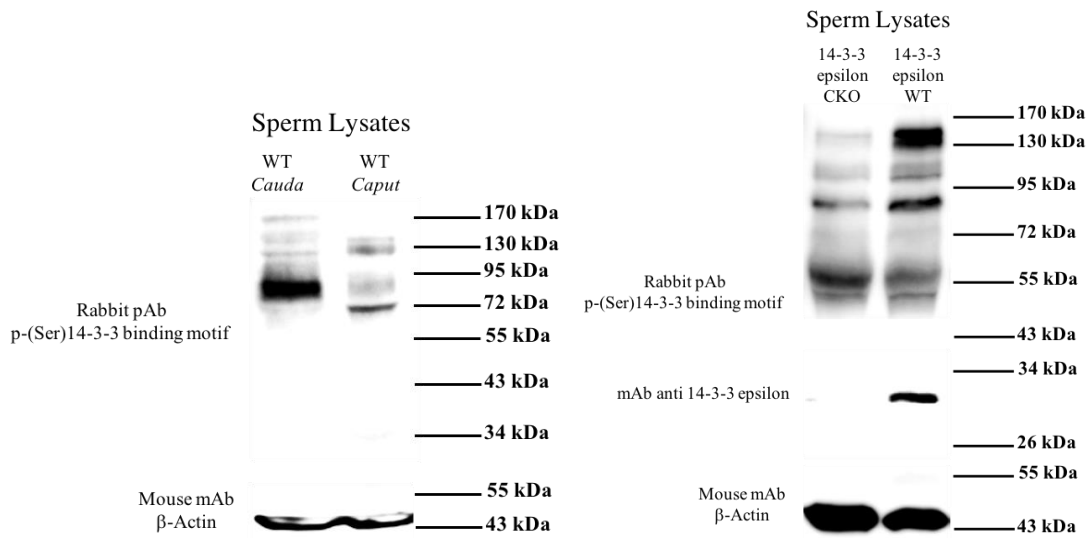


Figure 64. Western blot analysis of sperm extract probe with anti phospho(Ser)14-3-3 binding motif antibody. Left panel) sperm number adjusted to (1×10^7 sperm/ μ l). Mouse caput and caudal sperm extract were made as described after isolation in TBS. Right panel) WT vs KO sperm extract were made from sperm suspended in HTF for one hour to promote capacitation during the IVF. The blot later was probed with β -actin to show equal loading.

4.1.3 Discussion

The reason for the presence of seven isoforms of 14-3-3 produced from seven independent genes in higher organisms is not known. Determination of function is further complicated by the fact that some of the 14-3-3 isoforms can form heterodimers. Gene knockout has shown that some of the isoforms may have specific roles. The global knockout of 14-3-3 epsilon is embryonic lethal, apparently due to impaired heart development (Gittenberger-de Groot *et al.*, 2016; Kosaka *et al.*, 2012; Toyo-Oka *et al.*, 2003). Knockout of 14-3-3 zeta appears to cause neurological defects (P. S. Cheah *et al.*, 2012; Toyo-Oka *et al.*, 2014). A statement in one report on 14-3-3 zeta (Xu *et al.*, 2015) stated that males and females lacking this isoform are infertile; however there was no supporting data or examination and discussion of the infertility phenotype. The absence of 14-3-3 eta in knockout mice results in deafness and degeneration of cochlear cells (Buret *et al.*, 2016). There was also a mention in this report that 14-3-3 eta knock out males were infertile but there was no supporting data or discussion. The roles of any of the isoforms, based on gene knockout studies, in male or female fertility were not known.

We focused on two isoforms to begin the process of defining the role of 14-3-3 in male reproduction. Here we show that both 14-3-3 eta and epsilon are present in testis, whereas sperm contain only the epsilon isoform which is consistent with the published report of the mouse sperm proteome where they found the expression of 14-3-3 beta, epsilon and zeta (Baker *et al.*, 2008). The 14-3-3 epsilon isoform is present in the midpiece region. The expression of 14-3-3 epsilon mRNA in postnatal developing testis showed that expression increased temporally coinciding with the expected onset of

spermatogenesis and reaching the highest levels in the adult mice testis. Previous studies have also documented high levels of expression of 14-3-3 epsilon in human brain and testis (Aghazadeh & Papadopoulos, 2016).

Our results clearly show that genetic knockout of 14-3-3 epsilon leads to male infertility. Both global knockout (GKO) and testis-specific knockout (CKO) of 14-3-3 epsilon prevented males from producing pups when they were mated with wildtype females. Males were capable of mating, as indicated by copulation plugs in females that were shown to be otherwise fertile, but no offspring were produced. There was no other obvious phenotype observed in the males except infertility. In contrast global or testis-specific deletion of 14-3-3 eta did not reduce male fertility in *in vivo* breeding studies, suggesting this isoform is not required for normal testicular and sperm function in male mice. The role of any of the other five isoforms in males awaits further testing. Infertility of males lacking 14-3-3 epsilon may be associated with the lower sperm count in these animals, but also with many other factors. *In vitro* fertilization was significantly lower with sperm from the 14-3-3 epsilon CKO males (5% compared to 56% with WT sperm). The data suggest that impaired sperm function in penetrating the egg is also a likely reason for infertility. Factors responsible for this might include poor motility, reduced energy production, or due to abnormally shaped sperm.

The percent motility and velocity parameters of sperm from 14-3-3 epsilon KO mice were reduced. Mitochondrial potential and ATP levels were also reduced. The exact reasons for the reduced energy production and motility in mutant sperm are not known. Sperm morphology was affected with about 75% of knockout sperm displaying some

abnormalities including misshapen heads, and bent midpiece and head neck junctions. Similar sperm abnormalities are also seen in other KO mice where spermiogenesis is affected (Yan, 2009). The histological examination of 14-3-3 epsilon KO testis suggests spermiogenesis defects such as fewer sperm in seminiferous tubules, disorganized and abnormal sperm heads, sloughing cells, loss of elongating spermatids and vacuoles where cells have sloughed. The sperm abnormalities in were similar to those previously described in the germ cells of PP1 γ CKO mice (Sinha *et al.*, 2013). Previous studies on 14-3-3 in testis showed that the 14-3-3 theta isoform is present in Sertoli cells localized at the ectoplasmic specialization (ES), a type of adherent junction at the interface of the Sertoi cell and elongating spermatids. Localization of the 14-3-3 theta isoform was also found at the blood testis barrier (BTB). Knock down of 14-3-3 theta in Sertoli cells in culture resulted in reduced levels of proteins thought to be associated with the BTB and ES junction (Wong *et al.*, 2009). The role of the 14-3-3 in differentiating spermatids and Sertoli cells in promoting cell contacts essential for normal spermiogenesis require additional studies.

Previous work had identified 14-3-3 zeta in sperm, and also isolated a number of its binding proteins from sperm and testis. This same report was showed that two key signaling enzymes PP1 γ 2 and GSK3 are potential binding partners for 14-3-3 (Puri *et al.*, 2011, 2008). Loss of 14-3-3 epsilon may affect activity of these enzymes with further disruption of other enzymes involved in energy metabolism which are also 14-3-3 binding proteins. High protein phosphatase activity limits motility in caput epididymal sperm in WT type mice. Inhibiting Protein Phosphatase 1 by Calyculin A leads to

motility initiation in caput sperm and motility stimulation in caudal sperm. Thus PP1 activity is reduced while the cAMP level and PKA activity are increased during epididymal sperm maturation. A reduction in the PP1 activity is also associated with increased phosphorylation and decreased catalytic activity of GSK3 (Dey *et al.*, 2018). In the 14-3-3 epsilon KO mice caudal sperm, the phosphorylation of PP1 and GSK3 are low compared to the WT sperm which suggesting a role for 14-3-3 epsilon in changing the activity of the signaling during epididymal sperm maturation. Caudal sperm lacking 14-3-3 epsilon resemble WT caput sperm indicating impaired epididymal sperm maturation. Reduced GSK3 phosphorylation and high GSK3 catalytic activity seen in sperm lacking 14-3-3 epsilon is also seen in sperm from soluble Adenylyl Cyclase (sAC) and calcineurin KO mice (Dey *et al.*, 2018). Reduced phosphorylation of the phospho(Ser) binding motif containing proteins in testes extracts from testis-specific knockout 14-3-3 epsilon males is also seen with anti phospho(Ser) 14-3-3 binding motif antibodies. These antibodies largely detect proteins with a serine phosphorylation with proline at the +2 position an arginine at the -3 position. These antibodies were validated previously where it was shown that the antibodies reacted with proteins isolated using pull down with recombinant 14-3-3 (Puri *et al.*, 2008). Though unlikely, we cannot rule out the possibility that the reduced signal with 14-3-3 domain antibodies could be due reduced proteins levels rather than reduced phosphorylation. An assessment of the phosphor-proteome of sperm and testis lacking 14-3-3 epsilon should be instructive. Overall, our observations with sperm from 14-3-3 knock out mice are consistent with the

suggestion that 14-3-3 binding to phosphorylated proteins is part of mechanisms involved in the regulation of the catalytic activities of the sperm signaling enzymes.

The low ATP level and impaired mitochondrial function could be the reasons behind low motility in the 14-3-3 epsilon KO sperm. There is evidence that 14-3-3 epsilon plays a large role in mitochondrial function. It has been known that induction of the steroidogenesis in Leydig cells triggers the translocation of 14-3-3 epsilon from the cytosol into the outer membrane of mitochondria. The 14-3-3 epsilon is also named as mitochondrial import stimulation factor (MSF) when it forms a heterodimer with 14-3-3 zeta or gamma. At the outer mitochondrial membrane, Voltage Dependent Anion Channel (VDAC) competes with the Steroidogenic Acute Regulatory protein (STAR) to bind to 14-3-3 epsilon. The VDAC channel helps in transferring the fatty acids ions, reactive oxygen species, calcium, cholesterol and metabolites like ATP and ADP through the membrane. It also appears to mediate apoptosis (Aghazadeh, Martinez-Arguelles, Fan, Culty, & Papadopoulos, 2014). VDAC has three isoforms in mammals originating from VDAC genes 1, 2 and 3. Gene knockout of VDAC 1, 2 or 3 in a mouse cell line cause a reduction in respiration. VDAC 1 KO mice appears to be unaffected by the missing gene while VDAC 2 knockout mice were never generated due to the anti-apoptotic function. Surprisingly, VDAC 3 knockout mice show an infertility phenotype in mouse male. VDAC 3 is localized in the acrosomal and mid piece regions of mouse sperm (Messina, Reina, Guarino, & De Pinto, 2012). Future work should focus on changes that occur in sperm mitochondria in the absence of 14-3-3 epsilon.

Earlier studies from our lab identified a number of binding proteins with 14-3-3 zeta. The determination of the binding partners for 14-3-3 epsilon should now be done, given its importance in normal sperm function. Previous work showed that 14-3-3 zeta may form a heterodimer with 14-3-3 epsilon in testis (Puri et al., 2011). If this were the case, we predict knock out 14-3-3 zeta could have the same phenotype as the 14-3-3 epsilon knockout. Finally, it is feasible to envision possibilities of using disruption of 14-3-3 binding protein partners as a novel approach to male contraception.

In conclusion, our study has shown for the first time that out of the seven 14-3-3 isoforms one isoform (14-3-3 epsilon) is essential for spermiogenesis and normal sperm function. Absence of 14-3-3 epsilon alters male mouse fertility by causing oligospermia, asthenospermia and teratospermia. The deletion of 14-3-3 epsilon alone in male germ cells causes defects, indicating that other isoforms of 14-3-3 cannot compensate for loss of the epsilon isoform in testis. Absence of 14-3-3 epsilon alters spermiogenesis as well as altering other key proteins known to regulate sperm motility.

REFERENCES

- Acevedo, S. F., Tsigkari, K. K., Grammenoudi, S., & Skoulakis, E. M. C. (2007). In vivo functional specificity and homeostasis of *Drosophila* 14-3-3 proteins. *Genetics*. <https://doi.org/10.1534/genetics.107.072280>
- Adhikari, D., & Liu, K. (2014). The regulation of maturation promoting factor during prophase I arrest and meiotic entry in mammalian oocytes. *Molecular and Cellular Endocrinology*, 382(1), 480–487. <https://doi.org/10.1016/j.mce.2013.07.027>
- Aghazadeh, Y., Martinez-Arguelles, D. B., Fan, J., Culty, M., & Papadopoulos, V. (2014). Induction of androgen formation in the male by a TAT-VDAC1 fusion peptide blocking 14-3-3 ϵ protein adaptor and mitochondrial VDAC1 interactions. *Molecular Therapy*. <https://doi.org/10.1038/mt.2014.116>
- Aghazadeh, Y., & Papadopoulos, V. (2016). The role of the 14-3-3 protein family in health, disease, and drug development. *Drug Discovery Today*. <https://doi.org/10.1016/j.drudis.2015.09.012>
- Aitken, A. (2006). 14-3-3 proteins: A historic overview. *Seminars in Cancer Biology*, 16(3), 162–172.
- Aitken, A., Baxter, H., Dubois, T., Clokie, S., Mackie, S., Mitchell, K., ... Zemlickova, E. (2002). Specificity of 14-3-3 isoform dimer interactions and phosphorylation. *Biochemical Society Transactions*, 30, 351–360.
- Aitken, Alastair. (2006). 14-3-3 proteins: A historic overview. *Seminars in Cancer Biology*, 16(3), 162–172. <https://doi.org/10.1016/j.semcancer.2006.03.005>

- Aitken, Alastair. (2011). Post-translational modification of 14-3-3 isoforms and regulation of cellular function. *Seminars in Cell and Developmental Biology*. <https://doi.org/10.1016/j.semcdb.2011.08.003>
- Arnoult, C., Kazam, I. G., Visconti, P. E., Kopf, G. S., Villaz, M., & Florman, H. M. (1999). Control of the low voltage-activated calcium channel of mouse sperm by egg ZP3 and by membrane hyperpolarization during capacitation. *Proceedings of the National Academy of Sciences of the United States of America*. <https://doi.org/10.1073/pnas.96.12.6757>
- Arnoult, C., Zeng, Y., & Florman, H. M. (1996). ZP3-dependent activation of sperm cation channels regulates acrosomal secretion during mammalian fertilization. *Journal of Cell Biology*. <https://doi.org/10.1083/jcb.134.3.637>
- Bachvarova, R. (1985). Gene expression during oogenesis and oocyte development in mammals. *Developmental Biology (New York, N.Y. : 1985)*.
- Baker, M., Hetherington, L., Reeves, G., & Aitken, R. (2008). The mouse sperm proteome characterized via IPG strip prefractionation and LC-MS/MS identification. *Proteomics*, 8(8), 1720–1730.
- Bell, C. E., Calder, M. D., & Watson, A. J. (2008). Genomic RNA profiling and the programme controlling preimplantation mammalian development. *Molecular Human Reproduction*. <https://doi.org/10.1093/molehr/gan063>
- Bollen, M., & Stalmans, W. (1992). The structure, role, and regulation of type 1 protein phosphatases. *Critical Reviews in Biochemistry and Molecular Biology*, 27(3), 227–281. <https://doi.org/10.3109/10409239209082564>

- Borg, C. L., Wolski, K. M., Gibbs, G. M., & O'Bryan, M. K. (2009). Phenotyping male infertility in the mouse: How to get the most out of a “non-performer.” *Human Reproduction Update*. <https://doi.org/10.1093/humupd/dmp032>
- Bridges, D., & Moorhead, G. B. G. (2005). 14-3-3 proteins: a number of functions for a numbered protein. *Science's STKE : Signal Transduction Knowledge Environment*.
- Buffone, M. G., Foster, J. A., & Gerton, G. L. (2008). The role of the acrosomal matrix in fertilization. *International Journal of Developmental Biology*. <https://doi.org/10.1387/ijdb.072532mb>
- Buret, L., Delprat, B., & Delettre, C. (2016). Loss of function of Ywhah in mice induces deafness and cochlear outer hair cell's degeneration. *Cell Death & Disease*. <https://doi.org/10.1038/cddis.2016.88>
- Bury, L., Coelho, P. A., & Glover, D. M. (2016). From Meiosis to Mitosis: The Astonishing Flexibility of Cell Division Mechanisms in Early Mammalian Development. *Current Topics in Developmental Biology*, 120, 125–171. <https://doi.org/10.1016/bs.ctdb.2016.04.011>
- Chakrabarti, R., Cheng, L., Puri, P., Soler, D., & Vijayaraghavan, S. (2007). Protein phosphatase PP1 gamma 2 in sperm morphogenesis and epididymal initiation of sperm motility. *Asian Journal of Andrology*, 9(4), 445–452. <https://doi.org/10.1111/j.1745-7262.2007.00307.x>
- Chakrabarti, R., Kline, D., Lu, J., Orth, J., Pilder, S., & Vijayaraghavan, S. (2007). Analysis of Ppp1cc-Null Mice Suggests a Role for PP1gamma2 in Sperm Morphogenesis1. *Biology of Reproduction*.

<https://doi.org/10.1095/biolreprod.106.058610>

- Chaudhary, J., & Skinner, M. K. (2000). Characterization of a novel transcript of 14-3-3 theta in Sertoli cells. *J.Androl*, *21*(0196-3635 (Print)), 730–738.
- Cheah, P.-S., Ramshaw, H. S., Thomas, P. Q., Toyo-oka, K., Xu, X., Martin, S., ... Schwarz, Q. P. (2012). Neurodevelopmental and neuropsychiatric behaviour defects arise from 14-3-3 ζ deficiency. *Molecular Psychiatry*, *17*(4), 451–466. <https://doi.org/10.1038/mp.2011.158>
- Cheah, P. S., Ramshaw, H. S., Thomas, P. Q., Toyo-Oka, K., Xu, X., Martin, S., ... Schwarz, Q. P. (2012). Neurodevelopmental and neuropsychiatric behaviour defects arise from 14-3-3 ζ deficiency. *Molecular Psychiatry*. <https://doi.org/10.1038/mp.2011.158>
- Cheng, L., Pilder, S., Nairn, A. C., Ramdas, S., & Vijayaraghavan, S. (2009). PP1gamma2 and PPP1R11 are parts of a multimeric complex in developing testicular germ cells in which their steady state levels are reciprocally related. *PLoS ONE*, *4*(3). <https://doi.org/10.1371/journal.pone.0004861>
- Cohen, P. T. W. (2002). Protein phosphatase 1 - Targeted in many directions. *Journal of Cell Science*.
- Conti, M., Andersen, C. B., Richard, F., Mehats, C., Chun, S. Y., Horner, K., ... Tsafiriri, A. (2002). Role of cyclic nucleotide signaling in oocyte maturation. *Molecular and Cellular Endocrinology*, *187*(1–2), 153–159. [https://doi.org/10.1016/S0303-7207\(01\)00686-4](https://doi.org/10.1016/S0303-7207(01)00686-4)
- Cui, C., Ren, X., Liu, D., Deng, X., Qin, X., Zhao, X., ... Yu, B. (2014). 14-3-3 epsilon

- prevents G2/M transition of fertilized mouse eggs by binding with CDC25B. *Bmc Developmental Biology*, 14, 33. <https://doi.org/10.1186/s12861-014-0033-x>
- Darszon, A., Nishigaki, T., Beltran, C., & Treviño, C. L. (2011). Calcium channels in the development, maturation, and function of spermatozoa. *Physiological Reviews*. <https://doi.org/10.1152/physrev.00028.2010>
- De, S. (2014). *Protein 14-3-3 (YWHA) isoforms and their roles in regulating mouse oocyte maturation*. Kent State University.
- De, S., & Kline, D. (2013). Evidence for the requirement of 14-3-3eta (YWHAH) in meiotic spindle assembly during mouse oocyte maturation. *Bmc Developmental Biology*, 13, 10. <https://doi.org/10.1186/1471-213X-13-10>
- De, S., Marcinkiewicz, J. L., Vijayaraghavan, S., & Kline, D. (2012). Expression of 14-3-3 protein isoforms in mouse oocytes, eggs and ovarian follicular development. *BMC Research Notes*, 5(1), 57. <https://doi.org/10.1186/1756-0500-5-57>
- Dekel, N., & Beers, W. H. (1978). Rat oocyte maturation in vitro: relief of cyclic AMP inhibition by gonadotropins. *Proc. Natl. Acad. Sci. U.S.A.*, 75(9), 4369–4373. <https://doi.org/10.1073/pnas.75.9.4369>
- Detwiler, A. C. (2015). Evidence for the Role of YWHA in Mouse Oocyte Maturation. Kent State University.
- Dey, S., Goswami, S., Eisa, A., Bhattacharjee, R., Brothag, C., Kline, D., & Vijayaraghavan, S. (2018). Cyclic AMP and glycogen synthase kinase 3 form a regulatory loop in spermatozoa. *Journal of Cellular Physiology*. <https://doi.org/10.1002/jcp.26557>

- Dougherty, M. K., & Morrison, D. K. (2004). Unlocking the code of 14-3-3. *Journal of Cell Science*, 117(10), 1875–1884.
- Duckworth, B C, Weaver, J. S., & Ruderman, J. V. (2002). G2 arrest in *Xenopus* oocytes depends on phosphorylation of cdc25 by protein kinase A. *Proceedings of the National Academy of Sciences of the United States of America*, 99(26), 16794–16799.
- Duckworth, Brian C, Weaver, J. S., & Ruderman, J. V. (2002). G 2 arrest in *Xenopus* oocytes depends on phosphorylation of cdc25 by protein kinase A.
- Dym, M., & Fawcett, D. W. (1971). Further observations on the numbers of spermatogonia, spermatocytes, and spermatids connected by intercellular bridges in the mammalian testis. *Biology of Reproduction*.
<https://doi.org/10.1093/biolreprod/4.2.195>
- Eddy, E. M. (1998). Regulation of gene expression during spermatogenesis. *Seminars in Cell and Developmental Biology*. <https://doi.org/10.1006/scdb.1998.0201>
- Fardilha, M., Ferreira, M., Pelech, S., Vieira, S., Rebelo, S., Korrodi-Gregorio, L., ... Da Cruz E Silva, E. F. (2013). “oMICS” of human sperm: Profiling protein phosphatases. *OMICS A Journal of Integrative Biology*.
<https://doi.org/10.1089/omi.2012.0119>
- Forrest, A., & Gabrielli, B. (2001). Cdc25B activity is regulated by 14-3-3. *Oncogene*, 20(32), 4393–4401. <https://doi.org/10.1038/sj.onc.1204574>
- Freitas, M. J., Fardilha, M., & Vijayaraghavan, S. (2017). Signaling mechanisms in mammalian sperm motility. *Biology of Reproduction*.

<https://doi.org/10.1095/biolreprod.116.144337>

Gardino, A. K., Smerdon, S. J., & Yaffe, M. B. (2006). Structural determinants of 14-3-3 binding specificities and regulation of subcellular localization of 14-3-3-ligand complexes: A comparison of the X-ray crystal structures of all human 14-3-3 isoforms. *Seminars in Cancer Biology*.
<https://doi.org/10.1016/j.semcancer.2006.03.007>

Gilbert, S. F., & Barresi, M. J. F. (2017). DEVELOPMENTAL BIOLOGY, 11TH EDITION 2016. *American Journal of Medical Genetics Part A*.
<https://doi.org/10.1002/ajmg.a.38166>

Gilker, Eva Adeline, G. (2018). *Interactions and Localization of Protein Phosphatases, Ywha Proteins and Cell Cycle Control Proteins in Meiosis*. Kent State University.
Retrieved from
http://rave.ohiolink.edu/etdc/view?acc_num=kent1532699317257539

Gittenberger-de Groot, A. C., Hoppenbrouwers, T., Miquerol, L., Kosaka, Y., Poelmann, R. E., Wisse, L. J., ... Brunelli, L. (2016). 14-3-3epsilon controls multiple developmental processes in the mouse heart. *Developmental Dynamics*.
<https://doi.org/10.1002/dvdy.24440>

Goodson, S. G., Qiu, Y., Sutton, K. A., Xie, G., Jia, W., & O'Brien, D. A. (2012). Metabolic Substrates Exhibit Differential Effects on Functional Parameters of Mouse Sperm Capacitation1. *Biology of Reproduction*.
<https://doi.org/10.1095/biolreprod.112.102673>

Gottlieb, S. F., & Tegay, D. H. (2019). *Genetics, Meiosis. StatPearls*.

- Graf, M., Brobeil, A., Sturm, K., Steger, K., & Wimmer, M. (2011). 14-3-3 beta in the healthy and diseased male reproductive system. *Human Reproduction*, 26(1), 59–66. <https://doi.org/10.1093/humrep/deq319>
- Griswold, M. D. (1995). Interactions Between Germ Cells and Sertoli Cells in the Testis. *Biology of Reproduction*. <https://doi.org/10.1095/biolreprod52.2.211>
- Griswold, M. D. (1998). The central role of Sertoli cells in spermatogenesis. *Seminars in Cell and Developmental Biology*. <https://doi.org/10.1006/scdb.1998.0203>
- Grøndahl, M. L., Yding Andersen, C., Bogstad, J., Nielsen, F. C., Meinertz, H., & Borup, R. (2010). Gene expression profiles of single human mature oocytes in relation to age. *Human Reproduction*, 25(4), 957–968. <https://doi.org/10.1093/humrep/deq014>
- Grøndahl, Marie Louise, Borup, R., Vikesa, J., Ernst, E., Andersen, C. Y., & Lykke-Hartmann, K. (2013). The dormant and the fully competent oocyte: Comparing the transcriptome of human oocytes from primordial follicles and in metaphase II. *Molecular Human Reproduction*, 19(9), 600–617. <https://doi.org/10.1093/molehr/gat027>
- Ha, M., & Kim, V. N. (2014). Regulation of microRNA biogenesis. *Nature Reviews Molecular Cell Biology*. <https://doi.org/10.1038/nrm3838>
- Hermeking, H., & Benzinger, A. (2006). 14-3-3 proteins in cell cycle regulation. *Seminars in Cancer Biology*. <https://doi.org/10.1016/j.semcancer.2006.03.002>
- Hirshfield, A. N. (1991). Development of Follicles in the Mammalian Ovary. *International Review of Cytology*. [https://doi.org/10.1016/S0074-7696\(08\)61524-7](https://doi.org/10.1016/S0074-7696(08)61524-7)
- Honda, R., Ohba, Y., & Yasuda, H. (1997). 14-3-3 ζ protein binds to the carboxyl half of

- mouse wee1 kinase. *Biochemical and Biophysical Research Communications*.
<https://doi.org/10.1006/bbrc.1996.5933>
- Hu, M. W., Wang, Z. B., Teng, Y., Jiang, Z. Z., Ma, X. S., Hou, N., ... Sun, Q. Y. (2015). Loss of protein phosphatase 6 in oocytes causes failure of meiosis II exit and impaired female fertility. *Journal of Cell Science*. <https://doi.org/10.1242/jcs.173179>
- Ichimura, T., Isobe, T., Okuyama, T., Takahashi, N., Araki, K., Kuwano, R., & Takahashi, Y. (1988). Molecular cloning of cDNA coding for brain-specific 14-3-3 protein, a protein kinase-dependent activator of tyrosine and tryptophan hydroxylases. *Proceedings of the National Academy of Sciences of the United States of America*. <https://doi.org/10.1073/pnas.85.19.7084>
- Ichimura, Tohru, Kubota, H., Goma, T., Mizushima, N., Ohsumi, Y., Iwago, M., ... Isobe, T. (2004). Transcriptomic and proteomic analysis of a 14-3-3 gene-deficient yeast. *Biochemistry*, 43(20), 6149–6158. <https://doi.org/10.1021/bi035421i>
- Iguchi, N., Tobias, J. W., & Hecht, N. B. (2006). Expression profiling reveals meiotic male germ cell mRNAs that are translationally up- and down-regulated. *Proceedings of the National Academy of Sciences of the United States of America*. <https://doi.org/10.1073/pnas.0510999103>
- Inaba, K. (2003). Molecular Architecture of the Sperm Flagella: Molecules for Motility and Signaling. *Zoological Science*. <https://doi.org/10.2108/zsj.20.1043>
- Inaba, K. (2011). Sperm flagella: Comparative and phylogenetic perspectives of protein components. *Molecular Human Reproduction*. <https://doi.org/10.1093/molehr/gar034>

- Isobe, T., Hiyane, Y., Ichimura, T., Okuyama, T., Takahashi, N., Nakajo, S., & Nakaya, K. (1992). Activation of protein kinase C by the 14-3-3 proteins homologous with Exol protein that stimulates calcium-dependent exocytosis. *FEBS Letters*.
[https://doi.org/10.1016/0014-5793\(92\)81257-M](https://doi.org/10.1016/0014-5793(92)81257-M)
- Izumi, T., Walker, D. H., & Maller, J. L. (1992). Periodic changes in phosphorylation of the *Xenopus cdc25* phosphatase regulate its activity. *Molecular Biology of the Cell*.
<https://doi.org/10.1091/mbc.3.8.927>
- Jacob, A., & Jacob, A. (2012). The Male Reproductive System. In *A Comprehensive Textbook of Midwifery and Gynecological Nursing*.
https://doi.org/10.5005/jp/books/11532_7
- Jones, K. T. (2004). Turning it on and off: M-phase promoting factor during meiotic maturation and fertilization. *Molecular Human Reproduction*.
<https://doi.org/10.1093/molehr/gah009>
- Kang, M. K., Bang, A., Choi, H. O., & Han, S. J. (2017). Comparative analysis of two murine CDC25B isoforms. *Archives of Biological Sciences*.
<https://doi.org/10.2298/ABS160315062K>
- Kim, H., Fernandes, G., & Lee, C. (2016). Protein Phosphatases Involved in Regulating Mitosis: Facts and Hypotheses. *Molecules and Cells*, 39(9), 654–662.
<https://doi.org/10.14348/molcells.2016.0214>
- Kimmins, S., Kotaja, N., Davidson, I., & Sassone-Corsi, P. (2004). Testis-specific transcription mechanisms promoting male germ-cell differentiation. *Reproduction*.
<https://doi.org/10.1530/rep.1.00170>

- Kitagawa, Y., Sasaki, K., Shima, H., Shibuya, M., Sugimura, T., & Nagao, M. (1990). Protein phosphatases possibly involved in rat spermatogenesis. *Biochemical and Biophysical Research Communications*, *171*(1), 230–235. [https://doi.org/10.1016/0006-291X\(90\)91381-2](https://doi.org/10.1016/0006-291X(90)91381-2)
- Korrodi-Gregório, L., Esteves, S. L. C., & Fardilha, M. (2014). Protein phosphatase 1 catalytic isoforms: Specificity toward interacting proteins. *Translational Research*, *164*(5), 366–391. <https://doi.org/10.1016/j.trsl.2014.07.001>
- Kosaka, Y., Cieslik, K. A., Li, L., Lezin, G., Maguire, C. T., Saijoh, Y., ... Brunelli, L. (2012). 14-3-3epsilon Plays a Role in Cardiac Ventricular Compaction by Regulating the Cardiomyocyte Cell Cycle. *Molecular and Cellular Biology*, *32*(24), 5089–5102. <https://doi.org/10.1128/MCB.00829-12>
- Kumagai, A., Yakowec, P. S., & Dunphy, W. G. (1998). 4-3-3 Proteins Act as Negative Regulators of the Mitotic Inducer Cdc25 in Xenopus Egg Extracts. *Molecular Biology of the Cell*, *9*, 345–354.
- Laiho, A., Kotaja, N., Gyenesei, A., & Sironen, A. (2013). Transcriptome Profiling of the Murine Testis during the First Wave of Spermatogenesis. *PLoS ONE*. <https://doi.org/10.1371/journal.pone.0061558>
- Lan, Z. J., Xu, X., & Cooney, A. J. (2004). Differential oocyte-specific expression of Cre recombinase activity in GDF-9-iCre, Zp3cre, and Msx2Cre transgenic mice. *Biol Reprod*, *71*(5), 1469–1474. <https://doi.org/10.1095/biolreprod.104.031757>
- Lee, J., Kumagai, A., & Dunphy, W. G. (2001). Positive regulation of Wee1 by Chk1 and 14-3-3 proteins. *Molecular Biology of the Cell*. <https://doi.org/10.1091/mbc.12.3.551>

- Lesage, B., Beullens, M., Nuytten, M., Van Eynde, A., Keppens, S., Himpens, B., & Bollen, M. (2004). Interactor-mediated nuclear translocation and retention of protein phosphatase-1. *Journal of Biological Chemistry*. <https://doi.org/10.1074/jbc.M411911200>
- Lewandoski, M., Meyers, E. N., & Martin, G. R. (1997). Analysis of Fgf8 gene function in vertebrate development. In *Cold Spring Harbor Symposia on Quantitative Biology* (Vol. 62, pp. 159–168). <https://doi.org/10.1101/SQB.1997.062.01.021>
- Li, L., Lu, X., & Dean, J. (2013). The maternal to zygotic transition in mammals. *Molecular Aspects of Medicine*. <https://doi.org/10.1016/j.mam.2013.01.003>
- Lin, Q., Buckler, E. S., Muse, S. V., & Walker, J. C. (1999). Molecular evolution of type 1 serine/threonine protein phosphatases. *Molecular Phylogenetics and Evolution*, *12*(1), 57–66. <https://doi.org/10.1006/mpev.1998.0560>
- Lincoln, A. J., Wickramasinghe, D., Stein, P., Schultz, R. M., Palko, M. E., De Miguel, M. P., ... Donovan, P. J. (2002). Cdc25b phosphatase is required for resumption of meiosis during oocyte maturation. *Nature Genetics*, *30*(4), 446–449.
- Mack, S., Bhattacharyya, A. K., Joyce, C., Van Der Ven, H., & Zaneveld, L. J. D. (1983). Acrosomal Enzymes of Human Spermatozoa Before and After in Vitro Capacitation. *Biology of Reproduction*. <https://doi.org/10.1095/biolreprod28.5.1032>
- Mackintosh, C. (2004). Dynamic interactions between 14-3-3 proteins and phosphoproteins regulate diverse cellular processes. *Biochemical Journal*, *342*, 329–342. <https://doi.org/10.1042/BJ20031332>
- Mackintosh, Carol. (2004). Dynamic interactions between 14-3-3 proteins and

- phosphoproteins regulate diverse cellular processes. *Biochemical Journal*, 381, 329–342. <https://doi.org/10.1042/BJ20031332>
- Maekawa, M., Kamimura, K., & Nagano, T. (1996). Peritubular myoid cells in the testis : Their structure and function. *Archives of Histology and Cytology*. <https://doi.org/10.1679/aohc.59.1>
- Manova, K., Nocka, K., Besmer, P., & Bachvarova, R. F. (1990). Gonadal expression of c-kit encoded at the W locus of the mouse. *Development*.
- Margolis, S. S., Perry, J. A., Weitzel, D. H., Freel, C. D., Yoshida, M., Haystead, T. A., & Kornbluth, S. (2006). A role for PP1 in the Cdc2/cyclin B-mediated positive feedback activation of Cdc25. *Molecular Biology of the Cell*. <https://doi.org/10.1091/mbc.E05-08-0751>
- Margolis, S. S., Walsh, S., Weiser, D. C., Yoshida, M., Shenolikar, S., & Kornbluth, S. (2003). PP1 control of M phase entry exerted through 14-3-3-regulated Cdc25 dephosphorylation. *EMBO Journal*. <https://doi.org/10.1093/emboj/cdg545>
- Masciarelli, S., Horner, K., & Liu, C. (2004). Cyclic nucleotide phosphodiesterase 3A–deficient mice as a model of female infertility. *Journal of Clinical Investigation*, 114(2), 196–205. <https://doi.org/10.1172/JCI200421804.196>
- McGee, E. A., & Hsueh, A. J. W. (2000). Initial and cyclic recruitment of ovarian follicles. *Endocrine Reviews*. <https://doi.org/10.1210/er.21.2.200>
- Meek, S. E. M., Lane, W. S., & Piwnicka-Worms, H. (2004). Comprehensive proteomic analysis of interphase and mitotic 14-3-3-binding proteins. *Journal of Biological Chemistry*, 279(31), 32046–32054. <https://doi.org/10.1074/jbc.M403044200>

- Mehlmann, L. M. (2005). Oocyte-specific expression of Gpr3 is required for the maintenance of meiotic arrest in mouse oocytes. *Developmental Biology*, 288(2), 397–404.
- Mehlmann, L. M., Jones, T. L. Z., & Jaffe, L. A. (2002). Meiotic arrest in the mouse follicle maintained by a G(s) protein in the oocyte. *Science*, 297(5585), 1343–1345.
- Mehlmann, L. M., Saeki, Y., Tanaka, S., Brennan, T. J., Evsikov, A. V., Pendola, F. L., ... Jaffe, L. A. (2004). The G(s)-linked receptor GPR3 maintains meiotic arrest in mammalian oocytes. *Science*, 306(5703), 1947–1950.
- Mehlmann, Lisa M. (2005). Stops and starts in mammalian oocytes: Recent advances in understanding the regulation of meiotic arrest and oocyte maturation. *Reproduction*.
<https://doi.org/10.1530/rep.1.00793>
- Meng, J., Cui, C., Liu, Y., Jin, M., Wu, D., Liu, C., ... Yu, B. (2013). The Role of 14-3-3 epsilon Interaction with Phosphorylated Cdc25B at Its Ser321 in the Release of the Mouse Oocyte from Prophase I Arrest. *Plos One*, 8(1), e53633–e53633.
<https://doi.org/10.1371/journal.pone.0053633>
- Messina, A., Reina, S., Guarino, F., & De Pinto, V. (2012). VDAC isoforms in mammals. *Biochimica et Biophysica Acta - Biomembranes*.
<https://doi.org/10.1016/j.bbamem.2011.10.005>
- Mochida, S., & Hunt, T. (2012). Protein phosphatases and their regulation in the control of mitosis. <https://doi.org/10.1038/embor.2011.263>
- Moore, B. W., & Perez, V. J. (1967). Specific Acidic Proteins of the Nervous System. In *Physiological and Biochemical Aspects of Nervous Integration*.

- Morrison, D. K. (2009). The 14-3-3 proteins: integrators of diverse signaling cues that impact cell fate and cancer development. *Trends in Cell Biology*.
<https://doi.org/10.1016/j.tcb.2008.10.003>
- Mumby, M. C., & Walter, G. (1993). Protein serine/threonine phosphatases: structure, regulation, and functions in cell growth. *Physiological Reviews*, 73(4), 673–699.
- Muslin, A. J., Tanner, J. W., Allen, P. M., & Shaw, A. S. (1996). Interaction of 14-3-3 with signaling proteins is mediated by the recognition of phosphoserine. *Cell*.
[https://doi.org/10.1016/S0092-8674\(00\)81067-3](https://doi.org/10.1016/S0092-8674(00)81067-3)
- Neill, J. D., Plant, T. M., Pfaff, D. W., Challis, J. R. G., De Kretser, D. M., Richards, J. A. S., & Wassarman, P. M. (2006). *Knobil and neill's physiology of reproduction*. *Knobil and Neill's Physiology of Reproduction*.
- Oh, J. S., Han, S. J., & Conti, M. (2010). Wee1B, Myt1, and Cdc25 function in distinct compartments of the mouse oocyte to control meiotic resumption. *Journal of Cell Biology*, 188(2), 199–207. <https://doi.org/10.1083/jcb.200907161>
- Ohkura, H. (2015). Meiosis: An Overview of Key Differences from Mitosis. *Cold Spring Harbor Perspectives in Biology*, 7(5), a015859–a015859.
<https://doi.org/10.1101/cshperspect.a015859>
- Okano, K., Heng, H., Trevisanato, S., Tyers, M., & Varmuza, S. (1997). Genomic organization and functional analysis of the murine protein phosphatase 1c gamma (Ppp1cc) gene. *Genomics*, 45(1), 211–215. <https://doi.org/10.1006/geno.1997.4907>
- Pan, H., Ma, P., Zhu, W., & Schultz, R. M. (2008). Age-associated increase in aneuploidy and changes in gene expression in mouse eggs. *Dev Biol*, 316(2), 397–

407. <https://doi.org/10.1016/j.ydbio.2008.01.048>

Peng, C. Y., Graves, P. R., Thoma, R. S., Wu, Z., Shaw, A. S., & Piwnica-Worms, H. (1997). Mitotic and G2 checkpoint control: Regulation of 14-3-3 protein binding by phosphorylation of Cdc25c on serine-216. *Science*.

<https://doi.org/10.1126/science.277.5331.1501>

Perdiguerro, E., & Nebreda, A. R. (2004). Regulation of Cdc25C activity during the meiotic G2/M transition. *Cell Cycle*.

Petersen, C., Füzesi, L., & Hoyer-Fender, S. (1999). Outer dense fibre proteins from human sperm tail: Molecular cloning and expression analyses of two cDNA transcripts encoding proteins of ~70 kDa. *Molecular Human Reproduction*.

<https://doi.org/10.1093/molehr/5.7.627>

Pirino, G., Wesco, M. P., & Donovan, P. J. (2009). Protein kinase A regulates resumption of meiosis by phosphorylation of Cdc25B in mammalian oocytes. *Cell Cycle*, 8(4),

665–670. <https://doi.org/10.4161/cc.8.4.7846>

Plant, T., & Zeleznik, A. (2014). *Knobil and Neill's physiology of Reproduction 4th edition*. (Tony Plant and Anthony Zeleznik, Ed.).

Potireddy, S., Vassena, R., Patel, B. G., & Latham, K. E. (2006). Analysis of polysomal mRNA populations of mouse oocytes and zygotes: Dynamic changes in maternal mRNA utilization and function. *Developmental Biology*.

<https://doi.org/10.1016/j.ydbio.2006.06.024>

Pozuelo Rubio, M., Geraghty, K. M., Wong, B. H. C., Wood, N. T., Campbell, D. G., Morrice, N., & Mackintosh, C. (2004). 14-3-3-affinity purification of over 200

- human phosphoproteins reveals new links to regulation of cellular metabolism, proliferation and trafficking. *The Biochemical Journal*, 379(Pt 2), 395–408.
<https://doi.org/10.1042/BJ20031797>
- Puri, P., Acker-Palmer, A., Stahler, R., Chen, Y., Kline, D., & Vijayaraghavan, S. (2011). Identification of testis 14–3-3 binding proteins by tandem affinity purification. *Spermatogenesis*. <https://doi.org/10.4161/spmg.1.4.18902>
- Puri, P., Myers, K., Kline, D., & Vijayaraghavan, S. (2008). Proteomic analysis of bovine sperm YWHA binding partners identify proteins involved in signaling and metabolism. *Biology of Reproduction*, 79(6), 1183–1191.
<https://doi.org/10.1095/biolreprod.108.068734>
- Rebelo, S., Santos, M., Martins, F., da Cruz e Silva, E. F., & da Cruz e Silva, O. A. B. (2015). Protein phosphatase 1 is a key player in nuclear events. *Cellular Signalling*, 27(12), 2589–2598. <https://doi.org/10.1016/j.cellsig.2015.08.007>
- Rie Mils, V., Ronique Baldin, V., Oise Goubin, F., Pinta, I., Papin, C., Wayne, M., ... Ducommun, B. (2000). Specific interaction between 14-3-3 isoforms and the human CDC25B phosphatase. *Oncogene*, 19, 1257–1265.
<https://doi.org/10.1038/sj.onc.1203419>
- Robinson, M. O., McCarrey, J. R., & Simon, M. I. (1989). Transcriptional regulatory regions of testis-specific PGK2 defined in transgenic mice. *Proceedings of the National Academy of Sciences of the United States of America*.
<https://doi.org/10.1073/pnas.86.21.8437>
- Rossi, P., Albanesi, C., Grimaldi, P., & Geremia, R. (1991). Expression of the mRNA for

- the ligand of C-kit in mouse sertoli cells. *Biochemical and Biophysical Research Communications*. [https://doi.org/10.1016/S0006-291X\(05\)80272-4](https://doi.org/10.1016/S0006-291X(05)80272-4)
- Rothblum-Oviatt, C. J., Ryan, C. E., & Piwnica-Worms, H. (2001). 14-3-3 Binding regulates catalytic activity of human Wee1 kinase. *Cell Growth and Differentiation*.
- Ryves, W. J., Fryer, L., Dale, T., & Harwood, A. J. (1998). An assay for glycogen synthase kinase 3 (GSK-3) for use in crude cell extracts. *Analytical Biochemistry*. <https://doi.org/10.1006/abio.1998.2832>
- Sadate-Ngatchou, P. I., Payne, C. J., Dearth, A. T., & Braun, R. E. (2008). Cre recombinase activity specific to postnatal, premeiotic male germ cells in transgenic mice. *Genesis (New York, N.Y. : 2000)*, 46(12), 738–742. <https://doi.org/10.1002/dvg.20437>
- Sasaki, K., Shima, H., Kitagawa, Y., Irino, S., Sugimura, T., & Nagao, M. (1990). Identification of members of the protein phosphatase 1 gene family in the rat and enhanced expression of protein phosphatase 1 alpha gene in rat hepatocellular carcinomas. *Jpn.J.Cancer Res.*, 81(12), 1272–1280.
- Schäfer, M., Nayernia, K., Engel, W., & Schäfer, U. (1995). Translational control in spermatogenesis. *Developmental Biology*. <https://doi.org/10.1006/dbio.1995.8049>
- Schindler, K. (2011). Protein kinases and protein phosphatases that regulate meiotic maturation in mouse oocytes. *Results and Problems in Cell Differentiation*, 53, 309–341. https://doi.org/10.1007/978-3-642-19065-0_14
- Schoenwaelder, S. M., Darbousset, R., Cranmer, S. L., Ramshaw, H. S., Orive, S. L., Sturgeon, S., Jackson, S. P. (2017). Corrigendum: 14-3-3 ζ regulates the

- mitochondrial respiratory reserve linked to platelet phosphatidylserine exposure and procoagulant function. *Nature Communications*.
<https://doi.org/10.1038/ncomms16125>
- Scialli, A. R. (1993). A comparative overview of mammalian fertilization. *Reproductive Toxicology*. [https://doi.org/10.1016/0890-6238\(93\)90236-z](https://doi.org/10.1016/0890-6238(93)90236-z)
- Seung, J. H., Chen, R., Paronetto, M. P., & Conti, M. (2005). Wee1B is an oocyte-specific kinase involved in the control of meiotic arrest in the mouse. *Current Biology*, 15(18), 1670–1676. <https://doi.org/10.1016/j.cub.2005.07.056>
- Shapiro, H. M., Natale, P. J., & Kamentsky, L. A. (1979). Estimation of membrane potentials of individual lymphocytes by flow cytometry. *Proceedings of the National Academy of Sciences*. <https://doi.org/10.1073/pnas.76.11.5728>
- Shi, Y. (2009). Serine/Threonine Phosphatases: Mechanism through Structure. *Cell*. <https://doi.org/10.1016/j.cell.2009.10.006>
- Shima, Y., Miyabayashi, K., Haraguchi, S., Arakawa, T., Otake, H., Baba, T., ... Morohashi, K. I. (2013). Contribution of Leydig and Sertoli cells to testosterone production in mouse fetal testes. *Molecular Endocrinology*. <https://doi.org/10.1210/me.2012-1256>
- Shuhaibar, L. C., Egbert, J. R., Norris, R. P., Lampe, P. D., Nikolaev, V. O., Thunemann, M., ... Jaffe, L. A. (2015). Intercellular signaling via cyclic GMP diffusion through gap junctions restarts meiosis in mouse ovarian follicles. *Proceedings of the National Academy of Sciences of the United States of America*, 112(17), 5527–5532. <https://doi.org/10.1073/pnas.1423598112>

- Sinha, N., Puri, P., Nairn, A. C., & Vijayaraghavan, S. (2013). Selective Ablation of Ppp1cc Gene in Testicular Germ Cells Causes Oligo-Teratozoospermia and Infertility in Mice. *Biology of Reproduction*.
<https://doi.org/10.1095/biolreprod.113.110239>
- Smith, G D, Sadhu, A., Mathies, S., & Wolf, D. P. (1998). Characterization of protein phosphatases in mouse oocytes. *Developmental Biology*, 204(2), 537–549.
<https://doi.org/10.1006/dbio.1998.9043>
- Smith, Gary D, Sadhu, A., Mathies, S., & Wolf, D. P. (1998). Characterization of protein phosphatases in mouse oocytes. *Developmental Biology*, 204(2), 537–549.
<https://doi.org/10.1006/dbio.1998.9043>
- Solc, P., Saskova, A., Baran, V., Kubelka, M., Schultz, R. M., & Motlik, J. (2009). CDC25A phosphatase controls meiosis I progression in mouse oocytes, 317(1), 260–269. <https://doi.org/10.1016/j.ydbio.2008.02.028.CDC25A>
- Steinacker, P., Schwarz, P., Reim, K., Brechlin, P., Jahn, O., Kratzin, H., ... Otto, M. (2005). Unchanged survival rates of 14-3-3gamma knockout mice after inoculation with pathological prion protein. *Molecular and Cellular Biology*, 25(4), 1339–1346.
<https://doi.org/10.1128/MCB.25.4.1339-1346.2005>
- Swain, J. E., Wang, X., Saunders, T. L., Dunn, R., & Smith, G. D. (2003). Specific inhibition of mouse oocyte nuclear protein phosphatase-1 stimulates germinal vesicle breakdown. *Molecular Reproduction and Development*, 65(1), 96–103.
<https://doi.org/10.1002/mrd.10258>
- Swingle, M., Ni, L., & Honkanen, R. E. (2007). Small-molecule inhibitors of ser/thr

- protein phosphatases: specificity, use and common forms of abuse. *Methods in Molecular Biology (Clifton, N.J.)*, 365, 23–38. <https://doi.org/10.1385/1-59745-267-X:23>
- Tan, E. P., Duncan, F. E., & Slawson, C. (2017). The sweet side of the cell cycle. *Biochemical Society Transactions*. <https://doi.org/10.1042/BST20160145>
- Tang, A., Shi, P., Song, A., Zou, D., Zhou, Y., Gu, P., ... Gao, X. (2016). PP2A regulates kinetochore-microtubule attachment during meiosis I in oocyte. *Cell Cycle*, 15(11), 1450–1461. <https://doi.org/10.1080/15384101.2016.1175256>
- TOKER, A., ELLIS, C. A., SELLERS, L. A., & AITKEN, A. (1990). Protein kinase C inhibitor proteins: Purification from sheep brain and sequence similarity to lipocortins and 14-3-3 protein. *European Journal of Biochemistry*. <https://doi.org/10.1111/j.1432-1033.1990.tb19138.x>
- Toyo-Oka, K., Shionoya, A., Gambello, M. J., Cardoso, C., Leventer, R., Ward, H. L., ... Wynshaw-Boris, A. (2003). 14-3-3 ϵ is important for neuronal migration by binding to NUDEL: A molecular explanation for Miller-Dieker syndrome. *Nature Genetics*. <https://doi.org/10.1038/ng1169>
- Toyo-oka, K., Wachi, T., Hunt, R. F., Baraban, S. C., Taya, S., Ramshaw, H., ... Wynshaw-Boris, A. (2014). 14-3-3E and Z Regulate Neurogenesis and Differentiation of Neuronal Progenitor Cells in the Developing Brain. *The Journal of Neuroscience: The Official Journal of the Society for Neuroscience*, 34(36), 12168–12181. <https://doi.org/10.1523/JNEUROSCI.2513-13.2014>
- van Hemert, M. J., de Steensma, H. Y., & van Heusden, G. P. H. (2001). 14-3-3 Proteins:

- Key Regulators of Cell Division, Signalling and Apoptosis. *Bioessays*, 23(10), 936–946. <https://doi.org/10.1002/bies.1134>
- Varmuza, S., Jurisicova, A., Okano, K., Hudson, J., Boekelheide, K., & Shipp, E. B. (1999). Spermiogenesis is impaired in mice bearing a targeted mutation in the protein phosphatase 1cgamma gene. *Developmental Biology*, 205, 98–110. <https://doi.org/10.1006/dbio.1998.9100>
- Vijayaraghavan, S., Liberty, G. A., Mohan, J., Winfrey, V. P., Olson, G. E., & Carr, D. W. (1999). Isolation and molecular characterization of AKAP110, a novel, sperm-specific protein kinase A-anchoring protein. *Molecular Endocrinology*. <https://doi.org/10.1210/mend.13.5.0278>
- Walker, W. H., & Cheng, J. (2005). FSH and testosterone signaling in Sertoli cells. *Reproduction*. <https://doi.org/10.1530/rep.1.00358>
- Wang, X., Swain, J. E., Bollen, M., Liu, X. T., Ohl, D. A., & Smith, G. D. (2004). Endogenous regulators of protein phosphatase-1 during mouse oocyte development and meiosis. *Reproduction*. <https://doi.org/10.1530/rep.1.00173>
- Wang, Y., Jacobs, C., Hook, K. E., Duan, H., Booher, R. N., & Sun, Y. (2000). Binding of 14-3-3 β to the carboxyl terminus of Wee1 increases Wee1 stability, kinase activity, and G₂-M cell population. *Cell Growth and Differentiation*.
- Wera, S., & Hemmings, B. A. (1995). Serine/threonine protein phosphatases. *The Biochemical Journal*, 7(4), 17–29.
- Wong, E. W. P., Sun, S., Li, M. W. M., Lee, W. M., & Cheng, C. Y. (2009). 14-3-3 Protein regulates cell adhesion in the seminiferous epithelium of rat testes.

- Endocrinology*, 150(10), 4713–4723. <https://doi.org/10.1210/en.2009-0427>
- Wright, W. W., Musto, N. A., Mather, J. P., & Bardin, C. W. (1981). Sertoli cells secrete both testis-specific and serum proteins. *Proceedings of the National Academy of Sciences of the United States of America*.
- Xu, M., & Hecht, N. B. (2011). Polypyrimidine Tract-Binding Protein 2 Binds to Selective, Intronic Messenger RNA and MicroRNA Targets in the Mouse Testis. *Biology of Reproduction*. <https://doi.org/10.1095/biolreprod.110.087114>
- Xu, X., Jaehne, E. J., Greenberg, Z., McCarthy, P., Saleh, E., Parish, C. L., ... Schwarz, Q. (2015). 14-3-3 ζ deficient mice in the BALB/c background display behavioural and anatomical defects associated with neurodevelopmental disorders. *Scientific Reports*. <https://doi.org/10.1038/srep12434>
- Yaffe, M. B., Rittinger, K., Volinia, S., Caron, P. R., Aitken, A., Leffers, H., ... Cantley, L. C. (1997). The structural basis for 14-3-3:phosphopeptide binding specificity. *Cell*. [https://doi.org/10.1016/S0092-8674\(00\)80487-0](https://doi.org/10.1016/S0092-8674(00)80487-0)
- Yan, W. (2009). Male infertility caused by spermiogenic defects: Lessons from gene knockouts. *Molecular and Cellular Endocrinology*. <https://doi.org/10.1016/j.mce.2009.03.003>
- Yelick, P. C., Kwon, Y. K., Flynn, J. F., Borzorgzadeh, A., Kleene, K. C., & Hecht, N. B. (1989). Mouse transition protein 1 is translationally regulated during the postmeiotic stages of spermatogenesis. *Molecular Reproduction and Development*. <https://doi.org/10.1002/mrd.1080010307>
- Yeo, G., Holste, D., Kreiman, G., & Burge, C. B. (2004). Variation in alternative splicing

across human tissues. *Genome Biology*.

Yoshinaga, K., Nishikawa, S., Ogawa, M., Hayashi, S. I., Kunisada, T., & Fujimoto

Nishikawa, T. S. I. (1991). Role of c-kit in mouse spermatogenesis: Identification of spermatogonia as a specific site of c-kit expression and function. *Development*.

Zabludoff, S. D., Charron, M., Decerbo, J. N., Simukova, N., & Wright, W. W. (2001).

Male germ cells regulate transcription of the cathepsin L gene by rat Sertoli cells. *Endocrinology*. <https://doi.org/10.1210/endo.142.6.8106>

Zeng, Y., Clark, E. N., & Florman, H. M. (1995). Sperm membrane potential:

Hyperpolarization during capacitation regulates zona pellucida-dependent acrosomal secretion. *Developmental Biology*. <https://doi.org/10.1006/dbio.1995.1304>

Zhang, Y., Zhang, Z., Xu, X. Y., Li, X. S., Yu, M., Yu, A. M., ... Yu, B. Z. (2008).

Protein kinase A modulates Cdc25B activity during meiotic resumption of mouse oocytes. *Developmental Dynamics*, 237(12), 3777–3786.

<https://doi.org/10.1002/dvdy.21799>